Investigation into the role of DWNN in cell death

Tumelo Seameco

A thesis submitted in fulfilment of the requirements for the degree of Masters in

Science in the Department of Biotechnology, Faculty of Science, University of the

Western Cape

Supervisor: Prof DJG Rees

August 2004

ABSTRACT

Investigation into the role of DWNN in cell death

Tumelo Seameco

MSc thesis, Department of Biotechnology, Faculty of Science, University of the Western Cape

The efficient delivery of proteins into cells could previously only be achieved when molecules are small. There are currently a number of alternative means to overcome this difficulty. The transduction method utilised in this study results in protein delivery into both the cytoplasm and the nucleus. The methodology involves the transduction of cells with TAT-GFP fusion proteins, where TAT is the amino- or carboxy- terminal 11-amino acid protein transduction domain derived from HIV-TAT and green fluorescent protein (GFP), due to its flexibility as a non-involvement marker in cells, serves as a reporter protein. The means by which TAT delivers fusion proteins into cells is still unknown but it is thought to disrupt the cell membrane and thus enter the cell in a receptor independent fashion. We used fluorescence microscopy and flow cytometry to detect TAT mediated delivery of GFP fusion proteins, showing that we have successfully transduced CHO adherent cells.

TAT-GFP-fusion proteins were used to characterise a novel pro-apoptotic protein, DWNN, which has been identified from gene targeting experiments, and shown to play a role in the mechanism of apoptosis induced by cytotoxic T cells. DWNN consists of 76 residues that constitute a highly conserved domain.

The mode by which DWNN functions has been hypothesised to involve covalent linkage to some other proteins with Rb and p53 being important candidates. Transduction of TAT-GFP-DWNN$_{118}$ and TAT-DWNN$_{118}$ fusion proteins into cells resulted in localisation of the protein to the nucleus of the cells. Western Blot analysis demonstrated both TAT-GFP-DWNN$_{118}$ and TAT-DWNN$_{118}$ to be associated with a higher molecular weight protein. The nature of this protein complex is being evaluated.

This shows that the use of protein transduction technology can allow the detection of roles for proteins in apoptosis, using rapid introduction of protein into cells, which then allows the biochemical analysis of their function. This methodology holds hope for the development of vaccines and protein therapies for cancer and infectious diseases. In addition there is hope to eliminate HIV, infectious pathogens such as hepatitis C virus, cytomegalovirus and malaria.

August 2004

For the family

<u>Declaration</u>

I declare "*Investigation into the role of DWNN in cell death"* to be my work, which has not been submitted for any degree or examination in any other institution, and that all the sources I have used or quoted have been indicated and acknowledged by references.

Tumelo Seameco   August 2004

Signed:…………………………………..

TABLE OF CONTENTS   PAGE

CHAPTER 1: INTRODUCTION

CHAPTER 2: MATERIALS AND METHODS

Chapter 3: The Architecture and Construction of TAT-PTD

Fusion Proteins

CHAPTER 4: Expression and Purification of the Constructs

Chapter 5: Introduction of fusion proteins into cells by

Transduction

Chapter 6: General Discussion

List of Figures and Tables

Tables

Chapter 1

Chapter 2

Chapter 3

Figures

Chapter 1

Chapter 2

Chapter 3

q

release GFP.

Chapter 4

Chapter 5

ABBREVIATIONS

AIDS	**A**cquired **i**mmuno**d**eficiency **s**yndrome
Apaf-1	**a**poptotic **p**rotease-**a**ctivating **f**actor-**1**
bp	**b**ase **p**air
Bax	**B**cl-2 –**a**ssociated **x** protein
Bcl-2	**B c**ell **l**eukaemia-**2**
BPB	**B**romo**p**henol **b**lue
BSA	**B**ovine **s**erum **a**lbumin
CAD	**c**aspase-**a**ctivated **d**eoxyribonuclease
CARD	**ca**spase **r**ecruitment **d**omain
Caspases	**c**ysteine **asp**artic-specific prote**ases**
cDNA	**c**omplementary **DNA**
CED	**c**ell d**e**ath **d**efective
CHO	**C**hinese **h**amster **o**vary
C-terminal	**c**arboxy **terminal**
CTL	**C**ytotoxic **T l**ymphocyte
Da	**Da**lton
DAPI	4', 6'-**Di**a**a**midino-2-**p**henyl**i**ndole
DD	**d**eath **d**omain
DED	**d**eath **e**ffector **d**omain
dNTP	2'-**d**eoxy**n**ucleoside 5'-**trip**hosphate
DISC	**d**eath-**i**nducing **s**ignalling **c**omplex

w

DWNN	**D**omain **W**ith **N**o **N**ame
DMSO	**D**imethyl **s**ulphoxide
DNA	**D**eoxyribo**n**ucleic **a**cid
DTT	**Di**thio**t**hreitol
EDTA	**E**thylene **d**iamine **t**etra **a**cetic acid
egl-1	**e**xternal **g**erminal **l**ayer-**1**
FACS	**F**luorescence **a**ctivated **c**ell **s**orter
FADD	**F**as **a**ssociated **d**eath **d**omain
Fas	**F**ibroblast-**as**sociated
FasL	**Fas l**igand
FCS	**F**oetal **c**alf **s**erum
FGF-4	**f**ibroblast **g**rowth **f**actor-**4**
FITC	**f**luorescein **i**so**t**hio**c**yanate
GFP	**G**reen **f**luorescent **p**rotein
GST	**G**lutathione **S**-**T**ransferase
hid	**h**ead **i**nvolution **d**efective
HIV	**h**uman **i**mmunodeficiency **v**irus
IAP	**i**nhibitors of **ap**optosis
ICAD	**i**nhibitor of **CAD**
ICE	**i**nterleukin-1-B-converting **c**aspase **e**nzyme
IL-2	**i**nter**l**eukin-**2**
IPTG	**I**so**p**ropyl β-D-**t**hio**g**alactopyranoside
kb	**K**ilo **b**ase

kD	**K**ilo **D**alton
l	**l**itre
LB	**L**uria **B**roth
LCMV	**l**ymphocytic **c**horio**m**eningitis **v**irus
LMV	**l**ettuce **m**osaic **v**irus
loxP	**lo**cus of crossing-over
MAC	**m**embrane **a**ttack **c**omplex
MCS	**M**ultiple **c**loning **s**ite
MOPS	4-**Mo**rpholine **p**ropane**s**ulphonic acid
mRNA	**m**essenger **RNA**
MTS	**m**embrane-**t**ranslocating hydrophobic **s**equence
NK	**N**atural **k**iller cells
N-terminal	ami**no**-**terminal**
NLS	**n**uclear **l**ocalisation **s**equence
PACT	**p**53 **A**ssociated **c**ellular protein **t**estis derived
PAGE	**P**oly**a**crylamide **g**el **e**lectrophoresis
PBS	**P**hosphate **b**uffer **s**aline
PCD	**P**rogrammed **c**ell **d**eath
PCR	**P**olymerase **c**hain **r**eaction
PMSF	**P**henyl**m**ethyl**s**ulphonyl **f**luoride
PTD	**P**rotein **t**ransduction **d**omain
Rb	**R**etino**b**lastoma
RFP	**R**ed **f**luorescent **p**rotein

RNA	**R**ibo**n**ucleic **a**cid
rpr	**re**a**pe**r
SDS	**S**odium **d**odecyl **s**ulphate
SV-40	**s**imian **v**irus **40**
TAT	**t**ranscriptional **ac**t**i**vator
TEMED	*N*, *N*, *N*', *N*'-**Te**tra **m**ethyl**e**thylene**d**iamine
TNF	**T**umour **n**ecrosis **f**actor
UV	**U**ltra **v**iolet

z

ACKNOWLEDGEMENTS AND THANKS

Chinese Proverbs:

"Pure gold does not fear furnace."

"When eating bamboo sprouts, remember the man who planted them. "

"Our greatest glory is not in never falling, but in rising every time we fall. "

"Better to bend with the wind, than to break. "

"Peace only comes when reason rules."

"There are times, aren't there, when plants shoot but do not flower, and when they flower but do not produce fruit? "

"After the game, the king and the pawn go in the same box."

"Laws are useless when men are pure, unenforceable when men are corrupt."

"True words may not be pleasant, pleasant words may not be true."

"Lust and greed have no limit."

"Sow much, reap much; sow little, reap little. "

"Eloquence provides only persuasion, but truth buys loyalty."

You can only go halfway into the darkest forest; then you are coming out the other side. "

"Examine what is said, not who speaks."

"Man has two ears and one tongue so that he may listen twice as much as he speaks."

"Forget injuries, never forget kindnesses. "

"Everything has a price. Some things you think you must have, but the price, if you knew it beforehand you'd never, ever pay"……..

……. Nothing worth having comes without a serious price …..

This is how you recognise a man. He can change his name, his identity, even his face. But his gait will always give him away. Just as fingerprints can identify a man out of a million similar men, so can a man's gait. That never changes. Even if he breaks a bone, his body adapts and the peculiarities of the old gait re-emerge.

Solace is not absolution ……..

Pretending it's over when obviously it isn't, this thought defeats, it can't be explained, ………. complete lesson learnt ……….   Eric Lustbader…….Dark Homecoming.

>Don't count the days, make the days count!

There are chosen winners and chosen losers, but there's a higher force that determines winning …………….   Hidalgo, the movie.

It is a silent but patient hunter, possessing nothing but mass, but mass has gravity and it knows in time its victims will come, in this, it is ruthless, loud and impatient ………………

CHAPTER 1

INTRODUCTION

Genetic manipulation together with the arrival of novel and advanced technologies created a means of characterising and elucidating the functions of numerous identified genes. This aids in the refinement of biochemical understanding of such genes and those yet to be identified.

APOPTOSIS

Apoptosis is known to be the regulated destruction of a cell. This process is very complicated since the decision to die cannot be taken lightly. The activity of many genes influences the likelihood that a cell activates its self-destruction programme. When the decision is finalised, there is proper execution of the apoptotic programme. This programme requires coordinated activation and execution of multiple subprograms [Barisic *et al.*, 2003].

Apoptosis ("Primed" cell death) [apoptosis; Greek "a falling off" from apo, off, and ptosis, fall], a physiological, highly conserved program of cellular suicide is executed by a cascade of highly specific caspases, activated by complexation of initiator caspases [Holtz and Heinrich, 1999]. It is a suicide mechanism in which cell death occurs naturally during normal tissue turnover. It preserves homeostasis and usually occurs after activation of a calcium-dependent endogenous endonuclease [Ashwell *et*

al., 1994; Fanidi and Evan, 1994]. Apoptosis has been referred to as a physiologic cell death, in contrast to necrosis, which shows typical features of pathologic cell death (table 1.1).

Necrosis	Apoptosis
Morphology	
*Loss of membrane integrity	*Membrane blebbing, maintained integrity
*Swelling of cytoplasm and organelles	*Shrinkage of cytoplasm, condensation of cytoplasm
*Complete cell lysis	*Fragmentation of cell into membrane bound vesicles
Biochemistry	
*Passive process, no energy requirement	*Energy-dependent process
*Early loss of ion homeostasis	*Tightly regulated enzyme cascades
*Random digestion of DNA	*Non-random DNA-fragmentation
Physiology	
*Groups of cells affected at the same time	*Individual cells affected
*Evoked by non-physiological insult	*Induced by a physiologic stimuli
*Inflammatory response	*No Inflammatory response

Table 1.1: Necrotic versus Apoptotic features [Zador *et al.*, 2003].

1.1 An Overview of apoptosis

1.1.1 Introduction

There is a need for multi-cellular organisms to be able to eliminate excess or infected cells. As imperative as cell division and cell migration, regulated or programmed cell death is essential since it allows a given organism to tightly control cell numbers and the tissue size and it also allows an organism to protect itself from cells that may be a threat to homeostasis [Barisic *et al.*, 2003]. By that it should be obvious that the rogue cells have to be removed, thus for every cell there is time to live and a time to die.

Programmed cell death has been discovered and rediscovered. It acquired various names over the two previous centuries [Peter *et al.*, 1997]. The eventually adopted term is apoptosis, coined for the description of a common type programmed cell death that was repeatedly observed in various cell types and tissues. These dying cells were sharing many morphological features that were very distinct from the features in cells undergoing pathological, necrotic cell death. These morphological features might be due to the underlying common, conserved, endogenous cell death programme. In contrast to necrosis, apoptosis is a regulated, energy-dependent form of cell death leading to phagocytosis of cellular remnants by neighboring cells [Ziegler and Groscurth, 2004]. There are two ways by which cells die, namely, (i) they may be killed by injurious agents, or (ii) they may be induced to commit suicide.

Death by injury: Damage to cells by injury such as mechanical damage or being exposed to toxic chemicals yields a characteristic series of changes. Such cells and their organelles, mitochondria for an example, swell since there is disruption of the ability of the plasma membrane to control the passage of ions and water. This is due to necrosis being accompanied by rapid permeabilisation of plasma membrane [Proskuryakov *et al.*, 2003]. This results in the contents of the cell leaking out and consequently inflammation of the surrounding tissues occurs. This type of cell death is referred to as necrosis.

Death by suicide: Cells that are induced to commit suicide shrink since they are destined to be phagocytosed [Ohta and Ishibashi, 1999; Saraste and Pulkki, 2000; Soria Gonzalez and Orea Solano, 2002], and shrinkage is considerable in volume with the removal of water that may concentrate toxic products in the cell [Ahmad *et al.*, 1999; Lang *et al.*, 1999]. Their mitochondria break down and cytochrome c is released into the cytoplasm [Denecker *et al.*, 2001]. They then develop bubble-like blebs on their cell surfaces. Chromatin (DNA and protein) degradation in their nuclei occurs [Parrish *et al.*, 2001]. The break down of the cell into small membrane-wrapped fragments is a subsequent step. There is also an exposure, on the surface of the plasma membrane, of the phospholipid phosphatidylserine, that is, under normal conditions, located to the inner layer. These cells are then packaged into vesicles, bound by the receptors on the phagocytic cells such as macrophages and dentrictic cells that then engulf the cell fragments [Cory and Adams, 2002]. The phagocytic

cells then secrete cytokines that serve to inhibit inflammation [Ziegler and Groscurth, 2004]. In a case where the morphological pattern of a dying cell is shown to be different from this one (the distinct one for apoptosis), then such cell is definitely exhibiting some other death mode other than apoptosis itself, i.e., necrosis, where the death pattern shows a different morphological features (figure 1.1). The pattern of the events that occurs in death by suicide is so orderly that the whole process is often referred to as a **p**rogrammed **c**ell **d**eath or PCD [Abraham and Shaham, 2004].

The membrane of aged erythrocytes is inclined to shrink, stick out, from vesicle and lose lipid asymmetry. Aged erythrocytes were eliminated by phagocytosis. Both of the events are very similar to those observed in apoptotic nucleated cells. This suggested that aging of erythrocytes is also a process of apoptosis [Pan *et al.*, 1998].

Recent data indicate that, in contrast to necrosis caused by very extreme conditions, there are many examples when this form of cell death may be a normal physiological and regulated (programmed) event. Various stimuli (e.g., cytokines, ischemia, heat, irradiation, pathogens) can cause both apoptosis and necrosis in the same cell population [Proskuryakov *et al.*, 2003].

The cellular machinery of programmed cell death turns out to be as intrinsic to the cell such as mitosis for an example. Although apoptosis has been well documented in nematodes, insects and mammals, it is not yet clear how early in evolution apoptosis
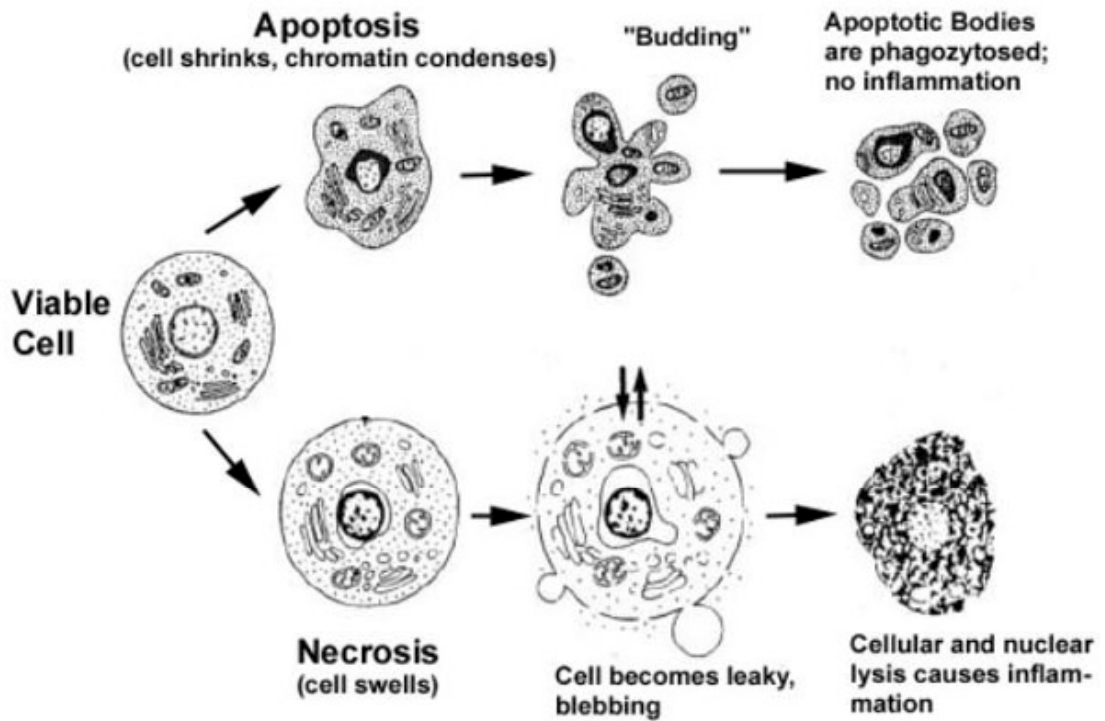
Figure 1.1: Apoptotic versus necrotic morphology. This depicts the Hallmarks of the apoptotic and necrotic cell death processes [Van Cruchten and Van Den Broeck, 2002].

or its component enzymes arose. In the simple metazoan *Hydra vulgaris*, cell death regulates cell numbers [Cikala *et al.*, 1999; Earnshaw *et al.*, 1999]. The importance of programmed cell death in various biological processes is a widespread phenomenon, which occurs in all kinds of metazoans [Tittel and Steller, 2000] such as in mammals, insects [Richardson and Kumar, 2002], nematodes [Liu and Hengartner, 1999], and cnidaria [Cikala *et al.*, 1999]. Moreover, programmed cell death also might play a role in plant biology [Solomon *et al.*, 1999], and apoptosis-like cell death mechanisms even have been observed and used as a model system in yeast [Skulachev, 2002; Frohlich and Madeo, 2000]. Programmed cell death is also an integral part of other unicellular eukaryotes and even prokaryotes sometimes undergo regulated cell death [Ameisen, 2002].

1.1.2 Reasons for a cell to be doomed or to commit suicide

There are about two reasons that differ:

Programmed cell death is as necessary for proper development as mitosis is. Metamorphosis into a frog acts as an example since the re-sorption of the tadpole's tail takes place by apoptosis. In vertebrates, removal by apoptosis of the tissue between fingers and toes of the foetus is required for their formation. In mammals, at the start of menstruation, the sloughing off of the inner lining of the uterus (the endometrium) occurs by apoptosis. In order for there to be the formation of the proper connections (synapses) between neurons in the brain, the surplus cells are eliminated by apoptosis. Other examples are the development of the brain, during
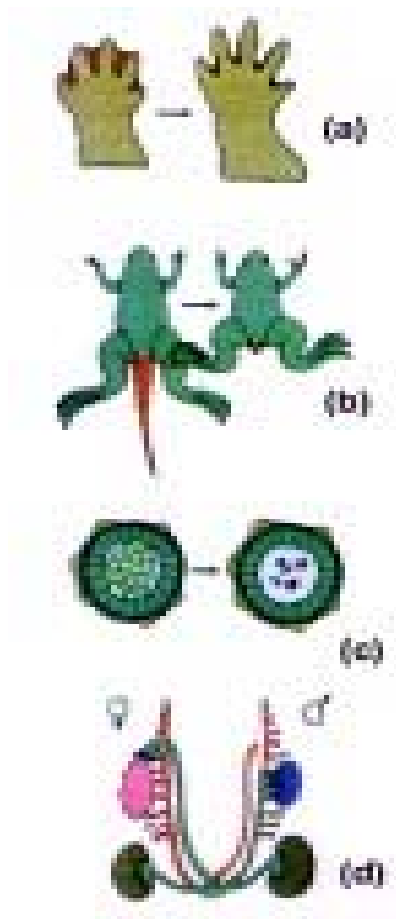
Figure 1.2: Apoptosis is involved in a variety of biological processes [Meier *et al.*, 2000; Vaux and Korsmeyer, 1999]. (a) Separate digits develop by tissue death during limb formation. (b) During metamorphosis, the unwanted tadpole tail is ablated (removed as no longer needed tissue). (c) Carving of hollow structures allowed by the downfall of cells. (d) Reproductive organs formation.

which half of the neurons that are initially created will die in later stages when the adult brain is formed [Hutchins and Barger, 1998, Nomura, 2004] and the development of the reproductive organs (figure 1.2) [Meier *et al.*, 2000]. Apoptosis is also a vital physiologic process in the ovary, and abnormalities in this process may lead to pathologic conditions [Palumbo and Yeh, 1995].

Programmed cell death is required to destroy cells representing a threat to the organism's integrity. Cells infected with viruses: One of the methods by which **c**ytotoxic **T** **l**ymphocytes (CTLs) kill virus-infected cells is by the induction of apoptosis. Cells of the immune system: The waning of the cell-mediated responses should be coupled with the removal of effector cells in order to prevent them from attacking the body constituents. CTLs induce apoptosis on each other. They also induce it upon themselves [Yeh, 1998]. Defects in the apoptotic machinery are associated with autoimmune diseases such as lupus erythematosus and rheumatoid arthritis. Cells with DNA damage: Damage to the cell's genome may lead to the disruption of proper embryonic development yielding birth defects. This damage may also cause a cell to be cancerous. Cells respond to damage by an increase in their p53 production, which potently induces apoptosis. There should not be any wonder that mutations in the p53 gene, producing a defective protein, are so often found in cancer cells (which represents a lethal threat to the organism). Cancer cells: Both chemicals and radiation utilised in cancer therapy induce apoptosis in some types of cancer cells [Gilman *et al.*, 2003; Ho *et al.*, 2003; Palumbo and Yeh, 1995; Yeh, 1998].

1.1.3 What happens when there is too much or too little apoptosis occurring in the body?

The physiological role of apoptosis is crucial and the malfunctions in this process may be detrimental since they have pathological consequences. Too little apoptosis results in cancers (it is widely accepted that some cancers are caused by cells not dying, rather than by a greater rate of proliferation), autoimmune diseases, and spreading of viral infections. Corruption of the machinery, that senses or implements DNA damage greatly influences cancer [Barisic *et al.*, 2003, Evan and Littlewood, 1998]. While too much apoptosis possibly plays a role in stroke damage or neuro-degeneration of Alzheimer's and Parkinson's diseases, which are consequential to excessive, premature apoptosis of neurons in the brain. The remaining neurons have no capability for regeneration to make up for the loss. AIDS and ischaemic diseases are also caused or enhanced by excessive apoptosis. In addition, dysregulated apoptosis signaling may intrude on other age-related disorders such as osteoporosis and atherosclerosis and perhaps on the process of aging itself [Barisic *et al.*, 2003, Deigner, 2000; Fadeel, 1999]. The manipulation of apoptosis thus has a potential for the treatment of diseases. Refining an understanding of the apoptotic mechanisms may aid in the research of novel effective drugs such as drugs for cancer combat.

1.1.4 Not All Programmed Cell Deaths Are Apoptotic

There may be several ways in which apoptosis may be triggered. In all cases, an initial event would prime or program the target cell, so that, apoptosis would be

triggered by the binding of antigens or super-antigens to the cell's T-cell receptors, which is not the case in other cell deaths [Chambers and Allison, 1999; Cohen, 1993; Gerschenson and Rotello, 1992; Haslett, 1999; Kerr *et al.*, 1972; Saraste and Pulkki, 2000].

1.1.5 What makes a cell make-up a decision to commit suicide?

There are two reasons for a cell to decide to prompt its own destruction: (i) the withdrawal of positive signals that are required for prolonged survival and (ii) the receipt of negative signals. **Withdrawal of positive signals:** The prolonged survival of most cells requires that they receive continuous stimulation from other cells and, for many, a continued adhesion to the surface on which they are growing. Some of the examples of positive signals are growth factors for neurons, and **i**nter**l**eukin-2 (IL-2), an essential for the mitosis of lymphocytes. **Receipt of negative signals:** These negative signals include (i) increased levels of oxidants within the cell, (ii) damage to DNA by these oxidants or other agents like ultraviolet light, X-rays and chemotherapeutic drugs, and (iii) the molecules that bind to the specific receptors on the surface of the cell to mark the beginning of the apoptosis program. These death activators include: (i) **T**umor **n**ecrosis **f**actor -α ("TNF") that binds the TNF receptor. (ii) Lymphotoxin (also referred to as tumor necrosis factor –β) that also binds the TNF receptor. (iii) **Fas l**igand (FasL), a molecule that binds the cell surface receptor known as Fas (also referred to as CD95) [Brossart and Bevan, 1996; Esser *et al.*,

1996]. After binding of FasL, the death receptor, Fas, assembles a **d**eath-**i**nducing **si**gnaling **c**omplex (DISC) [Ashkenazi A, 2002].

1.2 The Apoptosis Machinery

Intracellular regulators of apoptosis

The study of the mutations of the genes that are involved in apoptosis in the development of *Caenorhabditis elegans (C. elegans)* has identified two lethal genes, viz.; *ced-3* and *ced-4* (**c**ell d**e**ath **d**efective), essentials for cell death, and a gene for survival, *ced-9*, which is responsible for the prevention of death. Ced-3 is homologous to a mammalian protein called **i**nterleukin-1-B-converting **c**aspase **e**nzyme (ICE) [Cuende *et al.*, 1993]. Ced-9 inhibits apoptosis by binding to and thus neutralising ced-4, an activator of the caspase ced-3. Ced-3, a cysteine protease, cleaves certain proteins after a specific aspartic acid residue. It exists as a zymogen that is activated through self-cleavage. It is similar in sequence to the product of mammalian proto-oncogene Bcl-2 (**B c**ell **l**eukaemia-**2**). The fourth of the *C. elegans* genes is *egl-1* (**e**xternal **g**erminal **l**ayer-1), which is a pro-apoptotic gene that has a structural and functional similarity to the vertebrate *Bcl-2* gene family (figure 1.3). Egl-1 binds to ced-9 and disrupts the association between ced-4 and ced-9.

Mutations that yield either the inactivation of *ced-3* or *ced-4* result in the survival of almost all the cells that normally die during development [Hengartner, 1996; Henkart, 1995]. A third type of gene, *reaper* (*rpr*) encodes a protein that activates the death
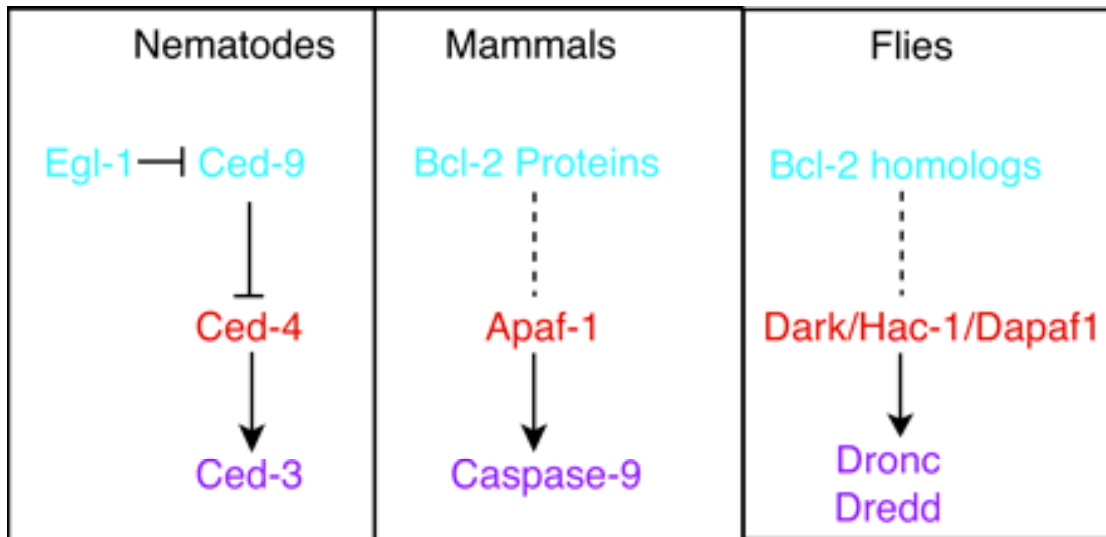
Figure 1.3 Schematic representation of conserved elements of the cell death machinery in nematodes, mammals and flies. The order of gene action is based on models established in the nematode, *C. elegans* [Chen and Abrams, 2000; Metzstein *et al.*, 1998].

program in *Drosophila*, but appears not to be directly involved itself. In *C. elegans*, there are additional genes that regulate later steps of the apoptotic process, such as cell engulfment and degradation. Genes that may be classified as sensors/triggers ("*reaper*-like"), effectors ("*ced-3/ced-4*-like"); and survival factors ("*ced-9*-like") have been identified in mammals [Hengartner and Horvitz, 1994; Hengartner *et al.*, 1992, Horvitz *et al.*, 1994, White, *et al.*, 1994]. Genetic regulation of apoptosis is surprisingly similar in nematode and vertebrate neurons [Putcha and Johnson, 2004]. In mammals, the ced-9 homologues Bcl-2 and Bcl-xL also block apoptosis by interfering with the activation of ced-3-like caspases [Conus *et al.*, 2000, Igaki and Miura, 2004]. Homologues have been identified in *Drosophila*, for ced-3, ced-4 and ced-9. Ced-9 belongs to the Bcl-2 family, which includes negative (Bcl-2) and positive (Bax: **B**cl-2 –**a**ssociated **x** protein) regulators of apoptosis. *Ced-4* gene encodes a protein that is primarily expressed during embryonic development and is homologous to mammalian *Apaf-1*. A *Drosophila* homologue of *ced-4* gene, *HAC-1,* has been identified [Schwartz *et al.*, 1993; Schwartz and Osborne, 1993]. HAC-1 has been shown to function during the embryonic development and radiation induced apoptosis. Loss of HAC-1 function yields reduced cell death. The recently discovered Bcl-2 family member named Drob-1 acts as a positive regulator of cell death [Gaumer *et al.*, 2000].

Ced-4 may interact with both ced-3 and ced-9. The binding of ced-4 to ced-3 leads to the activation of ced-3, while ced-9 binds to ced-4 and prevents it from activating

ced-3. Under normal conditions ced-9 complexes with ced-4 and ced-3, keeping ced-3 inactive. Apoptotic stimuli cause the dissociation of ced-9, thus allowing ced-3 activation and thereby committing the cell to apoptosis. Ced-4 promotes ced-3 activation by promoting proced-3 aggregation. Ced-4 interacts not only with ced-9 and ced-3, but also with itself. By interacting at the same time with proced-3 and with another ced-4 molecule, ced-4 brings multiple proced-3 molecules into close apposition.

Genetic experiments suggest that both *ced-3* and *ced-4* genes have to be expressed by those cells that are targeted to die, which indicates that the dying cell has an essential role in its demise being carried out. This suggests that apoptosis in *C. elegans* is a suicide process and it comes from the inside [Adams and Cory, 2002; Cecconi, 1999; Chinnaiyan *et al.*, 1996; Jacobson *et al.*, 1997; Metzstein *et al.*, 1998; Rodriguez *et al.*, 1998; *Weil et al.*, 1997].

1.2.1 How the Death Sentence is Delivered

The *Drosophila* genetic studies have led to the identification of a *reaper* gene. This gene plays a central role in cell death being initiated. The transcripts of this gene are found in doomed cells, and their presence precedes the morphological manifestations of apoptosis by one or two hours. The *reaper* gene is apparently encoding a small peptide without any homologies to known proteins in other species. The deletions of reaper suppress apoptosis in response to apoptotic stimuli. The reaper mutants thus

contain many extra cells. The reaper embryos have an intact apoptotic pathway that fails to be initiated. This gene is thought to integrate the information from diverse signalling pathways and put a cell on the apoptotic pathway. *Drosophila* activators of apoptosis mapping to the reaper region function, in part, by antagonising IAP (**i**nhibitors of **ap**optosis) proteins [Chen *et al.*, 2004].

Death inducers reaper, grim and hid (**h**ead **i**nvolution **d**efective) relay signals to trigger caspase function. Grim maps between reaper and hid. The cell deaths induced by each of these proteins are preceded by caspase activation [Abrams, 1999; Chen *et al.*, 1996]. A novel *Drosophila* gene, *dredd*, which shares an extensive homology to all members of the caspase gene family had been identified. Cells specific for programmed death in development display a striking accumulation of *dredd* RNA that requires signaling by the death activators reaper, grim, and hid [Chen *et al.*, 1998].

Induction of the release of cytochrome c from the mitochondria is instigated by many environmental and therapeutic agents, which thus initiate apoptotic cell death by activating Apaf-1 (**a**poptotic **p**rotease-**a**ctivating **f**actor-**1**) [Cain, 2003]. This protein is a mammalian homologue of ced-4 [Ohta and Ishibashi, 1999], an essential protein involved in programmed cell death in the nematode *C. elegans*. Apaf-1, after cytochrome c activation, oligomerises to form the Apaf-1 apoptosome, which is a caspase-activating complex. Caspase-9, an initiator caspase, is then recruited to the

complex by binding to Apaf-1 through CARD-CARD (**ca**spase **r**ecruitment **d**omain) interactions to form a holoenzyme complex. Subsequently, the Apaf-1/caspase-9 holoenzyme complex recruits the effector caspase-3 via an interaction between the active site cysteine in caspase-9 and the critical aspartate, which is the cleavage site that generates the large and small subunits of caspase-3 that constitute the activated form of caspase-3. This results in the initiation of the caspase cascade that is responsible for the execution phase of apoptosis [Cain, 2003].

1.2.2 Why Do Some Cells Die and Others Survive?

There is evidence from work on higher organisms that the intrinsic signals may protect cells from apoptosis by suppressing the suicide program. As an example, the survival of the developing neurons may be dependent upon neurotrophic factors that are secreted by their targets. Failure to receive a sufficient stimulation results in death. The advantage of the organism using extrinsic signalling to sustain cell survival entails one possibility, that it could provide a simple system for the elimination of cells that end up in the wrong place; without a signal to sustain them, the rogue cells would be eliminated [Raff, 1992]. When the primodial germ cells are taken as an example, in mammals, they originate in the hindgut and should migrate to the genital ridges, where they form the gametes. Those failing to reach the genital ridges are eliminated, presumably since they are deprived of the signal that is a requirement for their survival in the genital ridges [De Felici and Pesce, 1994].

A disadvantage of the mechanism that necessitates signalling for the prevention of apoptosis is that its failure, yielded by mutations, leads to the survival of unwanted cells, which paradoxically may lead to death of the organism itself. On the other hand though, there is an opportunity being presented by such mechanisms to allow the investigators to devise a means to target the unwanted cells for destruction, an example of which being the one presented by prostate cancer. The survival of the prostate cells depends on androgens; androgen depletion leads to the reduction in cell number by apoptosis. Recently, the dependence of prostate cells on the androgens to avoid cell death has been exploited therapeutically by the use of androgen ablation to invoke apoptosis in prostate cancer. Significantly resistance to androgen depletion correlates with the over expression of bcl-2, the human ced-9 homologue that acts to facilitate the brake-on of prostate cancer cell apoptosis. Thus the escape from androgen sensitivity by over expression of bcl-2 in a subset of prostate cancer cells leads to the proliferation of these cells and, ultimately, to the death of the patient. If bcl-2 could be down regulated, apoptosis of these cells could be invoked and the cancer controlled. Ironically, there may be an inverse correlation between cell death and the survival of the organism. Exploitation of this relationship is known to be holding much promise for the therapeutic control over diseases such as cancer [Bruckheimer *et al.*, 2003; Catz and Johnson, 2003; Rich *et al.*, 2000; Stein, 1999].

1.2.3 The apoptosis cascade

Apoptotic death is yielded by a complex cascade of incidences that eventually lead to the disassembly of the nucleus and that of the cell itself. This cascade can be divided into three stages that follow each other in sequence. These are initiation, execution and apoptotic death. During initiation, the cascade is induced and this leads to the first proteolytic events. Execution starts with the activation of execution caspases, where their activation is a "point of no return" since once carried out, the activation of these proteases leads to the degradation of a variety of proteins, the end result of which being irreversible damage to the cell. The cell does not release intracellular components even at this stage, thus the avoidance of the inflammatory response (figure 1.4) [Huppertz *et al.*, 1999].

1.3 CTL-KILLING

Cytotoxic **T** **L**ymphocytes (CTLs) are the key effectors in the cell-mediated immunity that destroys cells infected by viruses. After the adherence of the targeted cell to the CTL, their plasma membranes assimilate and the cytolytic granules migrate toward the contact site, thereby releasing their contents into the minute space between the cell membranes at the contact zone [Ju *et al.*, 1995]. This secretory process yields the basis of the lethal action of granule-mediated cytotoxicity. It is postulated that the molecules that are contained within the cytoplasmic granules are lytic effectors that bring about the targeted cell's apoptosis [Ju *et al.*, 1995, Peter and Krammer, 1998; Schulze-Osthoff *et al.*, 1998].

APOPTOSIS CASCADE

other inducers

induction via ligand-receptor interactions

initiation stages

PS-flip

DISC formation

proforms of initiator caspases

blebbing

active initiator caspases

degradation of actin, fodrin

bcl-2 family

APAF

bcl-2 family

proforms of execution caspases

execution stages

IAP

active execution caspases

shift of proteins

activation of nucleases

degradation of nuclear proteins

degradation of DNA

degradation of catenin, cytokeratin 18, Fak

apoptotic death

nuclear collapse

cellular collapse

Figure 1.4: The initiation, execution and apoptotic death stages of the apoptotic cascade. The effectors of apoptosis include the caspase family of proteases, which are selectively activated in a stimulus-specific and tissue-specific fashion [Papaconstantinou et al, 2001].

1.3.1 The mechanism by which the cytotoxic lymphocytes kill the targeted cells.

$CD8^+$ cytotoxic lymphocytes and lymphokine-activated killer cells depend on the perforin/granzyme system to kill their targets, while $CD4^+$ T cells employ Fas and other mechanisms to induce cell death [Aung and Graham, 2000]. The molecular mechanisms utilised by these pathways to induce apoptosis may converge on common death substrates. There are three mechanisms: viz., cytotoxic lymphokines, calcium-dependent and calcium-independent contact-dependent cytotoxicity. The contact-dependent mechanisms of cytotoxic-lymphocyte-induced death: The calcium-dependent mechanism relies on the secretion of cytotoxic granules onto the surface of the target cell and is thus called the granule exocytosis pathway. The calcium-independent pathway has now been shown to cause targeted cell death via the interaction of the Fas ligand on the CTL and the Fas receptor on the targeted cell [Ju *et al.*, 1995, Peter and Krammer, 1998; Schulze-Osthoff *et al.*, 1998].

After the activated T cell recognises its target, a tight junction is formed between the effector and the target cells, the CTL granules vectorially stream towards the contact site. At that site, the granules are thought to fuse with the effector T cell plasma membrane and the granule contents are directly exposed to the target cell membrane. C9 is a key terminal component of the complement cascade **m**embrane **a**ttack **c**omplex (MAC) [Johnson *et al.*, 1996]. One of the critical molecules of cytotoxic granules is perforin, a protein that is similar to some of the terminal components of the complement cascade. Perforin can polymerise, in the presence of calcium, to form

channel-like structures in the targeted cell membranes. The other key granule components are the granzymes, which are neutral serine proteases that activate the death machinery of appropriate targeted cells [Doherty *et al.*, 1997; Hahn *et al.*, 1994; Ju *et al.*, 1995; Mullauer *et al.*, 2001; Peter and Krammer, 1998; Schulze-Osthoff *et al.*, 1998].

1.3.2 The models of the perforin/granzyme and Fas systems

Granzymes belong to the serine proteases family. They are synthesised as zymogens and converted into active enzymes after cleavage of the leader peptide which result in a pro protein being formed. The pro-protein is then cleaved further [McGuire *et al.*, 1993]. All granzymes cleave at different specific sites. Granzymes A, and K display trypsin-like activity whereas granzyme H display chymotrypsin-like activity and granzyme M displays elastase-like activity [Pham *et al.*, 1998; Tooze *et al.*, 1991].

Granzymes play specific roles in apoptosis. Granzymes A and B are involved in apoptotic processes that lead to DNA damage and/or fragmentation, even if, they use alternative pathways [Darmon *et al.*, 1995]. In comparison to granzymes A and B, the role for the highly purified granzyme M in target cell lysis in combination with suboptimal levels of perforin has not been demonstrated yet [Smyth *et al.*, 1996]. One hypothesis has it that granzyme M may facilitate damage to virus during target cell destruction, which in turn can reduce the level of infection of *Ectromelia* virus. Viruses often encode various protease inhibitors that presumably benefit viral

replication by the inhibition of granzymes and caspases involved in target cell destruction [Sayers *et al.*, 2001].

It is a widely accepted that the granule-mediated killing by cytotoxic lymphocytes is initiated by the pore-forming molecule, perforin, thus facilitating the granzyme B entry into the targeted cell. In the presence of Ca^+, perforin polymerises and may form channels through which the granzymes may enter the target cell [Waterhouse and Trapani, 2002; White *et al.*, 1994].

Pore formation by perforin and the entry of granzymes through perforin formed pores

Recent *in vitro* experiments suggest that granzymes may sometimes enter target cells without passing through a perforin channel but the relative importance of this pathway *in vivo* is currently unknown [White *et al.*, 1994]. After entering the target cell, the granzymes are thought to pass into the cytoplasm of the cell, where they may act on the specific death proteases (caspases) involved with the ultimate death of the cell, and/or they are transported to the nucleus, where they may directly cleave and activate critical death substrates. Granzyme A and Granzyme B directly target critical caspase substrates in caspase-resistant cells [Behrens *et al.*, 2001; Isaaz *et al.*, 1995; Pinkoski *et al.*, 2001; Saunders, 1966; Schulze-Osthoff *et al.*, 1998; Waterhouse and Trapani, 2002; White *et al.*, 1994; Zhang *et al.*, 2001].

Microinjection of granzyme B directly into the cytoplasm of target cells resulted in apoptosis without the necessity of a second stimulus. This suggested that the key event is the presence of granzyme B in the cytoplasm, and that when the enzyme is internalised by a target cell, it streams to an intracellular compartment and accumulates until its release is stimulated by the addition of perforin [Pinkoski *et al.*, 1998].

CTL-killing through the Fas/Fas-ligand pathway

There are two different pathways documented through Fas. In one pathway, the death signal is disseminated by a cascade of caspases initiated by the activation of large amounts of caspase-8 at the DISC, followed by a rapid cleavage of caspase-3 and other caspases, which, ultimately cleave vital substrates in the cells (figure 1.5) [Cikala *et al.*, 1999; Earnshaw *et al.*, 1999; Varfolomeev, *et al.*, 1998; Vaux *et al.*, 1997; Yeh, *et al.*, 1998]. Another pathway is instigated by positively rescued cells, where a signaling pathway through CD40/CD154 is activated [Guzman-Rojas *et al.*, 2002].

The Fas system employs the Fas receptor, a member of the **t**umor **n**ecrosis **f**actor (TNF) family of death receptors and the Fas ligand, a membrane-associated ligand [White *et al.*, 1994]. Display of the Fas ligand on the T cell surface makes it feasible for the Fas ligand to interact with Fas receptors on the surface of target cells. Engagement of the Fas receptor results in the association of its intracellular death
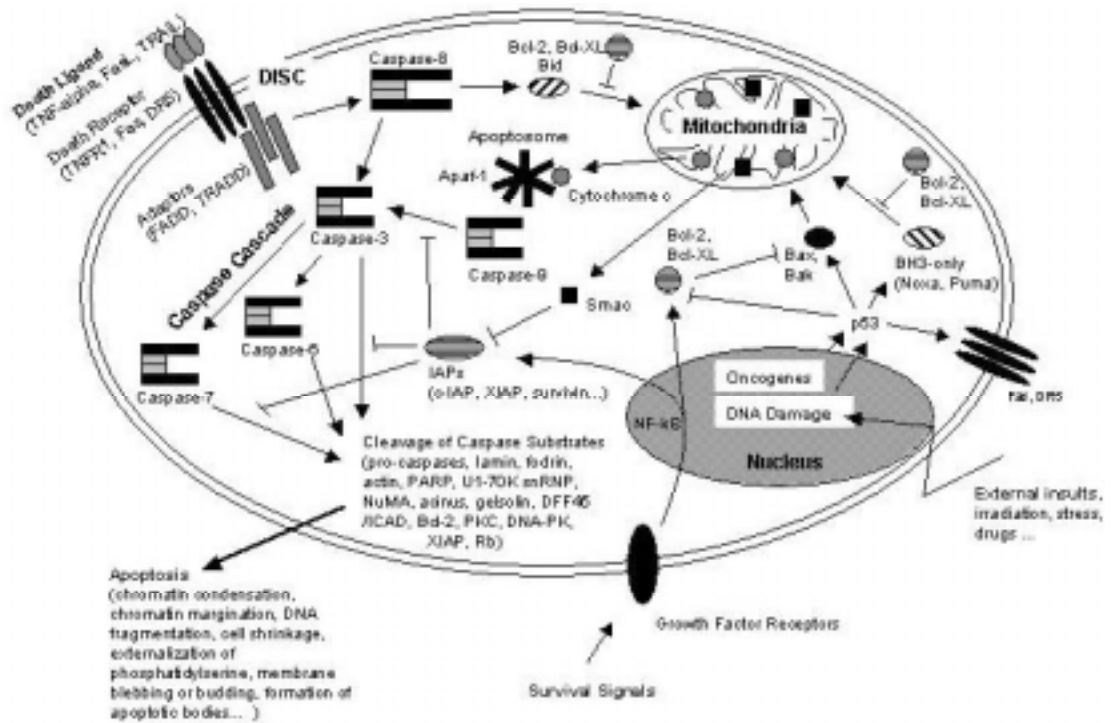
Figure 1.5: The pathways of caspases activation during apoptosis [Budihardjo et al, 1999].

domains, leading to the recruitment of the adaptor **F**as **a**ssociated **d**eath **d**omain (FADD) and procaspase-8 to form a **d**eath-**i**nducing **s**ignalling **c**omplex (DISC). In the DISC, FADD and Fas interact via their **d**eath **d**omain (DD), procaspase-8 then associates with FADD via the **d**eath **e**ffector **d**omains (DED) of these two molecules. Procaspase–8, a member of the caspase family of cysteine proteases, is then activated by the proteolytic cleavage after specific **asp**artic acid (Asp) residues, ultimately leading to the activation of procaspase-3. Activated caspase-3 then can cleave an inhibitor molecule that is tightly associated with a nuclease known as **c**aspase-**a**ssociated **D**Nase (CAD). Upon cleavage, the **i**nhibitor of **CAD** (ICAD) releases the nuclease from the CAD-ICAD complex, thereby allowing the nuclease to initiate DNA fragmentation and cause the ultimate demise of the cell [Behrens *et al.*, 2001; Isaaz *et al.*, 1995, Lee *et al.*, 2004; Saunders, 1966; Schulze-Osthoff *et al.*, 1998: Trapani, 2001,White *et al.*, 1994].

Several other proteins, such as intracellular signaling proteins (CAP1-4) have been described which bind to activated Fas and the DISC (**d**eath-**i**nducing **s**ignaling **c**omplex) but their precise roles and importance in apoptosis are not yet fully characterised. In the DISC, CAP1 and CAP2 represent FADD. CAP4 was identified as an ICE-like protease, FLICE, with two **d**eath **e**ffector **d**omains (DED) [Medema *et al.*, 1997].

Deficiency States of Cytotoxic Factors

The study of the deficiency states of the individual factors that may be important in the mediation of, or protection from, cytotoxicity makes it possible to obtain information on the pathophysiological importance of the effector molecules.

Perforin Deficiency

Mice that are deficient of this granule component are unable to clear **l**ymphocytic **c**horio**m**eningitis **v**irus (LCMV) infections that are normally eliminated by the CTL. The immunogenic tumors and tumors producing **i**nter**l**eukins (IL)-2 that are normally rejected, grow and kill mice that are perforin deficient [Reed, 1994]. Perforin-deficient mice were considerably more susceptible to tumor initiation by methylcholanthrene than granzyme A and/or B-deficient mice [Davis *et al.*, 2001].

Granzyme B Deficiency

Before the *in vivo* studies of this deficiency were reported a decade ago, it was anticipated that certain viral infections required a control by granzyme-mediated nuclear breakdown [Reed, 1994]. From tissues of granzyme B-deficient mice following intraperitoneal infection, virus clearance was impaired compared with control mice; however, the virus was ultimately eliminated. Clearance of lymphocytic choriomeningitis virus is delayed in the absence of granzyme B expression, but other CTL effector molecules can compensate for the absence of this granule constituent *in vivo* [Zajac *et al.*, 2003].

It is still controversial in regard to the biological role of granzyme serine proteases released with perforin from the cytotoxic granules of NK cells and CTL [Smyth *et al.*, 2003]. Splenocytes and allogeneic CTL of granzyme A and/or B-deficient mice were defective for induction of DNA fragmentation, but induced significant membrane damage and target cell death. Granzymes A and B are thus not critical for most anti-tumor effector functions of NK cells and CTL that are perforin mediated [Davis *et al.*, 2001]. Granzymes A and B have been shown to be critical for NK granule- mediated nucleolysis, with granzyme B being the main role player, while target cell lysis is due exclusively to perforin and independent of both proteases [Simon *et al.*, 1997, Smyth *et al.*, 2003].

Fas and Fas Ligand Deficiency

Based upon phenotype, these two deficiencies have almost identical biological results that include the development of polyclonal lymphoproliferative disorder that leads to the gross enlargement of the peripheral lymphodes; development of an autoimmune disease with a lupus-like syndrome; and early death. Lack of Fas or of Fas ligand expression results in the uncontrolled proliferation of activated T cells and the failure to eliminate them by programmed cell death [Reed, 1994], whereas its aggravation may cause tissue destruction [Nagata and Goldstein, 1995]. Germline deletion of the FasL gene, obtained after mating with mice expressing ubiquitous Cre recombinase mice exhibited an extreme splenomegaly and lymphadenopathy associated with

autoimmune disease. This severe phenotype led to the premature death [Karray *et al.*, 2004].

Bcl-2 Deficiency

The blockage of anti-apoptotic activity of Bcl-2 or its homologues triggers apoptosis [Bouillet *et al.*, 2001; Zhang *et al.*, 2001]. Bcl-2 thus prolongs cell survival [Vaux *et al.*, 1998]. Down-regulated levels of Bcl-2 resulted in increased apoptosis of lymphocytes [Ohman *et al.*, 2002]. The action of bcl-2 results in the protection of cells against apoptotic signals and against growth factor withdrawal, including IL-2. Inappropriate or over-expression of bcl-2 causes survival of cells normally destined to die and might thereby contribute to cancer. Conversely lack of bcl-2 results in premature death of cells that survive under normal conditions.

One of the consequences of bcl-2 deficiency is the loss of peripheral lymphocytes in the first few months of life. Regarding lymphocyte survival, bcl-2 seems to fulfill the opposite function of Fas/Fas ligand. The lack of the protecting factor results in the preponderance of the effects of Fas and the loss of cells and peripheral lymphocytes. This example supports the notion that Fas and bcl-2 play their roles at different stages of the pathway in the process of maintaining homeostasis of T cell proliferation and apoptosis. Deficiency of one component leads to the prevalence of the other and the subsequent dire consequences of either premature T cell death (bcl-2 deficiency) or lympho-proliferation and autoimmunity (deficiency of Fas/Fas ligand).

The combination of perforin with granzymes renders the attacked cells helpless in their attempt to repair the damage and is able to overcome the resistance of noncompliant (cells resisting apoptosis), parasitised cells. Death induced via the Fas ligand and its control by bcl-2 depends on target compliance and is primarily used to control and limit normal cell proliferation [Figueroa B Jr, 2001; Hoyes *et al.*, 2000; Reed, 1994].

1.4 Caspases

Caspase is a general term used for all the ICE-like family of aspartic-specific cysteine proteases (**c**ysteine **asp**artic-specific prote**ases**). These proteases employ cysteine as the nucleophilic group in their active sites to cleave peptide bonds C-terminal to aspartic acid residues within proteins. In the apoptotic pathways, the caspases are responsible for cell disassembly in the response to the pro-apoptotic signals [Thompson, 1995]. The caspases are amongst the most specific proteases, with an unusual and absolute requirement for cleavage after aspartic acid [White *et al.*, 1994; Nicholson, 1999].

The Role of Caspases in Apoptosis

Amongst their roles, the caspases inactivate proteins that protect the living cells from apoptosis. One example of which being the cleavage of ICAD, which serves to inhibit the nuclease responsible for DNA fragmentation referred to as **c**aspase-**a**ctivated **d**eoxyribonuclease (CAD). During apoptosis, ICAD is inactivated by caspases,

leaving CAD free to serve its role as a nuclease. Some other negative regulators of apoptosis that are cleaved by caspases are bcl-2 proteins [Hockenbery *et al.*, 1993]. Caspase-3 is known to cleave bcl-2. [Grunenfelder *et al.*, 2001; Kirsch *et al.*, 1999]. Cleavage inactivates these proteins, and it also produces a fragment that promotes apoptosis. Caspases contribute to apoptosis through a direct disassembly of the structure of the cell [Takahashi *et al.*, 1994]. During apoptosis, nuclear lamins, which maintain the structural integrity of the nuclear envelope [Zhang *et al.*, 2001], are cleaved at a single site by caspases, resulting in lamin collapse and thus contributing to the condensation of chromatin, which is a characteristic morphology of an apoptosing cell.

Granzyme B, the most powerful pro-apoptotic member of the granzyme family, like caspases, can cleave proteins after acidic residues, especially aspartic acid [Trapani, 2001], however, the specificities of granzyme B and the caspases are different. The precise nature of the interaction between the granzyme and the caspase pathways is not yet clear [Behrens *et al.*, 2001; Isaaz *et al.*, 1995, Saunders, 1966; Schulze-Osthoff *et al.*, 1998: White *et al.*, 1994]. Granzyme B induces apoptosis by means of perforin perforating the target cell's membrane. This results in osmotic swelling and activates caspase-3 to instigate cascade of caspases [Mullauer *et al.*, 2001]. This brings about the destruction of the targeted infected cells.

The table below lists the main caspases and some of their substrates and roles:

CASPASE	ALTERNATIVE NAME	SUBSTRATES	ROLE
Caspase-1	ICE	Pre-Interleukin-1b Lamins	Processing of interleukins. Can also induce apoptosis.
Caspase-2	Ich-1 (human) Nedd2 (rat, mouse)	Golgin-160	Apoptosis
Caspase-3	CPP32, YAMA, apopain	PARP Caspases-6, 7, 9 DNA-PK MDM2 Fodrin Lamins Topoisomerase I ICAD	Apoptosis
Caspase-4	Ich-2, ICE (rel)II	Caspase-1	Inflammation/Apoptosis
Caspase-5	ICE(rel)III	?	Inflammation/Apoptosis
Caspase-6	Mch2	PARP Lamins NuMA FAK Caspase-3	Apoptosis
Caspase-7	Mch3, ICE-LAP3, CMH-1	PARP Gas2 SREB1 EMAP II FAK Calpastatin	Apoptosis
Caspase-8	FLICE, MACH, Mch5	Caspases-3, 4, 6, 7, 9, 10, 13 PARP Bid	Apoptosis (death receptors)
Caspase-9	Apaf-3, ICE-LAP6, Mch6	Caspase-3, 7 Pro-caspase-9 PARP	Apoptosis
Caspase-10	FLICE-2, Mch4	Caspases-3, 4, 6, 7, 8, 9	Apoptosis (death receptors)
Caspase-11	Ich-3, ICE-B	?	Inflammation and apoptosis
Caspase-12	ICE-C	?	Apoptosis
Caspase-13	ERICE	?	Inflammation

Table 1.2: Caspase types and their role.

1.5 DWNN

DWNN (**D**omain **W**ith **N**o **N**ame), a novel protein domain that has a possible role in apoptosis and CTL-killing, consists of 76 residues that constitute a highly conserved domain and was recently identified in our laboratory, using promoter-trap mutagenesis [George, DPhil thesis, Oxford, 1995]. This technique was carried out upon CHO cells. DWNN knockout confers resistance to cytotoxic T-cell (CTL) killing and staurosporine-induced apoptosis, suggesting a probable task for the gene in CTL killing and apoptosis [George, 1995]. The alleged role is thus promotion of programmed cell death. Close homologues were identified in all the eukaryotic genomes examined, including plants (figures 1.6 and 1.7) [Rees *et al.*, unpublished data]. Though there are two copies in *Arabidopsis*, the domain occurs at only a single-copy in most completely sequenced genomes. Two major transcripts had been isolated from humans. One of them is a DWNN mRNA. The human DWNN gene encodes two overlapping proteins, termed DWNN-13 and DWNN-200 to date. The 1.1 kb mRNA encodes a 118 residue protein ($DWNN_{118}$) containing a highly conserved domain and a hydrophobic C terminal tail. The *DWNN* gene consists of 18 exons and exon 16 is alternatively spliced. Human DWNN consists of two promoters and at least six mRNA transcripts. Human DWNN and RbBP6 are adjacent on chromosome 16.

DWNN homologues associate with a number of other conserved domains. These include a zinc finger (CCHC), a RING finger (C3HC4) and [RBQ1] (p53-associated cellular protein testes-derived) domain: highly homologous to PACT (Sakai *et al*.,

```
DWNN-Arabidopsis-4        1:  . . MAI YYKFKSARDYDTI SMDGP. FI TVGLLKEKI YETKHLGSGKDLDI V : 47
DWNN-Medicago             1:  . . MAVYYKFKSAKDYNSI PMDGP. FI SVGTLKQSI FVSKHLGRGTDFDLL : 47
DWNN-Tomato               1:  . . MAVYI KYKSCKDYDSI PI LDH. FI SVGNLKSKI FESKRYGVGKDFDI L : 47
DWNN-Dictyostelium        1:  . . MSVHFKLKSEI DYDTVACEGG. FI SVADLKKFI QK. KRLGKSTDFDLL : 46
DWNN-Human                1:  . MSCVHYKFSSKLNYDTVTFDGL. HI SLCDLKKQI MGREKL. KAADCDLQ : 47
DWNN-Mouse                1:  . MSCVHYKFSSKLNYDTVTFDGL. HI SLCDLKKQI MGREKL. KAADSDLQ : 47
DWNN-Halocynthia          1:  . MSAI HYKFSSSNDYKNVTFDGL. SI SLLDLKKSI M REKL. KPTEVDLL : 47
DWNN-Drosophila           1:  . . MSVHYKFKSTLNFDTI TFDGL. HI SVGDLKREI VQQKRLGKI I DFDLQ : 47
DWNN-Saccharomyces        1:  MSGVI YYKFKSQKDPS RI TFDGTI GMSVFDVKREI I MQKKLGNGLDFDLL : 50
DWNN-Schizosaccharomyces. 1:  MS STI FYRFKSQRNTS RI LFDGT. GLTVFDLKREI I QENKLGDGTDFQLK : 49
DWNN-Arabidopsis-5        1:  . . MAI YYKFKSARDYDTI AMDGP. FI SVGI LKDKI FETKHLGTGKDLDI V : 47
DWNN-Candida              1:  MSSVVYYKFLHQKNKS VI HFDGT. SI SVFDLKKEI I LQNQLGSGQDFNLR : 49
DWNN-C.elegans            1:  . MSSI HYKFRAELDYKTLQFDGL. HI RGEQLVREI CAKENL. KLELFELQ : 47
DWNN-Chlamydomonas        1:  MASSI RFKFRAELSYSNLPFDGH. YI TVGELKRLI AERKGLGVDAANELQ : 49
DWNN-Cryptosporidium      1:  . . MAI YYKFKSEKKFKDLTHEFP. . ALVSHVRSKLREI LDI GEDMDI LAT : 46
```

```
DWNN-Arabidopsis-4        48:  I SNAQTN. . EEYLDEAMLI PKNTSVLI RRVPGRPRI RI : 83
DWNN-Medicago             48:  VTNAQTN. . EEYHDEEMLI PKNTSVLI RRVPGRPCLPI : 83
DWNN-Tomato               48:  LTNLQTN. . EDYVDHATLI PRSTSVLI RRVAGLPCFPI : 83
DWNN-Dictyostelium        47:  LTNSQTNE. EKYKDES FVI PKNTSVI VSRVPI VGNRS Y : 83
DWNN-Human                48:  I TNAQTK. . EEYTDDNALI PKNSSVI VRRI PI GGVKS T : 83
DWNN-Mouse                48:  I TNAQTI . . EEYTDDNALI PKNSSVI VRRI PI GGVKS Y : 83
DWNN-Halocynthia          48:  I TNAQSL. . QDYSDESTLI PKNTALLVRRI PLGAVPDT : 83
DWNN-Drosophila           48:  I TNAQSK. . EEYKDDGFLI PKNTTLI I SRI PI AHPTKK : 83
DWNN-Saccharomyces        51:  LYNANSN. . EEYDDDTFI I PRSTSVI VRRVPAQKSGK. : 85
DWNN-Schizosaccharomyces. 50:  I YNPDTE. . EEYDDDAFVI PRSTSVI VKRSPAI KSFS V : 85
DWNN-Arabidopsis-5        48:  VSNAQTN. . EEYLDEAMLI PKNTSVLI RRVPGRPRI TV : 83
DWNN-Candida              50:  LYHSEQPD. QEYELDQDVI PRSS YVLAKRSPAFVKLG. : 85
DWNN-C.elegans            48:  LQNAHTK. . KTYSDD. ELI PRNSSI I VQRFPRKDAAKV : 82
DWNN-Chlamydomonas        50:  LTDATSK. . RDYDNDAEQVMKNSAVI VRRVAGADKPTT : 85
DWNN-Cryptosporidium      47:  QSDKNGRVSNVYLSDYEI LKEGI YLNVVRLPKDLAKPL : 84
```

Figure 1.6: Sequence alignment of the unique and highly conserved DWNN domain from a range of eukaryotic genomes.

Figure 1.7: DWNN phylogenetic tree.

1995) (figure 1.8). Recent studies show that the RING fingers have a role in the regulation of proteins such as p53. This is due to a fact that these RING fingers catalyse the attachment of ubiquitin, which then serves to target them for degradation by the proteosomes. The cDNA that encodes a novel nuclear protein, designated PACT (p53-associated cellular protein testis derived) was isolated. This protein included a very basic lysine rich C terminus and a serine/arginine (SR) rich region. The human and mouse PACT domains are known to associate with Retinoblastoma (Rb) and p53, which are tumor suppressor proteins [Simons *et al.*, 1997].

P2P-R is a protein containing multiple domains including an N-terminal RING type zinc finger. P2P-R binds the p53 and the Rb1 tumor suppressors [Scott *et al.*, 2003]. P2P-R cDNA encodes protein domain involved in Rb1 binding and complement recent reports that localize Rb1 to sites of RNA processing in the nucleus [Witte and Scott, 1999]. Its function, amongst others, includes a role in apoptosis (P2P-R over-expression promotes apoptosis) [Gao *et al.*, 2002; Gao and Scott, 2003, Scott and Gao, 2002].

A search for known protein motifs in Mpe1p, an evolutionarily conserved protein, exposed a zinc knuckle between amino acids 182 and 195. A homology search on zinc knuckle led to an identification of genes from *S. pombe, A thaliana* and *D. melanogaster* in which Mpe1p domain is conserved. There is a region of Mpe1p that does not contain any known motifs. There is also a domain that has characteristic

Human 13 kDa DWNN ▪

Human 200 kDa DWNN ▪ Zinc Finger ▪ Ring Finger ▪ SR domain ▪ RbBP6 ▪ p53 binding

Figure 1.8: Domain arrangements of DWNN-containing proteins.

features of a RING finger [Aravind and Koonin, 2000; Vo *et al.*, 2001]. Results strongly suggest that Mpe1p is highly conserved and that a true human homologue occurs pending determination whether this human protein is the functional homologue of Mpe1p or if this protein takes on a different function in higher eukaryotic cells [Vo *et al.*, 2001]. One of the human cDNAs containing a conserved domain in Mpe1p codes for the RbBP6 protein, and it has been demonstrated that this protein interacts with the tumor suppressor pRB1 [Sakai *et al.*, 1995]. pRB1 is involved in cell differentiation and localises in the nucleus [Durfee *et al.*, 1994; Witte and Scott, 1997]. The sequence of the Mpe 1 protein includes the zinc knuckle, RING fingers and the N terminal $DWNN_{118}$ domain.
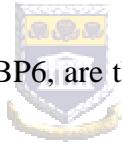
P2P-R, PACT and its homologue RbBP6, are thus all partial cDNA's of DWNN-200 (Fig 1.9).

Possible function of Proteins that contain DWNN

There are two possible functions suggested by a putative ubiquitin-like fold of DWNN: viz.: 1. Post-translational modification of target proteins: Ubiquitin and its structural homologue SUMO-1 become covalently bonded to target proteins through the action of specific enzymes referred generically as E1, E2 and E3. E3's, also referred to as "ubiquitin-ligases", typically contain RING (C3HC4) domains, which have an intrinsic ubiquitin-ligase activity. The presence of RING domains in RbBP6 (Rb-binding protein 6) and its murine homologue PACT (p53-associated protein),
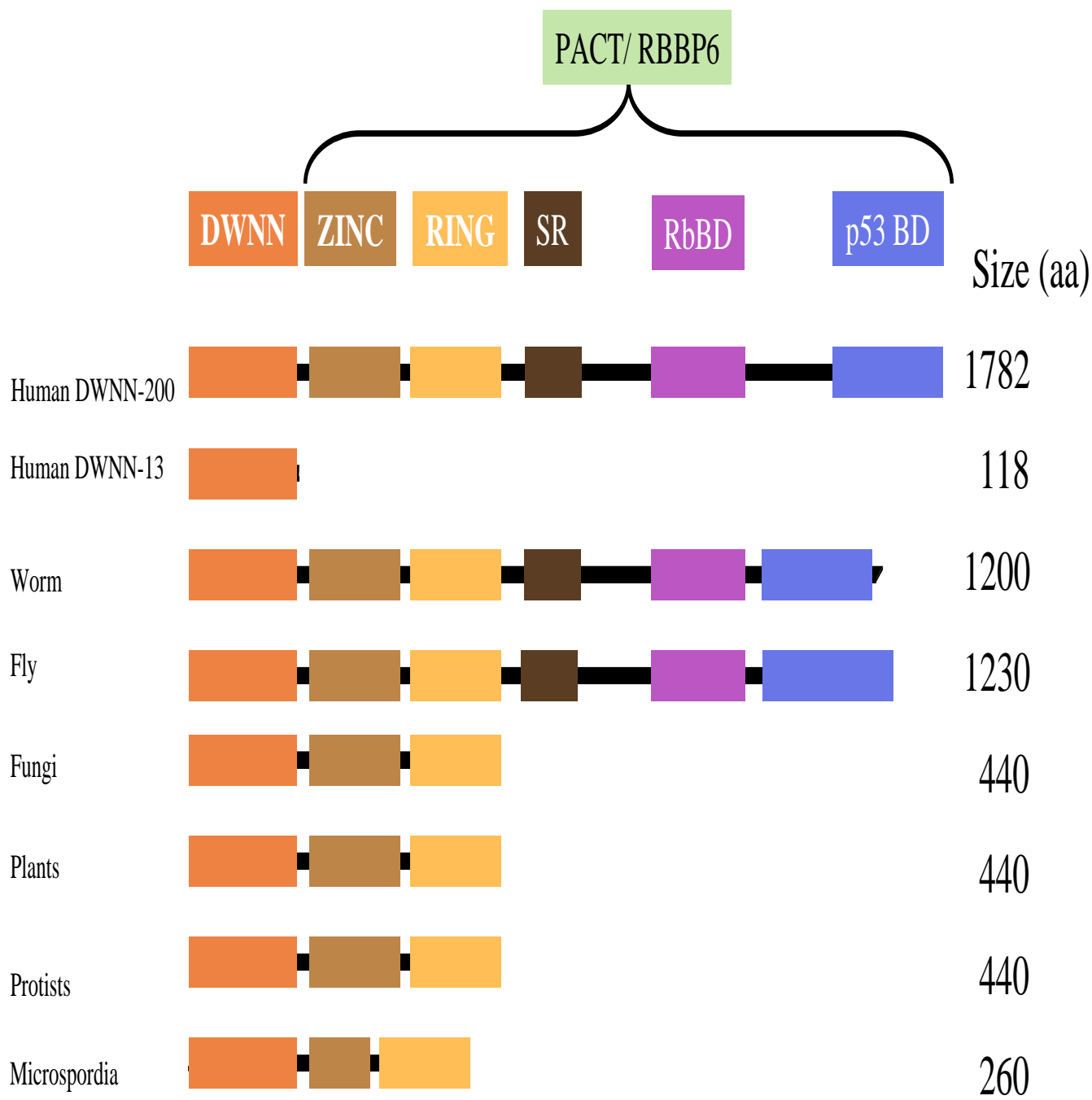
Figure 1.9: Domain arrangements of DWNN-containing proteins. BD = Binding.

which are both part of the DWNN-200, suggests that these proteins may serve as DWNN-ligases. The mode by which DWNN act in organisms in which it is covalently bonded to the PACT-homologue is not yet clear, hence the study that seeks to structurally and functionally characterise it.

2. <u>PACT domain is known to associate with tumor suppressors p53 and Rb:</u> DWNN proteins potentially function as p53 ubiquitin ligases. They may constitute a novel E3 ubiquitin ligase and play a role in regulating levels of p53 or Rb due to the presence of the RING finger domain, found in a number of E3 ubiquitin ligases where they target protein for degradation by catalysing the addition of ubiquitin-like proteins.

The presence of only one copy per genome means that dimerisation partners, if they exist, share little homology with DWNN. DWNN homologues are linked to a number of other conserved domains. The human homologue of PACT is the RbBP6 protein, which has been shown to bind to the product of the Retinoblastoma tumor suppressor gene. Following the "Rosetta Stone" hypothesis, it has been shown that the human DWNN is associated with RbBP6 *in-vivo* (Dlamini, unpublished). BLAST searches yield no significant homology between DWNN and any protein that is of a known structure. There is a current structure determination of the human DWNN domain by NMR in our laboratory. Secondary structure was predicted and confirmed to be consisting of α-helices and β-sheets. DWNN 3-D structure resembles that of ubiquitin [Pugh *et al*., unpublished].

Plants transformed to over-express DWNN are reported to severely have stunted growth and to develop defectively and appear bleached, while their untransformed counterparts look healthy and exhibit a healthy growth and development [Ludidi, MSc thesis, UWC, 2000]. The outcome suggests that DWNN over-expression leads to the induction of cell death programme. The DWNN knockout mutant plants showed a slightly more rapid growth rate than the wild type counterparts. These knockouts were reported to be taller, their leaves broader and their roots longer in comparison to the wild types. The absence of DWNN thus enhances the growth rate of the mutants presumably due to the suppression of regulated cell death. There are results suggesting a direct or indirect correlation between DWNN expression and cell death.

1.6 Green Fluorescent Protein

The green fluorescent protein, GFP, is a fluorescent protein that may be isolated from several bioluminescent coelenterates such as the pacific jellyfish *Aequorea victoria* [Miyawaki, 2002] or the sea pansy *Renilla reniformis* (these coelenterates emit green light from a green fluorescent protein). GFP's role is to yield a transduction, by energy transfer, of the blue chemi-luminescence of another protein into a green fluorescent light. The Green fluorescent proteins function as energy transfer acceptors, that receive energy from a Ca^{++} activated photoprotein or a luciferase-oxyluciferin in *A.victoria* and *R.reniformis*, respectively. When mechanically

stimulated, *A. victoria* emits green light, but when the photoprotein aequorin was purified from *A. victoria* photocytes, it generated blue, rather than green light. GFP thus act as a secondary fluorescent protein since it receives energy from the activated aequorin (figure 1.10) [Chalfie, 1995; Inouye and Tsuji, 1994]. It is suggested that radiation-less energy transfer is involved.

Fluorescent GFP is a useful reporter molecule for monitoring *in vivo* gene expression in eukaryotic and prokaryotic cells [Fortinea *et al.*, 2000]. It has been expressed in bacteria, yeast, slime mold, plants, *Drosophila*, zebrafish, and in mammalian cells. GFP may be exploited as a functional protein tag, in that it tolerates N-and C-terminal fusion to a wide variety of proteins, many of which have been shown to retain their native function [Chalfie, 1995; Chalfie, 1994; Cubitt *et al.*, 1995; Heim *et al.*, 1995; Liang *et al.*, 2003; Mitra *et al.*, 1996; Rosochacki, 2003; Ryu *et al.*, 2003].

Reporter genes such as GUS or GFP affect the biological properties of recombinant LMV (**l**ettuce **m**osaic **v**irus) isolates in both susceptible and resistant lettuce varieties when fused to the N-terminus of the viral protein [German-Retana *et al.*, 2003]. When wild type GFP is expressed into mammalian cells, its fluorescence is typically distributed throughout the cytoplasm and the nucleus. It is excluded from the nucleolus and vesicular organelles. Highly specific intracellular localisation including the nucleus, mitochondria, secretory pathway, plasma membrane and the cytoskeleton
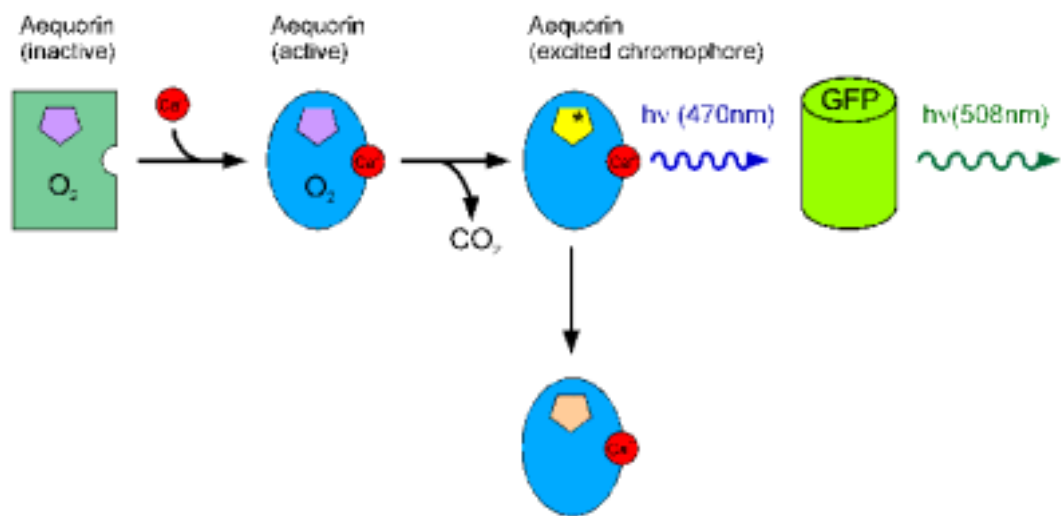
Figure 1.10: The figure summarises _A. victoria_ bioluminescence [Inouye and Tsuji, 1994].

may be achieved via fusions both to whole proteins and individual targeting sequences.

The enormous flexibility as a non-invasive marker in living cells allows for numerous other applications such as a cell lineage tracer, reporter of gene expression and as a potential measure of protein-protein interactions. The capability to detect multiple fluorescent proteins concurrently by flow cytometry provides the opportunity to distinguish non-invasively among various cell populations, or to assess gene function and monitor protein-protein interactions in individual cells. The combination of an enhanced blue-shifted emission variant of GFP termed enhanced cyan fluorescent protein and a red-shifted emission variant referred to as enhanced yellow fluorescent protein were found to be useful for this purpose [Chalfie, 1995; Chalfie, 1994; Cubitt *et al.*, 1995; Hawley *et al.*, 2004; Heim *et al.*, 1995; Mitra *et al.*, 1996].

The new variants of the wild type GFP (wt GFP) containing different mutations have been developed having characteristic properties, some of them being optimised for high expression in mammalian cells while others for use in the bacterial systems. The variants have usually a more intense fluorescence and may also have their own excitation and/or emission maxima [Cormack *et al.*, 1996, Delagrave *et al.*, 1995].

Physical and chemical studies on purified GFP have identified several important characteristics. GFP is shown to be highly resistant to denaturation requiring

treatment with 6 M guanidine hydrochloride at 90 ^{0}C or a pH of <4.0 or >12.0. Partial to near total renaturation takes place within minutes following reversal of denaturing conditions by dialysis or neutralisation [Bokman and Ward, 1981; Ward and Bokman, 1982].

1.7 Red Fluorescent Protein

The green fluorescent protein has, in the past few years, drawn much attention as a fluorescent marker in molecular and cell biology since it has an intrinsic chromophore and is capable of being inserted into cells at the DNA level. GFP has a setback though. This drawback is due to that its emission wavelength overlaps with the auto-fluorescence of many cells. This is partly why the mutants of GFP with red-shifted emission have been engineered.

In addition however, there is a new red fluorescent protein (DsRFP) that has recently been isolated from *Discosoma* reef coral. Due to its emission, DsRFP has a great potential as a marker for fluorescence experiments in cell biology. The structure of DsRFP is very similar to that of GFP [Cormack *et al.*, 1996, Delagrave *et al.*, 1995].

pDsRed1-C1

pDsRed1-C1 may be used as a means to construct fusion proteins to the C-terminus of DsRed1. In a case where a fusion construct retains the fluorescent properties of the native DsRed1 protein, its expression and localisation *in vivo* may be monitored by fluorescence microscopy and cytometry [Changsen *et al.*, 2003; Cormack *et al.*, 1996, Delagrave *et al.*, 1995]

1.8 PROTEIN TRANSDUCTION

1.8.1 What is "*In Vivo* Protein Transduction?"

"*In vivo*" implies in a living cell or a living organism and "protein transduction" takes place by several small regions of proteins called protein transduction domains (PTDs), which are cationic peptides [Snyder and Dowdy, 2004] identified to possess the ability to traverse biological membranes efficiently. Protein transduction is a relatively new molecular method, it provides a means of introducing large proteins across the cell membrane and the blood-brain barrier [Schwarze *et al.*, 1999; Wadia and Dowdy, 2002]. The protein of interest may be "transduced" to any cell type and will rapidly enter each cell such that an equivalent amount of the transduced protein is present in every cell. This technology opens a variety of new possibilities in the development of vaccines and protein therapies for cancer and infectious diseases and allows larger proteins to be introduced into a cell at lower doses. The lower doses may result in fewer side effects. There are also no permanent genetic modifications.

The introduction of proteins into cells is imprecise and indirect due to the current modes of introduction utilised. Such methods include microinjection, electroporation and others. These necessitate that recombinant DNA be introduced and subsequently expression and production of the protein by the cellular machinery occurs. Protein production may occur in a minority of target cells and this is undesirable since the production levels are not optimal. These methods, when employed in the delivery of the expression vectors, proteins, and/or pharmacologically active agents targeted at cells are challenging since besides low percentage of cells that are targeted, there is also over-expression, constraints in size and bio-availability. Despite these limitations, protein expression through DNA vectors yielded many insights on how cells function both in normal and diseased situations. Transfections yielded the efficiency within a range 50-90 % hence their popularity, but some were cytotoxic and more efficiency was a requirement. To alleviate these problems, a direct delivery of full-length proteins and domains by the concentration-dependent transduction can be employed. It has been shown that proteins linked to the HIV TAT transduction domain can transduce into cells [Ho *et al.*, 2001; Schwarze *et al.*, 2000; Vocero-Akbani *et al.*, 1999]. The ability to precisely control the amount of protein introduced into each cell is thus a powerful technique [Nagahara *et al.*, 1998; Schwarze *et al.*, 1999; Wadia and Dowdy, 2002, Wadia and Dowdy, 2003].

1.8.2. Transduction of Full-Length TAT Fusion Proteins Directly into

Mammalian Cells

The protein transduction domain (PTD) found in the HIV TAT protein (amino acids 47-57) has been documented to mediate the introduction of heterologous peptides and proteins, even of large sizes, into mammalian cells both *in vitro* and *in vivo* [Frankel and Pabo, 1988; Green and Lowenstein, 1988].

This methodology generates proteins that are efficiently transducible and yet biologically active and have broad potential in the manipulation of biological experimental systems.

In this method full-length fusion proteins that contain an NH_2 –terminal-eleven amino acid **P**rotein **T**randuction **D**omain (PTD), from the HIV virus, TAT protein, are generated. These proteins are then purified under denaturing conditions to increase the efficiency of transduction. Protein transduction appears not to be dependent upon receptors or transporters. Transduction is thought to target the lipid bi-layer component of the cell membrane. In this way, all the types of cells should be vulnerable or susceptible to such protein transduction. This technology has indeed been put to use by transducing a number of proteins that range in size between 15 and 120 kD into various human and murine cell types *in vitro* [Nagahara *et al.*, 1998].

In future, the TAT fusions may be used to combat genetic and hereditary diseases, and also the degenerative diseases of aging, through protein therapy. Transduction

also holds hope for new genetic and protein therapy, the development of vaccines, and cure for cancer and AIDS, contradictory though it may sound, since the latter was shown to be caused by the virus that the TAT domain is derived from

1.8.3 Cellular uptake

Due to their strong cell-surface binding, early assumptions regarding cellular uptake of TAT PTD's suggested a direct penetration mechanism across the lipid bilayer [Wadia *et al.*, 2004]. Understanding of the uptake pathway is ambiguous and controversial hence requires to be clarified. For clarity, TAT was fused to the N terminus of Gal protein. One possibility assumes that TAT-Gal enters the cell directly through plasma membrane (figure 1.11) [Bayley, 1999]. The schematic representation of Gal is shown as misfolded, rather than completely unfolded. The mechanism by which Gal translocates through the bi-layer is puzzling. Related unsolved issues remain in areas such as toxin penetration, anti-microbial peptide and polyamine action, and protein secretion. It may be that the domains are translocated as molten globules, or they may pass unfolded through a disordered bi-layer (as shown) or as an inside-out protein nucleated by the TAT sequence. The TAT peptide disrupts the bilayer, allowing the Gal sequences to enter. The translocation event or cytoplasmic chaperones promote refolding and coalescence of the domains. Finally, the enzymatically active tetramer is formed. Many proteins can be translocated by TAT, and it would be interesting to know more about their disulfide bond patterns, and whether they are readily unfolded or can exist in a molten globule state. Other
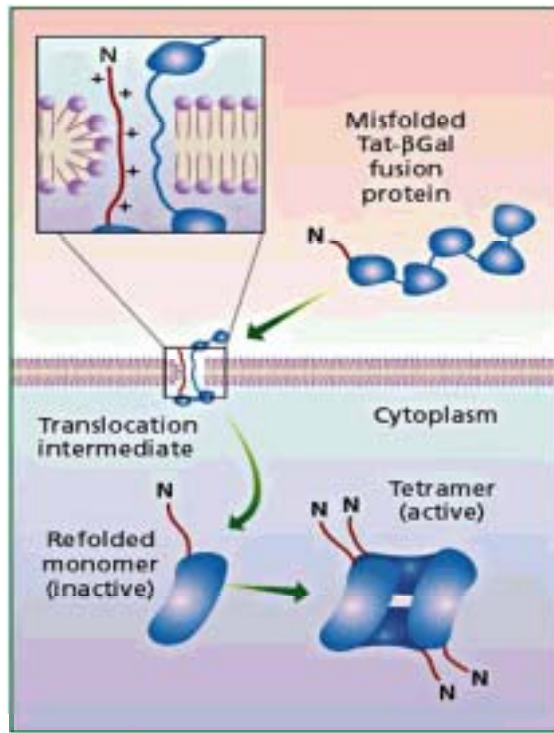
Figure 1.11: Possible mechanism for uptake of the TAT–Gal fusion protein by cells. The deliberately mis-folded protein contains the 11-residue TAT peptide (red) and the Gal sequence (1,023 residues), shown as five independently folded but disordered domains (green) [Bayley, 1999].

workers besides Dowdy and colleagues have claimed that extensive unfolding is required for ferrying by TAT [Bayley, 1999].

1.8.4 When to use this method?

Current methods efficiently delivered therapeutic compounds, peptidyl mimetics and proteins into cells *in vivo* only when such molecules are small. The typical size is usually less than 600 D. This limits the therapeutic proteins from entering cells and thus tissues and the blood-brain barrier. This method demonstrates that through protein transduction, it is possible to deliver a biologically active protein to each an every tissue in a living organism, the brain inclusive. Instead of a 600 D protein, a 100 kD (100,000 D) protein is being delivered, this marked difference was elaborated by comparing the size difference of the proteins with the tip of a pen and a fist [Schwarze *et al.*, 1999].

1.8.5 The Accomplishment of this method

Schwarze *et al.*, 1999 demonstrated that intraperitonial injection of the 120 kD β-galactosidase protein, fused to the protein transduction domain from the HIV TAT protein, would result in the delivery of the biologically active fusion protein to all tissues in mice, including the brain. Desired full-length fusion proteins were generated, containing an 11-amino acid TAT protein transduction domain (PTD: as referred to above) that was preceded by an NH_2-terminal fluorescein isothiocyanate [(FITC)-G-GGG-YGRKKRRQRRR]. The TAT-FITC peptide or the control free

FITC were then injected intraperitoneally into mice. Fluorescence was monitored and the results achieved showed that, twenty minutes after intraperitoneal injection of the TAT-FITC peptide or control free FITC, a strong fluorescence signal was detected in nearly all of the blood cells and splenocytes. There was evidence that the TAT-FITC peptide is capable of transducing into blood and splenic cells. Fluorescence confocal microscopy analysis, revealed a strong fluorescence signal in nearly all the areas of the brain and skeletal muscle tissue also [Schwarze *et al.*, 1999].

An NH_2-terminal TAT-β-Gal fusion protein (120 kD) and the control β-Gal fusion protein that lacked the NH_2-terminal leader (119 kD) were generated. The results obtained by fluorescence confocal microscopy showed that the FITC-labelled TAT-β-Gal fusion protein was present in the cells, while in the control, experiments using FITC-labelled β-Gal fusion protein, there was no β-Gal in the cells. These results revealed that there is a peak of concentration and enzymatic levels of TAT-β-Gal after thirty minutes, while the control counterpart (β-Gal) showed no increase in concentration in cells, nor in enzymatic activity levels after a two-hour period.

The transduction of peptides and proteins into mice lays the ground-work for the future epigenetic complementation experiments in model organisms and for the eventual transduction of therapeutic proteins into patients in the form of protein therapy. Therapy with biologically active full-length proteins will allow access to the built-in evolutionary specificity of these proteins for their targets, thereby potentially

avoiding the non-specific effects that are sometimes seen with small molecule therapies.

By the description of an experimental anti-HIV protein therapy based on a transducible HIV protease-activated caspase-3 that selectively induces apoptosis in HIV-infected cells, finally this methodology opens a number of new possibilities for the development of vaccines and protein therapies for cancer and infectious diseases. The imperative issues that remain to be examined in association with long-term transduction of proteins are potential immune responses and toxicity [Vocero-Akbani *et al.*, 1999].

1.8.6 Synthetic Protein Transduction Domains

There is growth in the amount of both natural and synthetic PTDs, since the need to test newly discovered PTDs for their ability to mediate the trafficking of the corresponding fusion proteins [Alexeyev *et al.*, 2004; Mai *et al.*, 2002]. Synthetic poly-Arginine, has been demonstrated to deliver numerous molecules, including synthetic small molecules, peptides and proteins, into animal models *in vivo* [Wadia and Dowdy, 2003].

On the basis of the modelled structure of the TAT PTD being a strong amphipathic helix, a series of synthetic PTDs that strengthen the α-helical content and optimise the arginine residues were synthesised. These synthetic domains significantly yielded

a remarkable enhancement of protein transduction potential compared to TAT both *in vitro* and *in vivo* [Ho *et al.*, 2001].

The *in vivo* role of this mechanism is to translocate desirable proteins into cells [Frankel and Pabo, 1988; Gius *et al.*, 1999; Green and Lowenstein, 1988; Hawiger, 1999; Ho *et al.*, 2001; Nagahara *et al.*, 1998; Schwarze *et al.*, 1999: Schwarze *et al.*, 2000; Vives *et al.*, 1997; Vocero-Akbani *et al.*, 1999].

It is likely that TAT PTD has not undergone evolutionary selective pressures for protein transduction, this thus suggests that the protein transduction potential may well be optimised synthetically. The structural motifs of a series of non-natural PTD peptides were enhanced and these novel domains demonstrated a significant enhancement of protein transduction potential into cells both *in vitro* and *in vivo* (figure 1.12) [Ho *et al.*, 2001].

The synthetic domains showed a great deal of improvement in the transduction potential. PTD-3 and PTD-6 domains demonstrated to be 5 fold more efficient than TAT, PTD-5 showed to be 8 fold more efficient, PTD-7 and PTD-8 yielded near identical transduction potentials with TAT, while PTD-4 provided the most dramatic improvement in relation to the original TAT, its potential was shown to be 33 fold more efficient than TAT (figure 1.12). This ability was tested *in vivo*, and PTD–4

Figure 1.12: The predicted α-helical wheels of TAT and non-naturally occurring PTDs [Ho *et al.*, 2001].

showed a significant increase relative to TAT peptide. It was thus concluded that PTD-4 exhibits increased transduction potential both *in vitro* and *in vivo.*

The researchers have in this way demonstrated, both *in vitro* and *in vivo*, that the optimisation of Arg residues plus the substitution with α-helical-promoting residues (Ala) resulted in the significant enhancements of the protein transduction potential.

1.8.7 Latest Transduction developments

The minimal sequence required for efficient transduction of TAT-GFP is the basic domain from 49-57 of HIV-1 TAT called the protein transduction domain (PTD) as mentioned earlier in the review. HIV-1 TAT PTD GFP fusion proteins in which HIV-1 TAT PTD is fused with the N- and/or C-termini of GFP have been generated. Various GFP fusion proteins were purified from *Escherichia coli* and characterised for their capability to enter mammalian cells using Western blot analysis, confocal microscopy and flow cytometry. The GFP fusion protein with TAT PTD at its C-terminus was taken up as proficiently as the GFP fusion protein with TAT PTD at its N-terminus. However, the same protein with PTDs at its both termini was taken up even more competently. All the GFP fusion proteins were present in both the nucleus and cytosol of the transduced cells. Uptake was demonstrated to be lower at $4\,^{0}C$ than at $37\,^{0}C$ [Ryu *et al.*, 2003].

1.9 Other Means of Protein Delivery

1.9.1 Protein delivery using VP22

The herpes simplex virus protein VP22 translocates between cultured mammalian cells. When VP22 is expressed in cultured cells, it is exported to the surrounding cells where it spreads and accumulates in the nuclei and binds chromatin. The activity of VP22 protein is such that it is also capable of delivering heterologous protein sequences [Elliott and O'Hare, 1997; Phelan *et al.*, 1998]

The import of VP22-green fluorescent protein (GFP) fusion purified from *E.coli* was detected by immuno-fluorescence microscopy, but there were difficulties in the detection of import by direct GFP fluorescence in both live and fixed cells. VP22-GFP protein in the nuclei of transfected cultures could only be detected by confocal microscopy and this suggested that the detection was made hard to achieve by the low level of GFP fluorescence [Lundberg and Johansson, 2001].

The limitation of GFP detection was overcome by the development of gene reporter assays that rely on the activity of the fusion partner that monitors the delivery of VP22. Such assays allowed the detection of VP22 translocation without the need for immuno-fluorescence or fixation of cells where there could possibly be potential artefacts that are associated with these protocols [Bennett *et al.*, 2002].

1.9.2 Delivery by a Short Peptide Carrier, Pep-1

A new protein delivery strategy, which is based on a short amphipathic peptide, Pep-1 (KETWWETWWTE WSQPKKKRKV), containing both hydrophobic tryptophan-rich, for efficient targeting to the cell membrane and hydrophobic interactions with proteins, and hydrophilic lysine-rich, derived from the **n**uclear **l**ocalisation **s**equence (NLS) of **s**imian **v**irus 40 (SV-40), regions, was presented. The Pep-1 carrier consists of 21-residues and can efficiently deliver various biologically active peptides and proteins into a wide range of cell lines with no requirement for covalent coupling or denaturation of the desired protein cargo. This aids in the protein stability and protection from degradation during the process of transfection [Morris *et al.*, 1999; Morris *et al.*, 2000]. This peptide crosses the plasma membrane of many cell types to carry and deliver proteins as large as antibodies [Taylor and Fernandez-Patron, 2003]. The delivery of peptides or proteins by any other means, than Pep-1 mediated mechanism, has major drawbacks in that there should be cross-linking to the target peptide or protein [Morris *et al.*, 2001]. The TAT-fusion-protein even requires target denaturation (Schwarze and Dowdy, 2000). VP22 requires fusion to the protein/peptide to be delivered, thus a suitable expression vector has to be constructed [Schwarze *et al.*, 2000].

The mixing of Pep-1 with peptides or proteins in a solution results in a rapid association through non-covalent hydrophobic interactions, and the final result is the formation of stable complexes. Pep-1 alone localises to the nucleus, but this does not

affect the sub-cellular localisation of the protein being delivered. This means of delivery is able to deliver peptides to the cytoplasm or the nucleus, depending on the signal motif expressed by the transported cargo. Pep-1 rapidly dissociates from the cargo in the cytoplasm once the complexes enter the cells and this confirms that it does not affect the final localisation of the cargoes it associates with [Morris *et al.*, 2000]. The cargo is thus at liberty to ensue its target organelle. Most importantly was that Pep-1 showed a very low level of toxicity, and seemed not to have any effect on the biological activity of the protein being transported and this had been demonstrated using the β-galactosidase enzyme.

Pep-1 localises rapidly and it has been indicated that its internalisation is independent of normal endosomal pathway (endocytosis). A similar behaviour has been reported for TAT-derived peptides [Fawell *et al.*, 1994, Vives *et al.*, 1997], VP22 and the other means of protein delivery, suggesting that the uptake of Pep-1 may occur by a similar mechanism [Morris *et al.*, 1997; Prochiantz, 2000]. The minimal threshold number of Pep-1 molecules to the targeted peptide or protein has to be attained for a successful intracellular delivery. This means that the ratio of Pep-1 to the cargo has to be immense, as 20:1 was shown to be optimal. The ratio of 5:1 result in no transfection while the ratio of 30:1 result in the decreased efficiency of delivery, which may be explained by either precipitation or the formation of large-size aggregates that are having a difficulty on entering the cells.

The efficiency of Pep-1-mediated peptide delivery is not affected by serum, which yields hope for the Pep-1 technology to be more attractive for *in vitro* and possibly *in vivo* applications. The efficiency of Pep-1 to deliver proteins has been characterised by the delivery of three very different types of proteins: 30 kDa GFP, 119 kDa β-Gal, and full-length specific antibodies. The efficiency of protein delivery was determined by counting fluorescent cells or by monitoring the β-Gal activity by staining with X-Gal. Approximately 80% efficiency was observed in both cases and all cells exhibited uniform and strong β-Gal activity and the presence of Pep-1 did not alter the activity of β-Gal. In the case of GFP, cells exhibited fluorescent GFP staining in the cytoplasm.

Pep-1 was demonstrated to be able to deliver antibodies into cells, while it preserved their ability to recognise their respective antigens within cells. That Pep-1 was shown to be able to deliver two different antibodies to their target antigens and yet attain their proper localisation, which is indicative that although it alone localises to the nucleus, it does not affect the appropriate sub-cellular localisation of the proteins it delivers. It is ideal for *in vivo* studies since fixing is not a requirement.

This means of delivery presents a number of advantages over the others in that rapid delivery with high efficiency, stability in physiological buffer, lack of or minimal cytotoxic effects at the recommended concentrations, and lack of sensitivity to serum are promised [Morris *et al.*, 2001]. The efficiency is no match to TAT-mediated

means of delivery in terms of the number of cells targeted though, which is an attribute that makes the TAT system preferable. It remains to be demonstrated whether Pep-1 will be as a successful carrier *in vivo* as it has shown to be *in vitro*, and what size limitations there will be on the molecules that can be transported.

1.9.3 Delivery by means of fusion between FGF-4 and a cell permeable Cre recombinase technologies

In this technology, the novel recombinant Cre recombinase that is permeable to the cell, was generated to be directly delivered into cells that contain lox-P flanked genes to cause genetic changes [Jo *et al.*, 2001]. Cre, is a site-specific DNA recombinase system that recognises the 34 base pair sequences called the lox-P sites. Cre catalyses the deletion of a DNA segment that is flanked by lox-P sites, thus leaving a single lox-P site intact. The placing of the lox-P sites in opposite orientation results in Cre also catalysing the inversion of the flanked (floxed) DNA segment [Prochiantz, 2000; Soriano, 1999].

The Cre/lox system enables the study of gene function and most prevalently used in conditional tissue-specific gene modifications, either gene knockouts or gene activations. The gene transfer by means of Cre has also made it possible for introduction into specific tissues. The direct delivery of the enzymatically active Cre protein into cells yields an alternative means of manipulating gene function [Akagi *et al.*, 1997]. A series of recombinant Cre proteins, with 12 of the 16 amino acids of the

membrane-**t**ranslocating hydrophobic **s**equence (MTS) from fibroblast growth factor-4 (FGF-4) fused at the C terminus, were generated. Protein transduction was thus combined with Cre/lox-P system so as to create a potentially exciting and powerful new tool for the genetic modification of cells. The FGF-4 MTS is capable to prompt the transfer of protein cargoes through the plasma membrane and into the cytoplasm of cells *in vitro*. A histidine tag, for purification and nuclear localisation signal (NLS) from simian virus 40 (SV40) T-antigen, containing recombinant Cre (His$_6$-NLS-Cre-MTS) was generated. The analysis of the exposure of 3T3 cells to this recombinant revealed nuclear localisation. The functionality of His$_6$-NLS-Cre-MTS was tested by the treatment of the cells containing floxed genes. The use of GFP and lacZ reporter assays and DNA analysis clearly demonstrated the protein transduction ability of His$_6$-NLS-Cre-MTS *in vitro*. Cultured cells were exposed to His$_6$-NLS-Cre-MTS for as little as 30 min, and this was a sufficient period to cause recombination in half of the treated cells, which is indicates how rapidly this recombinant protein can access entry into cells. This system is not as efficient as the TAT technology on the basis of the rapidity with which the proteins are delivered and the proportion of cells transduced.

The intravenous injection of the purified His$_6$-NLS-Cre-MTS into R26R mice that was expected to yield the β-Gal expression activity upon the expression of Cre resulted in the expression of β-Gal in many tissues throughout, thus demonstrating protein transduction *in vivo* and with no toxic effects, which is an attribute that,

amongst others, should render this delivery means favourable over many others. The brain was also susceptible to the Cre protein transduction, which indicates that the protein is capable of crossing the blood-brain barrier. This *in vivo* ability shows to be similar to the previously reported mode of transduction by HIV TAT-β-Gal protein. Although Cre was reported to have gained access to many of the organs, not all cells of the organs showed evidence of Cre-mediated recombination. The combination of the two technologies promises to be a productive union. [Jo *et al.*, 2001; Prochiantz, 2000; Lin *et al.*, 1995, Soriano, 1999, Schwarze *et al.*, 1999].

When purified recombinant Cre proteins with a heterologous protein transduction domain were compared with Cre proteins without, the outcome demonstrated that the unmodified Cre recombinase already intrinsically could cross the membrane boundary [Will *et al.*, 2002]. This stamps on the promising effect of the alleged union where translocation is supported by both parties in the marriage.

1.10 Mechanisms by which Carriers Deliver their Cargoes

The homeodomain of Antennapedia was internalised by several cell types, and by all of the cells present in culture, and the staining pattern suggested that the homeodomain has direct access to the cytoplasm. The deletion of certain sequences of the homeodomain eliminates the entry. Such sequences are within the third helix of the homeodomain, suggestive thus that this helix plays an important role in the internalisation process [Prochiantz, 2000].

The mechanisms by which VP22 and TAT internalise are not yet clear pending investigation. They, however, trigger the transportation of genetically fused cargoes. It may not have been a coincidence that the two viral proteins, TAT and VP22, are both secreted, internalised and conveyed to the nucleus of live cells. In case of TAT, there is a fragment including the nuclear localisation signal. The suggestion is that the structures responsible for the internalisation of TAT and homeo-proteins are evolutionarily related [Prochiantz, 2000].

1.11 The purpose of the project

Many genes are activated to influence the self-destruction programme of the cell. This programme entails synchronised instigation and implementation of numerous subprograms. The arrival of gene targeting aided in the determining of the functions of novel genes. Such genes may have been sequenced, but not functionally characterised. The fulfillment of this requirement through gene targeting technology has swiftly developed.

The mode by which DWNN operate in organisms in which it is thought to be covalently linked to some other proteins, which have a definite role in apoptosis, is not yet unraveled. This study attempted the functional characterisation of DWNN in light to the hypothesis that it may be involved in CTL killing and apoptosis.

In this study, TAT protein transduction domain was fused to a *GFP* reporter gene (due to its flexibility as a non-interfering marker in cells). *DWNN* gene was covalently linked to the cassette and functional studies were conducted with the resultant fusion protein. Protein transduction was exploited since it is a powerful tool for introduction of proteins and peptide mimetics into cells.

The proposed experimental layout was to generate recombinant TAT-PTD fusion proteins (GST-TAT-GFP, GST-TAT-GFP-DWNN$_{118}$, and GST-TAT-DWNN$_{118}$) and their negative controls (GST-GFP and GST-GFP-DWNN$_{118}$). Subsequently these were tested for their capability to traffic into cells in a receptor-less and endocytosis independent manner. The final part of the program was to partially characterise the manner by which a novel gene, with a presumed task in CTL killing and apoptosis, operates.

The manipulation of apoptosis presents a promise for dealing with diseases. Refining an understanding of the apoptotic mechanisms may promote research of novel effective drugs such as drugs for cancer treatment.

CHAPTER 2

MATERIALS AND METHODOLOGY

2.1 General Chemicals and Enzymes

40 % 19:1 Acrylamide:bis-acrylamide	Bio-Rad
40 % 37.5:1 Acrylamide:bis-acrylamide	Bio-Rad
Agarose	Promega
Ammonium persulphate	Merck
Ampicillin	Roche
Bacteriological agar	Merck
Boric acid	Merck
Bovine serum albumin	Roche
Bromophenol blue	Sigma
Buffer saturated phenol	Invitrogen
Chloroform	BDH
Coomassie Brilliant Blue R 250	Sigma
DAPI (4', 6'-diamidino-2-phenylindole)	Sigma
DMSO (Dimethyl sulphoxide)	Sigma
DTT (Dithiothreitol)	Roche
EDTA (Ethylene diamine tetra acetic acid)	Merck
Ethanol	BDH
Ethidium bromide	Promega

Glacial acetic acid	Merck
Glucose	BDH
Glutathione	Sigma
Glycine	BDH
Hydrochloric acid	Merck
IPTG (Isopropyl β-D-thiogalactopyranoside)	Promega
Methanol	Merck
N-Z-Amine A	Sigma
Paraformaldehyde	Sigma
PMSF (phenylmethylsulphonyl fluoride)	Roche
Ponceau S	Sigma
Premixed Protein markers	Roche
SDS (Sodium dodecyl sulphate)	Promega
Sodium azide	Roche
Sodium hydroxide	Merck
TEMED (*N*, *N*, *N'*, *N'*-Tetra methylethylene-diamine)	Promega
Tris (Tris[hydroxymethyl] aminoethane)	BDH
Triton X-100 (iso-octylphenoxypoly-ethoxyethanol)	Roche
Tryptone	Merck
Tween 20 (Polyoxyethylene [20] sorbitan)	Merck

Urea	Amersham Pharmacia
Xylene cyanol	BDH
Yeast extract	Merck

The chemicals used were of AnalaR or equivalent grade. Restriction endonucleases were supplied by New England Biolabs or Roche Diagnostics. T4 DNA ligase was obtained from Promega. *Taq* DNA polymerase was obtained from Takara Biotechnology.

2.2 Stock Solutions, Buffers And Additional Materials

1 x TAE:

40 mM Tris-acetate, 1 mM EDTA, pH 7.8.

1 x TBE:

90 mM Tris-borate and 2 mM EDTA, pH 8.3.

4× Stacking gel Buffer:

0.5 M Tris-HCl, pH 6.8.

5× SDS Electrophoresis Buffer:

25 mM Tris, 0.1 % SDS and 250 mM glycine, pH 8.3.

6× Glycerol BPB Gel-loading Buffer:

30 % glycerol, 0.25 % Bromophenol blue and 0.25 % Xylene cyanol.

8× Separating gel Buffer:

3 M Tris-HCl, pH 8.8. This buffer was stored at 4 °C.

10 x M9 Salts:

0.2 M NH_4Cl, 0.2 M KH_2PO_4, 0.5 M Na_2HPO_4.

TE:

10 mM Tris-Cl, 1 mM EDTA, pH 7.5.

Ammonium persulphate:

A 10 % stock solution was prepared in deionised water.

Ampicillin:

100 mg/ml ampicillin in dH_2O.

Cell lysis buffer:

137 mM NaCl, 27 mM KCl, 80 mM Na_2HPO_4, 1.5 mM KH_2PO_4, pH 7.4, 1 % Triton X100, 1 mM DTT, 1 mM EDTA, 1 mM PMSF and 100 mg/ml Lysozyme, 100 µg/ml DNAse.

Chloramphenicol:

100 mg/ml in absolute ethanol.

Coomassie Staining Solution:

0.25 g Coomassie Brilliant Blue R 250, 45 % methanol and 5 % acetic acid.

DNA Loading buffer:

0.25 % Bromo-phenol-blue, 0.25 % xylene cyanol, 30 % glycerol.

De-staining Solution:

30 % methanol and 10 % acetic acid.

DTT:

A 1 M stock solution was prepared in 0.01M Sodium acetate, pH 5.2. This solution was sterilised by filtration.

EDTA:

A stock solution was prepared at a concentration of 0.5 M in deionised water, pH 8.

Elution Buffer (sDNA):

300 mM Sodium acetate, 1 mM EDTA.

GTE:

25 mM Tris-Cl, 10 mM EDTA, 50 mM glucose, pH 8.0.

IPTG:

A 1 M stock solution was prepared in deionised water. The solution was sterilised by filtration.

Kanamycin:

50 mg/ml Kanamycin.

LB Media:

10 g/l Bacto-tryptone, 5 g/l Bacto-Yeast Extract, 5 g/l NaCl and 2 g/l glucose.

Lysozyme:

A stock solution was prepared at a concentration of 50 mg/ml in deionised water.

M9ZB:

10 g/l NZ-Amine A, 5 g/l NaCl, 20 mM NH_4Cl, 20 mM KH_2PO_4, 50 mM Na_2HPO_4, 0.04 % Glucose and 1 mM $MgSO_4$.

NaOH/SDS or Lysis solution:

0.2 N NaOH, 1% SDS.

Paraformaldehyde Fixative:

16 g paraformaldehyde was dissolved in 80 ml deionised water by stirring at 70 °C (in fume cupboard). One drop of 2 M NaOH was added. The solution was cooled down to room temperature and the volume adjusted to 100 ml with deionised water. This solution was filter sterilised through a 0.45 micron filter and a 100 ml 2× PBS was added.

PBS: phosphate-buffered saline:

137 mM NaCl, 27 mM KCl, 80 mM Na_2HPO_4, 1.5 mM KH_2PO_4, pH 7.4.

Phenol/Chloroform:

1:1 phenol:chloroform, (v/v).

PMSF:

A 10 mM stock solution was prepared in isopropanol.

Potassium acetate/Neutralising solution:

3 M potassium acetate, pH 5.

PreScission^TM Protease cleavage buffer:

50 mM Tris-HCl, pH 7.0, 150 mM NaCl, 1 mM DTT, 1 mM EDTA.

Protein Elution Buffer:

10 mM glutathione and 50 mM Tris-HCl, pH 8.0.

RNAse (DNase free):

A 20 mg/ml stock solution was prepared in a buffer containing 0.1 M sodium acetate and 0.3 mM EDTA (pH 4.8, with acetic acid). This solution was boiled for 15 min and cooled quickly by placing it in ice water.

TBS:

20 mM Tris-HCl and 150 mM NaCl, pH 7.5.

TBS-MT:

5 % Low fat dried milk powder and 0.1 % Tween 20 in TBS.

TBS-T:

0.1 % Tween 20 in TBS.

Tfb1 Buffer:

30 mM Potassium acetate, 50 mM $MnCl_2$, 0.1 M KCl, 6.7 mM $CaCl_2$ and 15 % glycerol (v/v).

Tfb2 Buffer:

9 mM MOPS, 50 mM $CaCl_2$, 10 mM KCl and 15 % glycerol (v/v).

Tissue culture media:

The following tissue culture medium and supplements were supplied by Invitrogen: nutrient mixture Ham's F12, 100× penicillin-streptomycin, and Foetal calf serum (FCS).

Transfer Buffer:

25 mM Tris, 192 mM glycine and 20 % methanol.

TYM Broth

20 g/l bacto-tryptone, 5 g/l yeast extract, 3.5 g/l NaCl, 2 g/l $MgCl_2$.

ZB:

10 g/l NZ-Amine A, 5 g/l NaCl.

ZB agar:

10 g/l NZ-Amine A, 5 g/l NaCl and 14 g/l Bacteriological agar.

2.3 Gel electrophoresis of DNA

2.3.1 Agarose gel electrophoresis

Gel preparation and electrophoresis

Gels were prepared by adding the required volume of 1 X TBE or TAE to the appropriate mass of electrophoresis grade agarose. The agarose was then boiled and cooled to 55 °C. Ethidium bromide was added to the agarose solution to a final

concentration of 0.5 μg/ml. This was then set in the appropriate gel form. All gels were electrophoresed in 1 x TBE or 1 x TAE at 8 V/cm.

Sample preparation

Approximately 1 μl (0.5 vol) of DNA loading buffer was mixed with DNA in 5-20 μl and loaded into the gel.

Detection of DNA

Gels contained ethidium bromide, thus DNA was visualized by illuminating the gel with wavelength UV light on a trans-illuminator. For DNA recovery from the gel purposes, a 360 nm wavelength lamp was used to avoid damage to the DNA.

Electro-elution of DNA gel slice

DNA was electrophoresed until the fragments of interest were well separated from other fragments, monitoring the process with a 360 nm UV lamp. Each fragment was excised using a clean sterile scalpel blade and placed into a 1.5 ml tube. The fragments were gene cleaned as per manufacturer's manual. Purification of DNA fragments by GFX entailed the weighing of the fragments and 10 μl of the capture buffer was added for every 10 mg of agarose and the mixture was vigorously mixed by vortexing. The tube was placed $60\,^{0}$C for 5-15 min to melt the agarose. The sample was then transferred to a GFX column within a collection tube and centrifuged for 30 seconds at 13 000 g. The flow through was discarded and the

column placed back in the collection tube. 500 µl of wash buffer was added to the column and the tube centrifuged for a minute at 13 000 *g*. The collection tube was removed and placed in a 1.5 ml tube and 20 µl of elution buffer was directly put on the matrix of the column and incubated at room temperature for a minute. The tube was centrifuged for a minute at 13 000 *g* to gather the DNA. DNA was pure for cloning procedure.

2.3.2 SDS-PAGE electrophoresis

Elution of small DNA fragments from PAGE

The synthesised oligonucleotides or DNA samples after a PCR reaction were electrophoresed in a 5 % Polyacrylamide gel prepared from 40 % 19:1 acrylamide:bis-acrylamide, and the gel was stained for 10-20 minutes in 0.5 µg/ml ethidium bromide.

The bands of interest were excised out of the gel, macerated, and placed in 1.5 ml tubes. Elution buffer was added to the pieces of the gel so as to just cover the pieces (approximately two times the original volume of the gel slice) and incubated overnight at 37 °C with gentle shaking. DNA fragments smaller than 250 bp were eluted in 3-4 hours. The samples were centrifuged at room temperature and the supernatant that contained the DNA was transferred to a clean 1.5 ml tube and was again centrifuged at 10 000 *g* for a minute to remove the remaining acrylamide gel pieces. The supernatant was again transferred to another clean tube and the DNA was

precipitated with 2.5 volumes of absolute ethanol for an hour at –20 °C. The pellet (DNA fragments) was recovered by centrifuging at 10 000 g for 10 min, then washed twice with 70 % ethanol, dried at 37 °C and then re-suspended in 1 x TE buffer.

SDS-polyacrylamide gel electrophoresis (SDS-PAGE).

Proteins were separated on SDS-PAGE gels. Gels were made from a 40 % of pre-mix acrylamide: bisacrylamide (37.5:1) (Bio-Rad). The separating gel consisted of 12 to 16 % acrylamide: bisacrylamide (37.5:1), 0.375 M Tris-HCl, pH 8.8, 0.1 % SDS, 0.5 %, ammonium persulphate and 0.1 % TEMED. The stacking gel consisted of 4 % acrylamide: bisacrylamide (37.5:1), 0.125 M Tris-HCl, pH 6.8, 0.1 % SDS, 0.5 % ammonium persulphate and 0.1 % TEMED. The samples were mixed with an equal volume of 2× Sample Buffer, boiled for 5 min, centrifuged for 10 min at 10 000 g, and electrophoresed in 1× SDS Electrophoresis Buffer at 100 V/cm (constant voltage) for about 25 min using a Hoefer Mighty Small II Gel electrophoresis system (Amersham Pharmacia). The voltage was increased to 150 V/cm (constant voltage) when the bromophenol blue dye front reached the separating gel. Electrophoresis was stopped when the bromophenol blue dye front reached the bottom of the gel. The gel was incubated in Coomassie Staining Solution for 30 min and then incubated in De-staining solution, until suitably de-stained.

2.4 DNA Quantification

The absorbance of DNA was measured (optical density or O.D) to determine the sample quantity at 260 nm in a spectrophotometer.

The following formulas derived from Beer's Law were used:

[DNA] for ds DNA   O.D x 50 µg/ml x dilution factor

[DNA] for ss DNA/RNA   O.D x 40 µg/ml x dilution factor

[DNA] for oligonucleotides   O.D x 2 µg/ml x dilution factor

2.5 Phenol- Chloroform Inactivation/cleaning and Ethanol Precipitation

One volume of phenol/chloroform (1:1) was added to the sample. The samples were centrifuged at 10 000 *g* for 10 minutes to recover the top aqueous layer. This step was repeated to ensure that all impurities were removed. The DNA was precipitated with 1/10 volume of 3 M sodium acetate and 2.5 volume of 96 % ethanol. The solution was thoroughly mixed and left on ice for 5 min and after that, the samples were centrifuged for 10 min at 10 000 *g*. The supernatant was discarded and the pellet washed with 70 % ethanol and centrifuged for 5 min. The ethanol was decanted and the last few drops were aspirated with a pipette. The pellet was left to air dry or the process was facilitated by brief incubation at 37 °C, so as to remove excess drops by evaporation. The reasonably dry pellet was dissolved in an appropriate amount (depending on amount of DNA) of 1 x TE.

2.6 Sequencing

Sequencing Using the ABI 310 Genetic Analyzer

Sequencing reactions were performed using the DNA Sequencing Kit, BigDye[TM] Terminator v3.0 Cycle Sequencing Ready Reaction (Applied Biosystems). The PCR sequencing reactions were performed in a 20 µl final volume containing 3.2 pmol of the sequencing primer, 4 µl Terminator Ready Reaction mix (Applied Biosystems) and 4 µl 2.5× Sequencing Buffer. For plasmid DNA templates 500 ng of DNA was added, while the DNA concentration for PCR fragments was dependent on the size of the PCR fragment. For each of the reaction the reagents were added as follows:

Reagent	Quantity
Terminator Ready Reaction Mix	4.0 µl
2.5 X Sequencing Buffer	4.0 µl
Template	-
SsDNA	50-100 ng
DsDNA	200-500 ng
PCR products DNA	1-100 ng
Primer	3.2 pmol
De-ionized water	to final volume of
Total Volume	20 µl

The samples were well mixed and briefly centrifuged. The tubes were then placed into a PCR machine/thermal cycler and the volume calibration of the machine was set

in accordance to the volume of the samples. Reactions were carried out according to the manufacturer's protocol.

The contents of the tubes were centrifuged. For the extension precipitation of samples in micro-centrifuge tubes the following was done: The entire contents of each extension reaction were aspirated out with a pipette and transferred into a 1.5 ml micro-centrifuge tube. After transfer of contents, 16 µl of de-ionized water and 64 µl of 95 % ethanol were added to the 1.5 ml tube with samples to precipitate the DNA. The samples were briefly mixed by vortexing. Samples were left at room temperature for 30 minutes to precipitate the extension products. Thereafter the tubes were placed into a micro-centrifuge in a marked orientation and the tubes were centrifuged for 20-30 min at 10 000 g. The supernatant was discarded by aspirating it with care, with a separate pipette tip for each sample so as to avoid contamination. At this stage the pellet might or might not be visible. Importantly, the supernatant was completely removed, as the unincorporated dye terminators should not dissolve. The pellet was washed twice with 250 µl of 70 % ethanol. Ethanol was added and the samples were briefly mixed by vortexing and the tubes were placed into the micro-centrifuge in the same orientation as before. The samples were centrifuged for 10 min at 10 000 g. The supernatant was again carefully aspirated and the pellet was dried at 37 °C for 10-15 min. The pellet was stored at –20 °C for further use in a sequencing reaction. The pellet was dissolved in 25 µl of Template Suppressor Buffer (TSR) [Applied Biosystems]. The sample was then heat denatured at 95 °C for 2 min. After

denaturing the samples were then transferred immediately to ice for 5 min and sequencing using the ABI 310 PRISM^{TM} Genetic Analyzer (Applied Biosystems) followed. Data collection was conveyed using the ABI 310 PRISM^{TM} Collection Software (Applied Biosystems) and the analysis was done using Sequence Analysis 3.3 Software (Applied Biosystems).

2.7 Cloning Vectors

2.7.1 pGEM$^{®}$-T Easy.

The pGEM$^{®}$-T Easy Vector System (Promega) is capable of direct cloning of PCR fragments. This cloning strategy utilises terminal extendase activity of *Taq* polymerase which adds an extra base (usually an adenosine) on the 3' end of PCR products (Clark, 1988). The pGEM$^{®}$-T Easy Vector, as supplied for cloning by the manufacturer, contains single 3'-T overhangs at the insertion site, and is able to accommodate the ligation of PCR fragments (Figure 2.1).

2.7.2 pGEX-6P-2.

The Glutathione S-Transferase (GST) gene fusion system (Amersham Pharmacia) is a protein expression system, which can be used for the expression, purification and detection of recombinant fusion proteins produced in *E. coli*. This system is designed for the inducible, high-level intracellular expression of genes or gene fragments as fusions with *Schistosoma japonicum* GST (Smith and Johnson, 1988). The GST domain acts as an affinity tag that allows for the purification of the fusion protein by
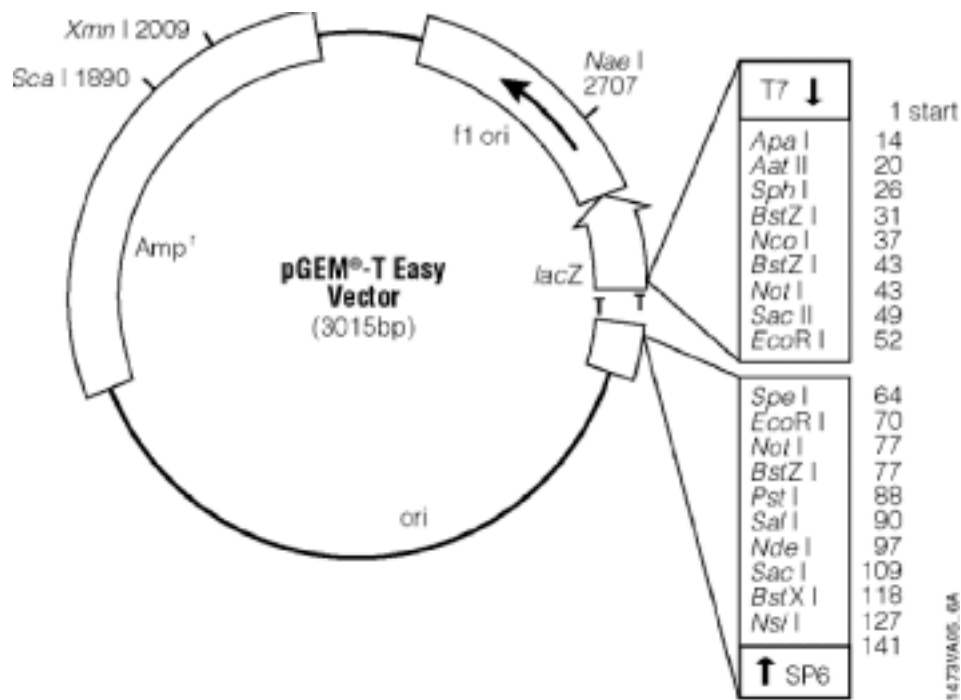
Figure 2.1: The pGEM®-T Easy Vector System (Promega) for direct cloning of PCR fragments. This map shows the multiple cloning site and the T overhangs.

affinity chromatography using glutathione agarose. A number of glutathione S-transferase fusion vectors have been developed. One such vector is pGEX-6P-2 (Figure 2.2).

Separation of the protein of interest from GST can be achieved by using a site-specific protease whose recognition sequence is located between the GST domain and the protein of interest. In the case of pGEX-6P-2 this protease is PreScission™ Protease (Amersham Pharmacia). This protease is a genetically engineered fusion protein consisting of human rhinovirus 3C protease and GST. This enzyme specifically cleaves between the Gln and Gly residues of the recognition sequence of Leu-Glu-Val-Leu-Phe-Gln/Gly-Pro (Cordingley *et al*., 1990).

2.7.3 Annealing of complementary oligonucleotides

Complementary oligonucleotides, with desirable overhangs, were annealed at the same concentration and volume, each, in TE buffer containing a small amount of salt (NaCl). The reaction mixture was incubated at 95 °C for 5 minutes and allowed to cool down slowly to room temperature. The annealed fragment was ready for cloning into a vector.

2.7.4 Restriction enzyme digestion of DNA

Restriction enzymes were used according to manufacturer's instructions. In general 1 µg of DNA was digested with 1 unit of enzyme in the appropriate buffer and

pGEX-6P-2

PreScission™ Protease

Leu Glu Val Leu Phe Gln↓Gly Pro┃Leu Gly Ser Pro Gly Ile Pro Gly Ser Thr Arg Ala Ala Ala Ser
CTG GAA GTT CTG TTC CAG GGG CCC CTG GGA TCC CCA GGA ATT CCC GGG TCG ACT CGA GCG GCC GCA TCG

BamH I   EcoR I   Sma I   Sal I   Xho I   Not I

Ball I

glutathione S-transferase

Ptac
BspM I

pSj10ΔBam7Stop7

Tth111 I
Aat II

Amp^r

Pst I

pGEX
~4900 bp

Nar I
EcoR V
BssH II
Apa I
BstE II
Mlu I

lac I q

p4.5

AlwN I

pBR322
ori

Figure 2.2: A circular map of the pGEX-6P-2 expression vector.
This map shows the GST (Glutathione S-transferase) domain next to
the multiple cloning site and the position of the PreScission Protease
cleavage site between the GST domain and the multiple cloning site.

temperature. Restriction enzymes were inactivated by either heating the reaction mixture at 70 °C for 10 min, or by phenol/chloroform extraction if the enzyme is heat stable.

2.7.5 Re-circularization of digested Vectors/Ligation of DNA

Ligation reactions were set up according to the manufacturer's instructions. Reactions were performed in 1× ligase buffer (30 mM Tris-HCl, pH 7.8, 10 mM $MgCl_2$, 10 mM DTT and 1 mM ATP) using T4 DNA ligase (Promega). It was necessary to make sure that the entire contents in the tubes were at the bottom of the tubes. Ligations were performed according to the manufacturer's instructions. The enzyme was heat inactivated by incubation 70 °C for 10 min.

A ligation reaction was set up as follows:

Tubes	Vector (10 ng/µl)	Insert	2x Rapid Ligation Buffer	T4 Ligase (3 U/µl)	dH$_2$O
Positive Control	1 µl	-	5 µl	1 µl	3 µl
Negative Control	1 µl	-	5 µl	-	4 µl
Experimental Tube	1 µl	1 µl	5 µl	1 µl	2 µl

Table 2.1: Ligation reactions for cloning

The samples were mixed by vortexing and then incubated at room temperature for 3 hours. After ligation, 100 µl of competent cells were added to the ligation mix and the transformations were conducted (Section 2.10).

2.8 Bacterial cultures.

2.8.1 Strains used.

(1). *Escherichia coli* MC1061 (Casadaban and Cohen, 1980):

F$^-$, *ara*D139, (*ara leu*) 7697, Δ*lac*x74, *gal*U$^-$, *gal*K$^-$, *hsm*$^+$, *str*A.

(2). *E. coli* BL21 Star^{TM} pLys (DE3) (Stratagene):

F$^-$ *omp T hsdS$_B$ (r$_B^-$ m$_B^-$) gal dcm rne131* (DE3*)*

2.8.2 Cultures

Escherichia coli MC1061 was used to produce plasmid DNA, while *E. coli* BL21 Star^{TM} pLys (DE3) was used to express recombinant fusion proteins. *E. coli* was grown in L broth and on L agar plates with or without ampicillin. When required ampicillin was added to L broth and L agar plates to a final concentration of 100 µg/ml. All cultures were grown at 37 °C.

Glycerol stocks were prepared directly from overnight cultures, grown under selectable conditions, by dilution of the culture with an equal volume of 80 % sterile glycerol. These were then stored at – 70 °C.

2.9 Preparation of competent cells for transformation

Competent cells were prepared and stored as is indicated below for *E.coli*. The *E.coli* colony was taken from a freshly streaked L agar plate and transferred to 10 ml of TYM broth and grown, by shaking vigorously, at 37 °C to OD$_{550}$ = 0.2. The cells

were then transferred to 500 ml of TYM broth and grown as previously stated above to $OD_{550} = 0.2$. The cells were then quickly chilled on ice and the bacteria were centrifuged to pellet by centrifugation at 5000 g for 10 min. Thereafter, the bacterial pellet was re-suspended in 250 ml of transformation buffer (Tfb1) at 0 °C and were left to stand for 30 min. The bacterial pellet was recovered by centrifugation at 5000 g for 10 min at 4 °C, the pellet was re-suspended in 50 ml of transformation buffer (Tfb2) at 4 °C. This was followed by aliquoting the re-suspended samples into 250 μl or 500 μl aliquots and then quick freezing in liquid nitrogen, this was done before storage at –70 °C. This method of preparation routinely resulted in transformation efficiencies of $3x10^6$ to 10^7 transformants/μg supercoiled DNA.

2.10 Transformation

High efficiency competent cells (MC 1061) of 1 X 10^7 cfu/μl were used for transformations. To each ligation reaction that was prepared above, 100 μl of competent cells were added. These samples were then incubated for 30 min on ice. While these samples were incubated, 2 plate per reaction with LB + Ampicillin (100 μg/ml) were prepared. To the sample tubes, 900 μl LB without ampicillin was added and incubated at 37 °C for an hour. The plates were in duplicate; 100 μl of each transformation were plated and then incubated overnight at 37 °C. The colonies that grew were counted and some of the colonies were selected. The chosen colonies were re-suspended in about 10 μl sterile deionised water (dH$_2$O) and these were

stored at 4 °C. Colony PCR to identify positive clones was performed to screen for recombinant clones.

2.11 PCR

2.11.1 Amplification of DNA by PCR.

PCR reactions were performed in 1× reaction buffer according to the manufacturers instructions. The enzyme *Taq* polymerase (Takara Biotechnology) was used at 0.2 units per reaction. The primers were present at 1 pmol and between 1 and 10 ng of DNA template was used in each reaction. The $MgCl_2$ concentration was 1.5   M.

2.11.2 Colony PCR: Screening for positive clones

The positive colonies were screened for as follows:

A reaction was prepared as follows:

Forward primer:	[10 pmol]	1 µl
Reverse primer	[10 pmol]	1 µl
dNTPs		1 µl
$MgCl_2$		1 µl
10 X Buffer		2.5 µl
Taq polymerase		0.2 µl
dH_2O		17.3 µl
		24 µl

1 µl bacterial cell suspension (section 2.10) was added to this mixture and the samples were well mixed and briefly centrifuged. A negative control which substituted the 1 µl bacterial cell suspension with 1 µl of water was also performed. Samples were then placed into a PCR machine and colony PCR was conducted under the following specifications:

30 cycles were repeated as follows:

Rapid thermal ramp to 95 °C

95 °C for 2 min

Rapid thermal ramp to 94 °C

94 °C for 30 seconds

Rapid thermal ramp to 92 °C

92 °C for 10 min

Rapid thermal ramp to 68 °C

68 °C for 30 seconds (Annealing temperature)

Rapid thermal ramp to 75 °C

75 °C for 1 min

Rapid thermal ramp to 4 °C

This protocol was used since the annealing temperature of the pGEX-6p-2 was at the specified temperature to determine, which chosen bacterial colonies represented the recombinant clones. The samples were analysed by agarose gel electrophoresis and

positive clones were prepared by small-scale plasmid DNA isolation for further screening by restriction digestion.

2.12 Small Scale Plasmid DNA Isolation

After the positive clones were identified the remaining samples from the re-suspended tubes were inoculated into 15 ml LB medium with the appropriate antibiotic (ampicillin), and grown overnight at 37 °C with vigorous shaking. About 900 µl of the overnight cultures were removed and was added to 100 µl sterile glycerol or dimethyl-sulphoxide (DMSO) for storage at –70 °C. The remaining cell suspension was centrifuged at 6 000 g for 10 min. The supernatant was discarded and 200 µl of GTE solution was added and the sample was vortexed and incubated on ice for 5 min. 400 µl of lysis solution (section 2.2) was then added and the samples were mixed and then incubated on ice for 5 min. 300 µl of neutralising solution added and the samples were gently mixed. The samples were centrifuged at 10 000 g for 15 min. 800 µl of the supernatant was transferred carefully to fresh tubes and 600 µl of isopropanol was added and the samples were vortexed and left at –20 °C for 30 min. The samples were then centrifuged at 10 000 g for 10min and the supernatant was discarded. The pellet was washed with 70 % ethanol. The pellet was dissolved either in 500 µl or 50 µl (if no further purification was intended) of 1 X TE. An RNAse treatment was carried out by an addition of 5 µl of RNAse (100 µg/µl) to the 500 µl and incubation at 37 °C for an hour. 800 µl of phenol/chloroform (1:1) was added,

and the sample was vortexed and centrifuged at 10 000 *g* for 5 min. The aqueous layer was carefully removed and added to a tube. Half the initial volume of 7 M ammonium acetate and 2.5 times the initial volume of ethanol were added and the samples were vortexed and then incubated at –20 °C for 30 min. The samples were then centrifuged at 10 000 *g* for 10 min, the pellet was washed twice with 70 % ethanol and dried at 37 °C for 10-15 min. The dried pellet was re-suspended in 50 µl of 1 X TE and stored at –20 °C.

2.13 Expression

2.13.1 Expression screening of the transformants

The positive clones were transformed in *E.coli* BL21 pLys S (DE3) competent cells and after overnight growth on L agar plate, a colony was inoculated into a 1 ml of appropriate media containing 0.3 % glucose, and 100 µg/ml ampicillin in a 1.5 ml tube. The samples were shaken at 37 °C for 4 hours. After incubation, 1 ml was equally split into two 0.5 ml samples where one was to be induced and the other not. To the induced tube, 0.3 mM IPTG was added and further incubation at 37 °C followed. Incubation was carried out on the un-induced samples also. Cells were centrifuged for 1 min and the supernatant was discarded. The cells were then re-suspended into 100 µl of PBS. 20 µl's of the cell suspension and 5 µl of 2x SDS sample buffer were thoroughly mixed and incubated at 95 °C for about 5 min and electrophoresed on a 12 % separating gel and 5 % stacking gel. The gel was then stained and de-stained to view the samples as protein fragments of particular sizes.

2.13.2 Large-scale expression of recombinant protein

2.13.2.1 Expression in LB

Large-scale expression was performed by an inoculation of a single colony in to 100 ml of LB containing 100 µg/ml ampicillin. The culture was incubated at 37 °C overnight and 900 ml of LB containing 100 µg/ml ampicillin was added and incubated at 37 °C until the OD_{550} equaled 0.4-0.6. IPTG was added to a final concentration of 0.3 mM. The sample was then incubated with shaking at 25 °C for 4 hours. Bacteria were recovered by centrifugation at 5000 g for 10 min. The supernatant was discarded and the pellet could be stored at –20 °C until further use. The pellet was re-suspended in 20-25 ml of Lysis buffer. Lysis was carried out by freezing at –70 °C for 5 min, and thawing at 37 °C for 5 min. The freeze thawing process was done three times or more for successful lysis. The protein lysate was stored at 4 °C until purification. Immediate purification was preferable since degradation by proteases (proteolysis) could occur. 0.2 % of sodium azide was included to inhibit bacterial growth.

2.13.2.2 Expression in M9ZB

The positive clones were transformed in *E.coli* BL21 pLys S (DE3) Gold competent cells and after overnight incubation on M9ZB plates containing 100 µg/ml ampicillin and 10 µg/ml chloramphenicol, a colony was picked and inoculated into 200 ml of M9ZB containing 100 µg/ml ampicillin and 10 µg/ml chloramphenicol. This was

incubated, with shaking, in a 2 l flask at 37 °C for 6 hours. 800 ml of media was added and the samples were further incubated until the OD$_{550}$ reached between 0.4 and 0.6, usually for 30 min. IPTG was added to a final concentration of 0.3 mM. The cultures were incubated with shaking at room temperature for 4 hours. Lysis was carried out as in 2.13.2.1 above.

2.14 Protein purification on GST column

2.14.1 Preparation of Glutathione–agarose beads

To swell 2 ml of gel, 140 mg of the lyophilised powder was mixed with de-ionized water (200 ml/g). The mixture was incubated overnight at 4 °C for 100 % swelling to occur. After swelling, the agarose beads were thoroughly washed with 10 volumes of water and then with an equilibration buffer (PBS) to remove the lactose present in the lyophilised product.

2.14.2 Storage and stability

The beads were properly stored at 4 °C. The swollen resin was stored in 1 M NaCl and 1 mM sodium azide was included.

2.14.3 Purification

In a case of a previously used column, a wash with a 3 column volumes (CV) of 1 M NaCl was the first step. The column was then equilibrated with 5 CV of PBS. The protein sample was added to the column and the flow through was collected. The

column was then washed with 5 CV of PBS-Triton X. The flow through was collected and 15 mM glutathione, 50 mM Tris pH 8.0 was used for elution. 3-5 ml fractions were collected and the column was washed with 5 CV of 1 M NaCl. The resin was then stored in this solution with sodium azide (section 2.14.2).

2.14.4 PreScission Protease cleavage of recombinant protein

The recombinant proteins were cleaved with PreScission [TM] Protease (Amersham Pharmacia Biotech) to release the fusion proteins from GST. 12 units (6 μl) of protease were added to 15 ml of recombinant protein in a dialysis tube (molecular weight cut off (MWCO) 3500 Da). The dialysis tube was placed in a cleavage buffer (50 mM Tris-HCl, 150 mM NaCl, 1 mM EDTA and 1 mM DTT, pH 7.0). Cleavage was done overnight at 4 °C. Subsequent to cleavage, the fusion proteins were recovered using a glutathione agarose column as described in Section 2.14.3.

2.15 Tissue Culture

2.15.1 Cell Thawing and Seeding

Cell vial was removed from –150 °C, briefly incubated in a water bath at 37 °C until just thawed. The contents of the vial were transferred into 5 ml media, containing serum and antibiotics, in a 15 ml tube. The tube was centrifuged at 300 g for 2 min to pellet cells. The supernatant was discarded and the cells were re-suspended into 5 ml of media and transferred into a 25 cm^2 flask. The cells were then incubated at 37 °C with 5 % CO_2.

2.15.2 Changing media

The media on cells was discarded and cells were thoroughly washed with PBS, which was also discarded. Fresh media was added and the cells were re-incubated at 37 °C with 5 % CO_2.

2.15.3 Trypsinisation of cells

Media was removed from the flask and the cells were treated with a single PBS wash. PBS was removed and 5 ml of 0.125 % trypsin in PBS was added to the cells. The cells were incubated at 37 °C with 5 % CO_2 for about 10 min and 2 ml of media was added to stop the action of trypsin. The cells were transferred into a 15 ml tube and centrifuged at 300 g for 2 min. The supernatant was discarded and the pellet was re-suspended into 10 ml of media.

2.15.4 Splitting of cells

The re-suspended cell suspension above was split between 1:3 and 1:10 cell ratio into flasks. The flasks were topped with an appropriate amount of media to make each up to 5 ml. The flasks were then incubated at 37 °C with 5 % CO_2.

2.15.5 Freezing down of cells

The cell suspension after trypsin activity was made up to 9 ml with media and 1 ml of 1 % DMSO (90 %:10 %) was added. The suspension was divided into cryo-vials (1.5 ml/vial). These vials were stored at –150 °C.

2.15.6 Isolation of proteins from cultured cells.

Cells were removed by trypsinisation and recovered by centrifugation for 5 min at 200 g. The cells were then washed twice with 5 ml ice cold PBS. The cell pellet was re-suspended in 100 µl PBS. An equal volume of 1× Reducing Loading Buffer was added to the sample. The cells were mixed by three cycles of rapid vortex for 5 sec each and lysed by boiling at 95 °C for 5 min. The mixing was repeated, and the samples were boiled again for another 5 min. This sample was either stored at –70 °C or centrifuged for 5 min at 10 000 g before electrophoresis on a SDS-PAGE gel.

2.16 Transduction

2.16.1 Protein Denaturation

Purified protein samples (contained in Tris pH 8.0) for transduction were denatured in 8 M urea and incubated at room temperature for at least 10 min. The volumes used were 500 µl or 1000 µl depending on the concentration desired.

2.16.2 Purification/Buffer exchange by G25 Sephadex

G-25 Sephadex beads were prepared in 1 X TE, autoclaved, and a 4.5 ml G-25 column was prepared in a 5 ml syringe. The column was equilibrated with media without serum and antibiotics. The denatured protein sample was loaded onto the

column and eluted with the equilibration media. Three fractions of about 2 ml were collected and the first two fractions containing the denatured protein were mixed and put on ice.

2.16.3 Tissue culture based *in vivo* protein transduction

The purified protein sample was made up to the required volume with media and an appropriate amount of serum was added. This protein sample was added to the previously split cells, in a dish with heat sterilised cover slips, for transduction to take place. The cells were incubated at 37 °C for 30 min and the media was changed. Incubation occurred until cells were ready to be analysed.

2.16.4 Microscopic detection

A cover slip was obtained from the dish and thoroughly washed with PBS. It was then mounted on 1:1000 diluted DAPI, for 20 min, to stain the nuclei. Vecta Shield was used to mount for 10 min, and the cover slip was left until dry. The slide was viewed by fluorescence microscopy both with DAPI and fluorescence filters for comparative purposes.

Immuno-fluorescence staining

Cells that were transduced with no reporter gene were cultured on heat-sterilised cover slips. After transduction, the cells were washed twice with PBS, fixed with 4 % paraformaldehyde fixative for 15 min and washed three times (5 min each wash) with 2 ml PBS (100 mM glycine was included in one wash). Cells were then

permeabilised by incubation in 2 ml PBS containing 0.1 % Triton X-100 for 2 min. Cells were washed twice with 2 ml PBS (3 min each wash) and then blocked by incubation in PBS containing 1 % BSA (PBS-BSA). Cells were incubated for an hour in 50 µl anti-DWNN primary antibody [Faro, MSc thesis, UWC, 2004] diluted (1:10 000) in PBS-BSA. Cells were washed three times in PBS (30 sec each wash) and incubated for an hour in a secondary antibody diluted (1:10 000) in PBS-BSA. Cells were washed with PBS as was the case after primary antibody treatment. Cells were then incubated for 30 min in DAPI diluted (1:10 000) in PBS-BSA. Cells were then washed thrice in PBS before mounting in Vecta Shield on microscope slides and were viewed using a Zeiss Axioplan fluorescence microscope. A Spot RT Digital camera was used to capture images.

2.16.5 Flow cytometric analysis

Cells that were growing on the dish were thoroughly washed with PBS, treated with 500 µl trypsin, and incubated at 37 °C for a minute or until they had rounded. They were then suspended in 1 ml media and transferred into a test tube to be analysed on a FACScan.

2.17 Western blotting

Protein samples were electrophoresed on PAGE gels as described in Section 2.3.2. The proteins were transferred onto a PVDF-P membrane (Amersham Pharmacia) using a Mini Protean II™ system (Bio-Rad). Before transfer the membrane was pre-

wetted in methanol for a few seconds, washed in deionised water for 5 min and equilibrated in Transfer Buffer for 10 min. The SDS PAGE gels were also equilibrated in Transfer Buffer for 10 min. Transfer was performed at 4 °C, 100 V (constant voltage) for 1 hr in pre-cooled Transfer Buffer. After transfer the membranes were stained with Ponceau S (Sigma) to check for protein transfer. The membranes were incubated in TBSMT for 1 hr. The purified primary antibody was diluted 1:5 000 in TBSMT and the membranes were incubated in the primary antibody (anti-DWNN) for 30 min. The membrane was washed three times for 10 min in TBSMT. The secondary antibody, anti-rabbit Ig horseradish peroxidase (Amersham Pharmacia) was diluted (1:20 000) in TBSMT and the membranes were incubated in this antibody for 30 min. The membrane was washed three times for 10 min in TBSMT. This was followed by three more washes with TBST. Detection was performed using the ECL + plus Western Blotting Detection System (Amersham Pharmacia), which was added to the membrane. The membrane was exposed to the film at 1 minute and 5 minutes intervals and then developed.

Blot stripping

The blot was stripped for another primary antibody incubation. The stripping was performed by the pre-wetting of the membrane in methanol for a few seconds, 5 min wash in deionised water, 5 min incubation in 0.2 M NaOH, another 5 min wash in deionised water and a final 5 min wash in TBST. The membrane could be used again by carrying on from the blocking with TBSMT incubation for 1 hr step.

2.18 Primers and Oligonucleotides

Primers and oligonucleotides (Table 3) were synthesised using a PCR-Mate EP™ Model 391 DNA Synthesiser (Applied Biosystems). They were synthesised at a 0.2 M scale on the suitable synthesis column as per manufacturer's recommendation. They were then were eluted from the column by manual deprotection and cleavage as per manufacturer's manual prescription. The quality of the primers was confirmed by electrophoresis on polyacrylamide gels as described in Section 2.3.2. Quantification of primers was conveyed by measuring the optical density at 260 nm in a spectrophotometer (one OD_{260} unit of single stranded DNA equals 33 ng/ l).

Primer/Oligonucleotide	Sequence
PGEX 5' sequencing primer	5'-d[GGGCTGGCAAGCCACGTTTGGTG]-3'
PGEX 3' sequencing primer	5'-d[CCGGGAGCTGCATGTGTCAGAGG]-3'
TAT 1	5'[GATCTGGTTACGGTCGTAAAAAACGTCGTCAGCGT CGTCGTG]-3'
TAT 2	3'[ACCAATGCCAGCATTTTTTGCAGCAGTCGCAGCAG CACCTAG]-5'
TAT 3x	5'-[GATCCGGTCTAGAGGCGAGATCTCAG]-3'
TAT 4x	3'-[GCCAGATCTCCGCTCTAGAGTCTTAA]-5'

Table 2.2: Primer and oligonucleotides sequences.

CHAPTER 3

The Architecture and Construction of TAT-PTD Fusion Proteins

3.1 Introduction

The plasma membrane of the eukaryotes was thought to be impermeable to almost all peptides and proteins. This has been demonstrated to have a rare exception with the identification of several **P**rotein **T**ransduction **D**omains (PTDs) that have the ability to penetrate into cells and can equally transduce their cargo across the poorly permeable and selective cell membrane, resulting in the accumulation of proteins inside the cell [Nagahara *et al.*, 1998; Morris *et al.*, 2001, Prochiantz, 2000; Ryu *et al.*, 2003; Schwarze *et al.*, 2000; Vocero-Akbani *et al.*, 1999].

The three widely studied and exploited PTDs are from the *Drosophila* homeotic transcription protein antennapedia (Antp), the Herpes Simplex virus structural protein VP22, and the **H**uman **I**mmunodeficiency **V**irus 1 (HIV-1) transcriptional activator TAT protein. The mechanism by which transduction by these PTDs occurs is still not yet unraveled but it is known to be independent of receptors, transporters and endocytosis. This suggests that all cell types can be potential targets. Transduction takes place through a rapid process that, at both 37 °C and 4 °C, essentially targets 100 % of cells in a protein concentration-dependent manner [Frankel and Pabo, 1988;

Gius *et al.*, 1999; Green and Lowenstein, 1988; Hawiger, 1999; Ho *et al.*, 2001; 1999; Morris *et al.*, 2001; Nagahara *et al.*, 1998; Schwarze *et al.*, 1999: Schwarze *et al.*, 2000; Vives *et al.*, 1997; Vocero-Akbani *et al.*, 1999].

Recombinant fusion proteins, containing these PTDs, can be used for the delivery of biologically active proteins into cells. This was demonstrated by the delivery of active β-galactosidase into cells [Bayley, 1999]. The delivered proteins are found both in the cytoplasm and the nucleus. The rate of cellular uptake has been found to correlate with number of arginine basic residues present in a PTD [Futaki *et al.*, 2001; Ho *et al.*, 2001]. There is thus a common mechanism that probably depends on an interaction between the basic charges on the PTD and the negative charges on the surface of the cell. Recent studies identified at least one structural membrane component that is required for PTD internalisation. It has been shown that an increase in the amount of heparin resulted in competition with TAT-PTD internalisation. Attributed to their highly basic charge, TAT peptides bind to heparin, which could possibly hinder internalisation [Nagahara *et al.*, 1998; Vocero-Akbani *et al.*, 1999].

Presently, the fusion proteins whose architecture contains TAT-PTD exhibit markedly better cellular uptake than similar fusion proteins of a 16 amino acid sequence from antennapedia. The recently devised peptoid transducers like retro-inverso form of TAT or homopolymers of arginine seem to increase cellular uptake several fold [Ho *et al.*, 2001]. The efficiency with which Antp transduces into cells

dramatically decreases with incorporation of larger proteins. VP22 internalisation has been reported, but less information about the efficiency of this PTD delivery mode is known [Wadia and Dowdy, 2002; Wadia and Dowdy, 2003].

Recombinant fusion proteins bearing the 12 amino acid **m**embrane-**t**ranslocating hydrophobic **s**equence (MTS) from the Kaposi **f**ibroblast **g**rowth **f**actor (FGF-4) are capable of transducing enzymatically active proteins directly into mammalian cells. The delivery by FGF-4 MTS was demonstrated by the transfer of protein cargoes through the plasma membrane and into the cytoplasm of cells *in vitro*. Protein transduction by FGF-4 has been combined with Cre/lox-P system so as to establish a would-be exciting and compelling innovative tool for the genetic modification of cells [Jo *et al.*, 2001].

The aim of this chapter is to describe the structural design and construction of the following TAT-PTD fusion proteins, GST-TAT-GFP, GST-TAT-GFP-DWNN$_{118}$, GST-TAT-DWNN$_{118}$ and their controls, GST-GFP and GST-GFP-DWNN$_{118}$. The constructs were generated by cloning into the pGEX-6P-2 vector, which consists of glutathione-S-transferase (GST) for expression and purification of the fusion proteins. Figs 3.1 A and B illustrate a general layout of the construction of these vectors.

Green fluorescent protein (GFP) is commonly used as a marker for genetic manipulation and cell biological studies [Chalfie, 1995; Chalfie, 1994; Cubitt *et al.*,
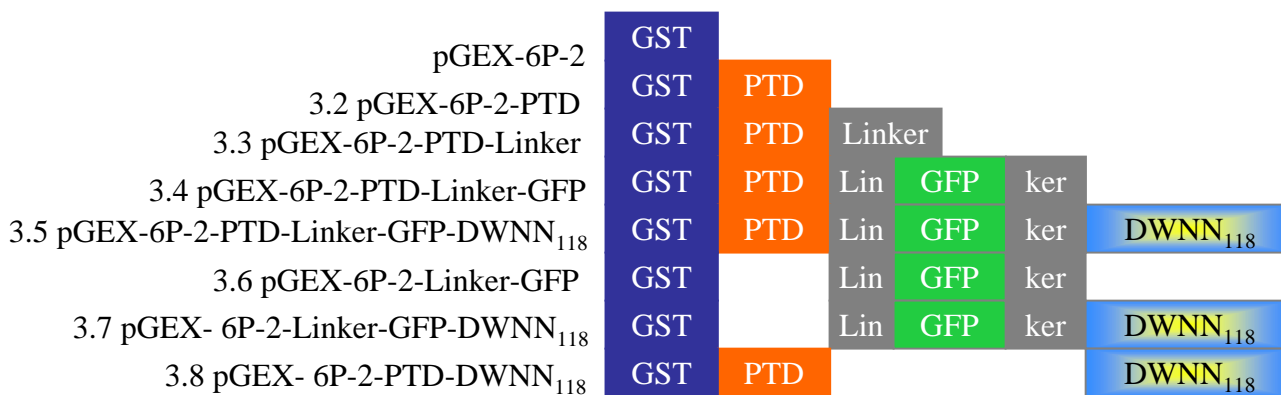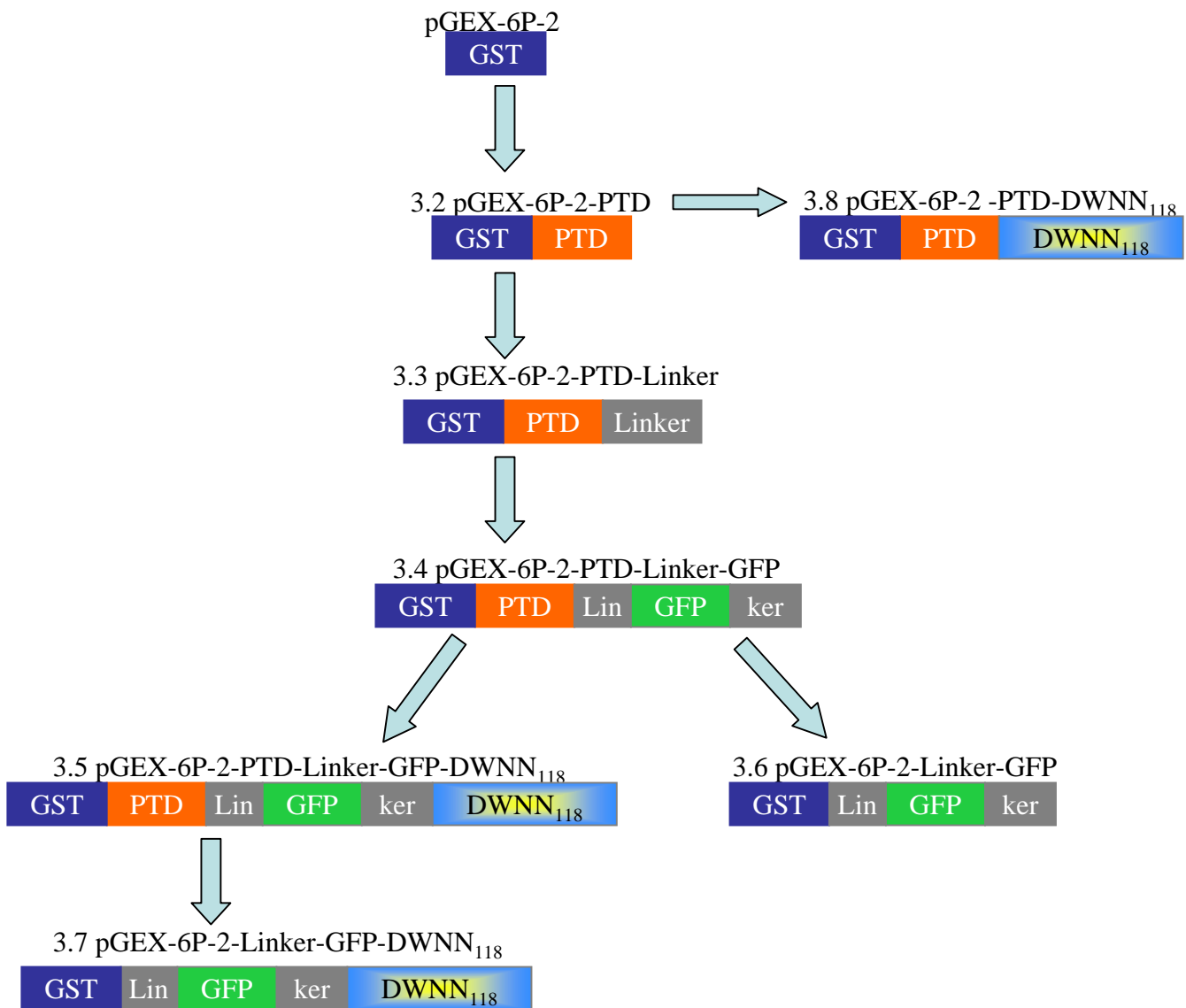
Figure 3.1A: An out-line of the engineered fusion proteins.

The representations delineate the construction of the recombinants.
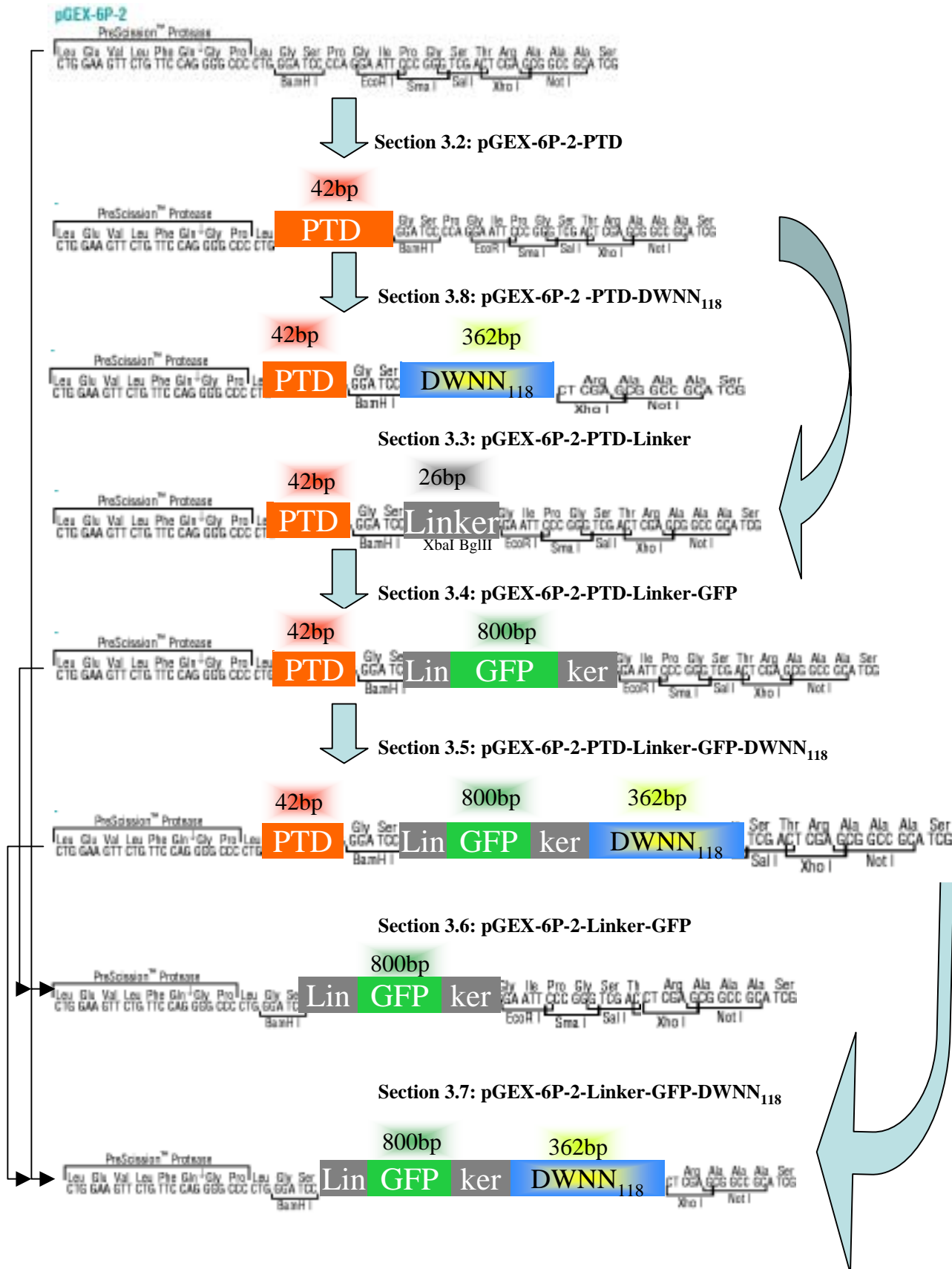
Figure 3.1B: An out-line of the engineered fusion proteins showing insertion into the multiple cloning site of the pGEX-6P-2 vector and the restriction site for the 3-C protease.

1995; Hawley *et al.*, 2004; Heim *et al.*, 1995; Mitra *et al.*, 1996]. In this study, GFP was used to report the presence of the protein of interest after transduction, as it fluoresces green and can easily be observed (section 1.6). It is widely reported not to interfere with the function of the fusion protein partner [Fortinea *et al.*, 2000; Hawley *et al.*, 2004], and is therefore a suitable fusion partner in studies of proteins of unknown functions.

A screen for genes involved in antigen processing and CTL killing led to the identification of DWNN (section 1.5). Subsequent studies revealed that this protein might be involved in apoptosis (section 1.5). This study aims to develop tools for use in the functional analysis of DWNN. The TAT-PTD provides a means of delivering DWNN into cells and allows for the *in vivo* study of the function of this protein. The construction of TAT-DWNN$_{118}$ was to show, in an undisputable manner, that GFP does not affect the correct conformation of the protein of interest, thus interfering with its function. The localisation track of this construct was to be carried out by means of primary and secondary antibodies using Western blot analysis (section 2.17), and by primary antibody and fluorescein or rhodamine using immuno-fluorescence staining (section 2.16.4) then fluorescein or rhodamine fluorescence. The negative control constructs were manufactured to demonstrate that the cellular uptake is TAT-PTD mediated rather than by any other means like by a transporter, receptor or by endocytosis.

3.2 The cloning of the Protein Transduction Domain (PTD) into pGEX-6P-2

The complementary single stranded DNA sequences, TAT 1 and 2 (Table 2.2: section 2.18), coding for the protein transduction domain (PTD) were synthesised to have *Bgl*II and *Bam*HI restriction site at the 5' and 3' ends respectively. The oligonucleotides were annealed (section 2.7.3) (Fig 3.2), diluted in series for vector insert molar ratio to vary from 1:1 to 1:10 000, and cloned by ligation into the *Bam*HI digested pGEX-6P-2 vector (Fig 3.3), since *Bam*HI and *Bgl*II are compatible, i.e. one site is capable of cloning or ligating onto another, the ligation end of these sites (*Bam*HI and *Bgl*II) was disrupted and could never be used though, while the other ligation end remained intact in that linear digestion product projected two *Bam*HI overhangs.

The vector insert molar ratio was determined using the formula:

$$\frac{\text{Vector in ng x Insert size in kb}}{\text{Vector size in kb}} \text{ x Insert vs Vector ratio}$$

So:

$$\frac{1 \text{ ng x } 0.042 \text{ kb}}{4.9 \text{ kb}} \text{ x } 1 = 0.0086 \text{ ng} \text{ for 1:1 molar ratio and}$$

and:

Figure 3.2 Annealed oligonucleotide sequences (TAT 1 and 2) coding for the PTD sequence. ⌐¬ = Amino acid translation, where Y=Tyrosine, G=Glycine, R=Arginine, K=Lysine, and Q=Glutamine.

Figure 3.3: 1 %Agarose gel electrophoresis of the *Bam*HI digested pGEX-6P-2.

Lane 1: Molecular weight marker and Lane 2: *Bam*HI Digested vector.

Dilution	pGEX-6P-2	PTD	Vector:Insert Molar ratio	Cloning/Ligation
-	1 ng	0	1:0	-
1	1 ng	0.0086 ng	1:1	+
2	1 ng	0.086 ng	1:10	+
3	1 ng	0.86 ng	1:100	+
4	1 ng	8.6 ng	1:1000	+
5	1 ng	86 ng	1:10000	No growth

Table 3.1 Test for vector re-circularisation vs insertion of pGEX-6P-2 and PTD.

The ligation mixtures were transformed into *E.coli* MC1061 (section 2.10) and plated on the nutrient agar plates containing ampicillin. Colonies were randomly picked and a colony PCR with pGEX reverse and forward primers (Table 2.2: section 2.18) was used to screen for recombinant colonies and the results showed a 42 bp size difference between the transformants (229 bp) and the negative (187 bp) colonies (Fig 3.4). This was due to the amplification of the multiple cloning site (mcs: 187 bp) in the negatives and of both the mcs and the inserted sequence in the recombinants. The most concentrated insert was, in theory, expected to yield less colonies due to successful insertion than a mere vector re-circularisation. The successful insertion depended on absolute concentration of the insert, hence the higher the insert concentration the more the insertion likelihood, where fewer colonies thus insertion would be expected. Insertion was equally dependent on the vector length after

Figure 3.4: 1 % Agarose gel electrophoresis of colony PCR screening for the cloning of the PTD sequence into pGEX-6P-2.

A. Lane 1: Molecular weight marker, Lanes 2, 4, 6, 7, 9, 11, & 12 : Successful insertion (positive clones), Lanes 3, 5, 8 and 10: Negative clones.

The positive clones were 42 bp bigger than the negative clones hence the 42 bp noticeable size difference.

linearisation, where there would be less likelihood of vector self-ligation in long linear vectors. The expected colony pattern hence successful insertion was thus, in a descending dilution manner, 5, 4, 3, 2 and 1 (Table 3.1). In practice, of this experiment in particular, the colony background pattern, due to transformation efficiency, hence successful insertion was, in a descending dilution manner, 4, 3, 1, 2 and 5 (in which there were no colonies at all). There was growth in all but one plate, the one with the highest concentration of the PTD. The plate with no PTD (Table 3.1), where re-circularisation (vector self-ligation) was expected, had more colonies than the rest. Insertion resulted in the generation of pGEX-6P-2-PTD illustrated in Fig 3.5. Small-scale plasmid DNA isolation (section 2.12) of the transformants was performed (Fig 3.8) (section 3.3). Restriction digestion would not yield any convincing results as to the successful insertion of the PTD since the disrupted *Bam*HI site would not allow the release of the insert hence a sequence analysis (section 2.6), using a pGEX reverse primer, was used to verify the presence of PTD (Figs 3.6 A and B) that was shown by colony PCR at an earlier stage above.

pGEX-6P-2-PTD was transformed into *E.coli* BL21 pLys S (DE3) to screen for the expression of GST-PTD (Fig 3.29) (section 3.9).

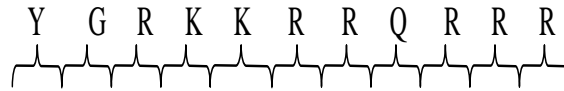### 3.3 The cloning of the linker sequence into pGEX-6P-2-PTD

Oligonucleotides (designated TAT 3x and TAT 4x in this study), coding for a linker sequence containing internal *Xba*I and *Bgl*II restriction sites, for the insertion of the
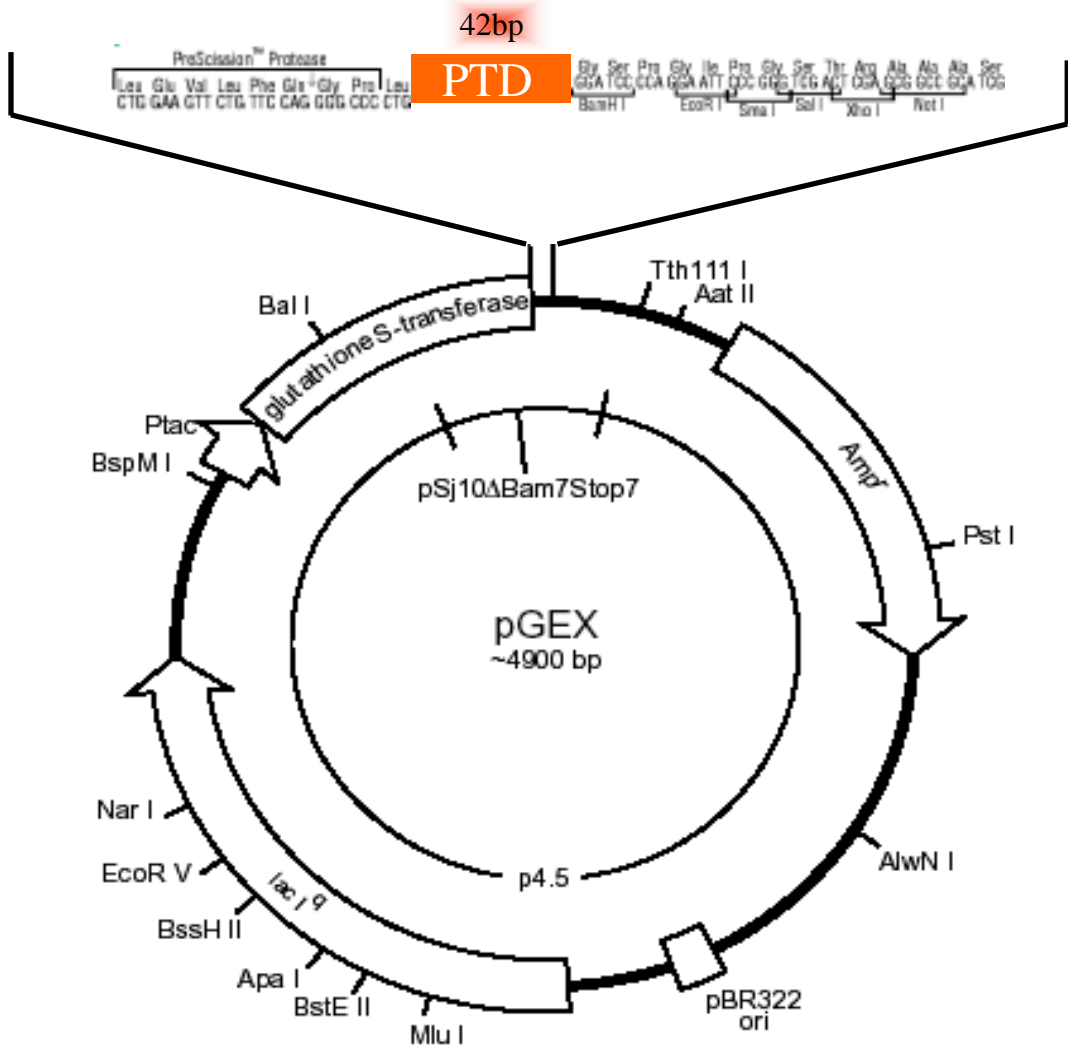
Figure 3.5 Diagrammatic representation of PTD insertion into pGEX-6P-2.

This diagram serves the illustration of how the *Ba*mHI and *Bgl*II generated PTD was inserted into the pGEX-6P-2 *Ba*mHI site.

Y   G   R   K   K   R   R   Q   R   R   R

GTTC TGTTCCA**GGGGCCCCT**GGGATCTGGTTACGGTCGTAAAAAACGTCGTCAGCGTCGTCGTGGATCCCCAGGAATTCCC
CAAGACAAGGT<u>CCCCGGGGA</u>CCCTAGACCAATGCCAGCATTTTTTGCAGCAGTCGCAGCAGCACCTAGGGGTCCTTAAGGGG

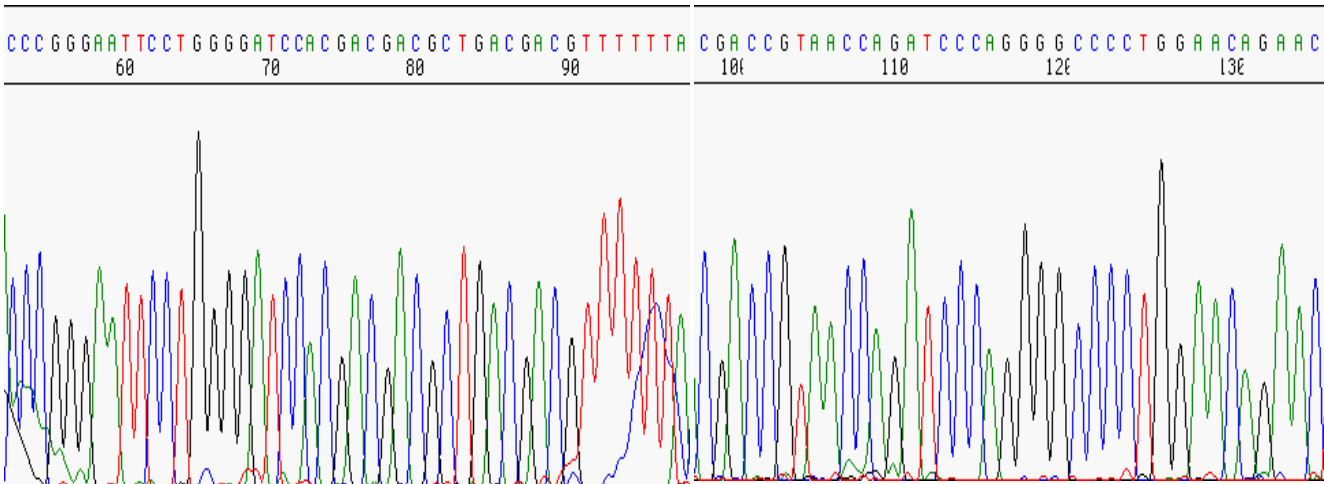pGEX-6P-2 Mcs

| PTD sequence | Bam HI | Eco RI |

Figure 3.6A: Sequence analysis verifying the presence of the PTD sequence.

The PTD sequence is shown and is flanked by *Bam HI* restriction sites.

Mcs= Multiple cloning site.

B.

Figure 3.6B: Sequence data generated for the confirmation of the presence of the PTD sequence. This
was sequenced with the pGEX reverse primer hence an opposite orientation of the PTD sequence.

GFP reporter gene, were synthesised (Table 2.2: section 2.18). This sequence was created to have *Bam*HI and *Ec*oRI restriction sites for cloning fusion protein inserts, which could be used as diagnostic sites for linker incorporation into pGEX-6P-2-PTD (Fig 3.7). The pGEX-6P-2-PTD construct was digested with *Bam*HI and *Ec*oRI (Fig 3.8). The construct was first digested with each enzyme, separately, to test their capability to successfully digest. The linker sequence was cloned into pGEX-6P-2-PTD. The vector insert molar ratio was determined using the formula:

$$\frac{\text{Vector in ng x Insert size in kb}}{\text{Vector size in kb}} \text{ x Insert vs Vector ratio}$$
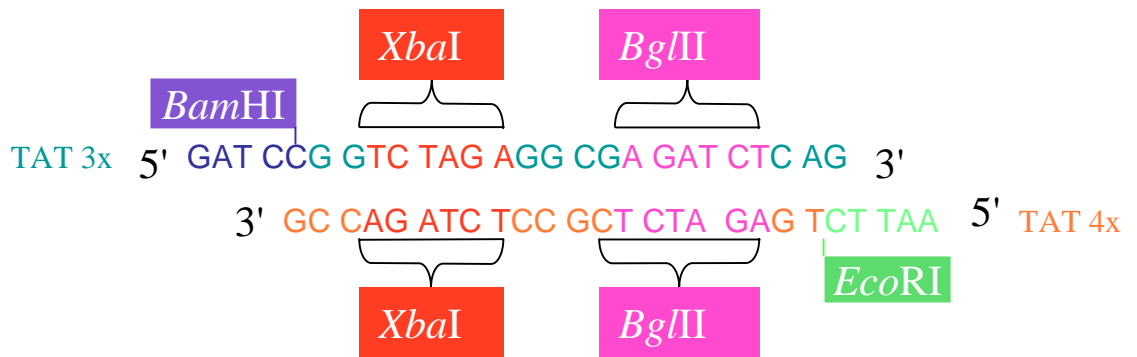
So:

$$\frac{1 \text{ ng x } 0.026 \text{ kb}}{4.942 \text{ kb}} \text{ x } 1 = 0.0053 \text{ ng for 1:1 molar ratio and}$$

| Dilution	pGEX-6P2-PTD	Linker	Vector:Insert Molar ratio	Cloning/Ligation
-	1 ng	0	1:0	-
1	1 ng	0.0053 ng	1:1	+
2	1 ng	0.053 ng	1:10	+
3	1 ng	0.53 ng	1:100	+
4	1 ng	5.3 ng	1:1000	+
5	1 ng	53 ng	1:10000	+

Table 3.2 Test for vector re-circularisation vs insertion of pGEX-6P-2-PTD and Linker sequence.

Figure 3.7: Annealed oligonucleotide sequences (TAT 3x and 4x) coding for the linker sequence.

The oligonucleotides were generated with *Ba*mHI and *EcoR*I for insertion into the pGEX-6p-2-PTD vector and with *Xba*I and *Bgl*II for inserting the *GFP* reporter gene.
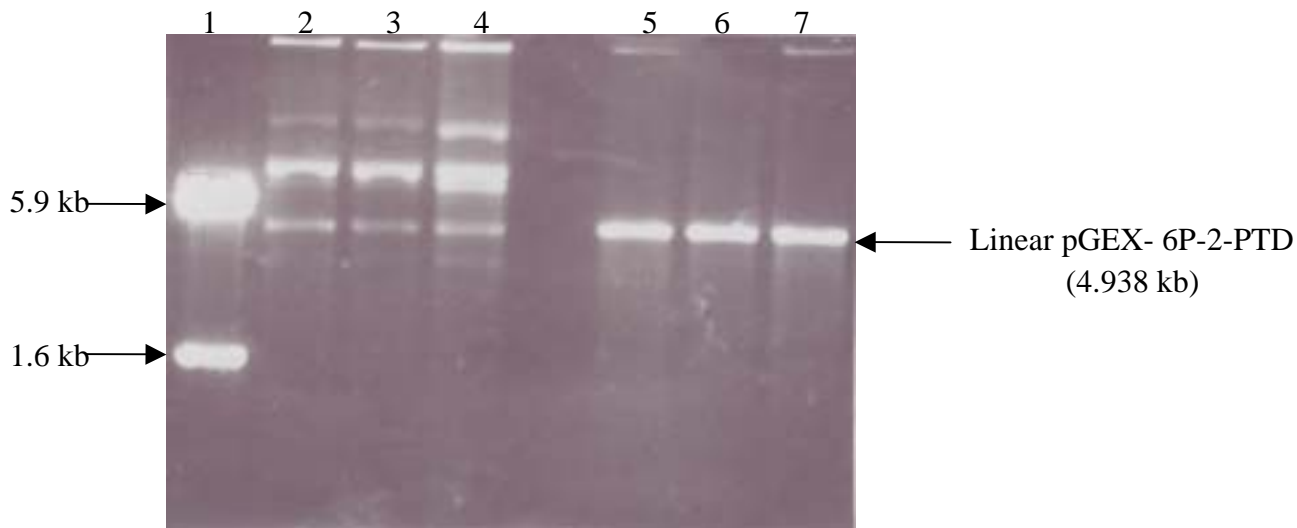
Figure 3.8: 1 % Agarose gel electrophoresis of the small scale plasmid isolation of pGEX-6P-2-PTD and its digestion with *Bam*HI and *Eco*RI double digest.

Lane 1: Molecular weight marker , Lanes 2, 3 & 4: Undigested small scale plasmid isolation (clones),   Lanes 5, 6 & 7: *Bam*HI and *Eco* RI digestion products (digests).

Colony PCR was used to screen for positive colonies and showed a 26 bp size difference between the transformants (255 bp) and the negative (229 bp) clones (Fig 3.9). Restriction digestion would not show the insert since the size of the linker sequence was small (the vector:insert size ratio was immense, that was an attribute accounting for an insert not being visible by gel electrophoresis in fig 3.10 after being released). Small scale DNA isolation (section 2.12) was performed and the presence of the linker sequence was confirmed by restriction digestion using *Xba*I and *Bgl*II separately (Fig 3.10). Since there were neither *Xba*I nor *Bgl*II sites on pGEX-6P-2-PTD, the successful digestion of the transformants with these enzymes would verify the presence of the linker sequence. Successful insertion of the linker sequence into pGEX-6P-2-PTD generated pGEX-6P-2-PTD-Linker (Fig 3.11). Sequence analysis (section 2.6), using pGEX reverse primer, served further confirmation of the successful insertion (Fig 3.12).

pGEX-6P-2-PTD-Linker was transformed into *E.coli* BL21 pLys S (DE3) to screen for the expression of GST-PTD-Linker (Fig 3.29) (section 3.9).

3.4 The cloning of GFP into pGEX-6P-2-PTD-Linker

The GFP cDNA fragment was removed from the pGFPC₁ vector (Clontech) by restriction digestion of this plasmid with *Bam*HI and *Nhe*I (Fig 3.13 A and D) and gel purified. pGEX-6P-2-PTD-Linker was digested with *Bgl*II and *Xba*I, the sites that were engineered with the linker (Fig 3.13 B and C), to generate complementary
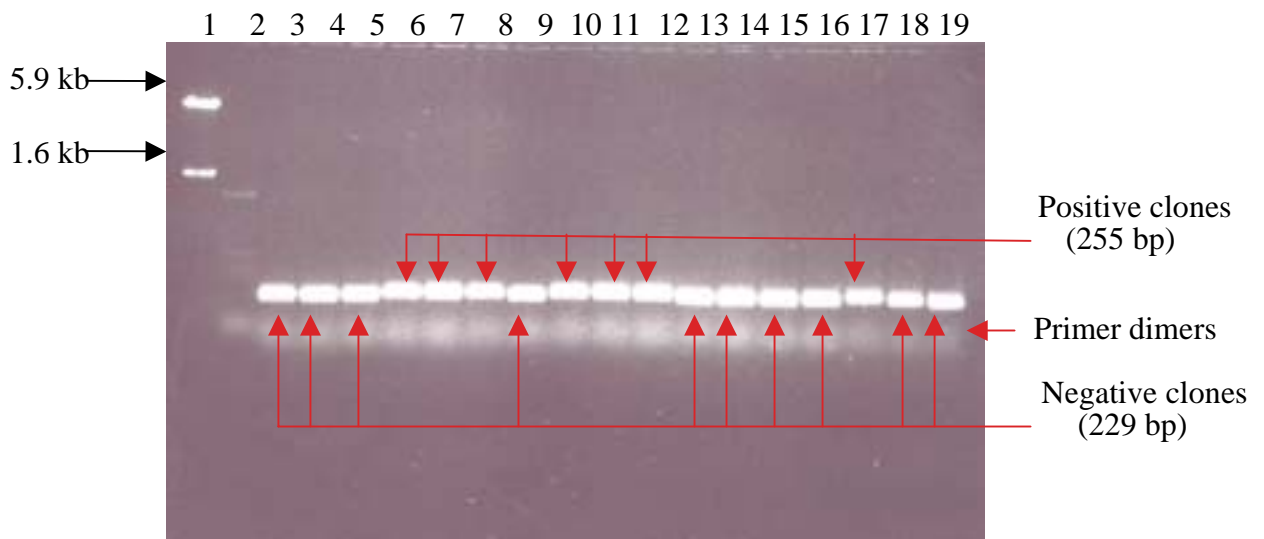
Figure 3.9: 1 % Agarose gel electrophoresis of colony PCR screening for the cloning of the Linker sequence into pGEX-6P-2-PTD.

Lane 1 and 2: Molecular weight markers, Lanes 3-19: Clones.

The positive clones were 26 bp bigger than the negative clones hence the 26 bp noticeable size difference.
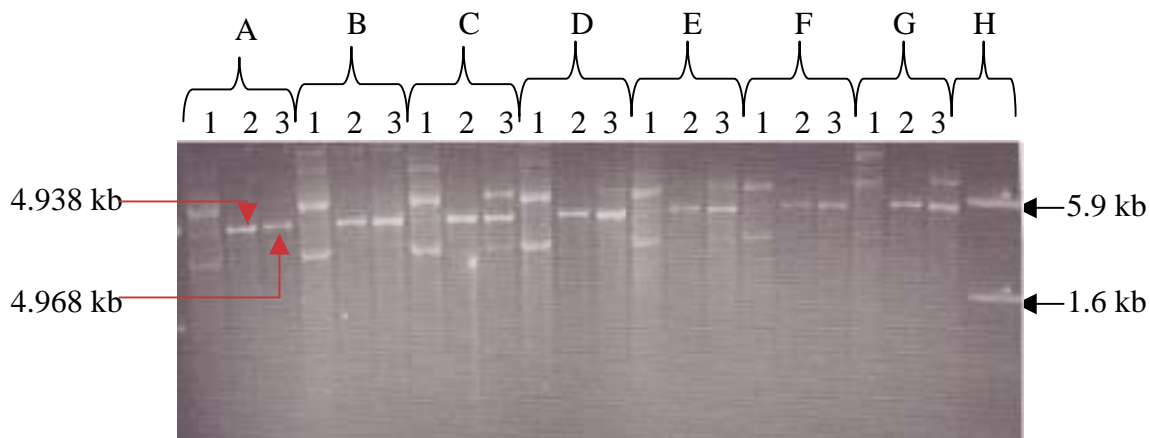
Figure 3.10: 1 % Agarose gel electrophoresis of the small scale isolation of pGEX-6p-2-PTD-linker and its digestion with *Bam*HI/*Eco*RI or with *Xba*I to screen for the presence of the linker sequence.

Regions: A, B, C, D, E, F, and G: different clones of the same construct, Lane 1: Undigested small scale plasmid DNA isolation, Lane 2: Digestion with *Bam*HI/*Eco*RI, Lane 3: Digestion with *Xba*I, Lane H: Molecular weight marker.

The multiple bands in C3, E3 and G3 could be due to incomplete digestion or to the clones being negative, but since they were screened by colony PCR the explanation is that of incomplete digestion.
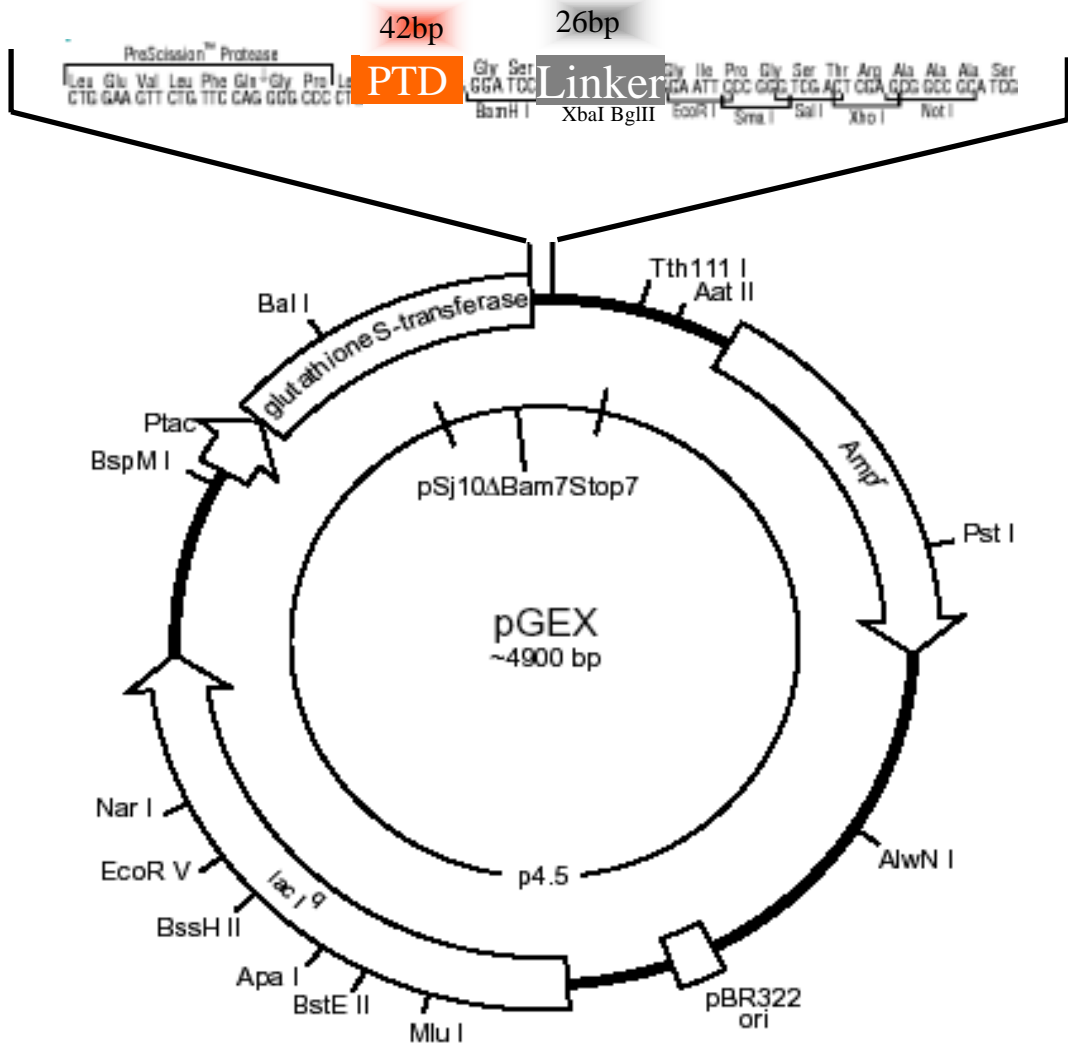
Figure 3.11: Diagrammatic representation of the insertion of the linker sequence into pGEX-6P-2-PTD.

An illustration on how the linker sequence, generated with *Ba*mHI and *EcoR*I, was inserted into the pGEX-6P-2-PTD *Ba*mHI and *EcoR*I sites. The *Xba*I and *Bgl*II sites are within the linker sequence.
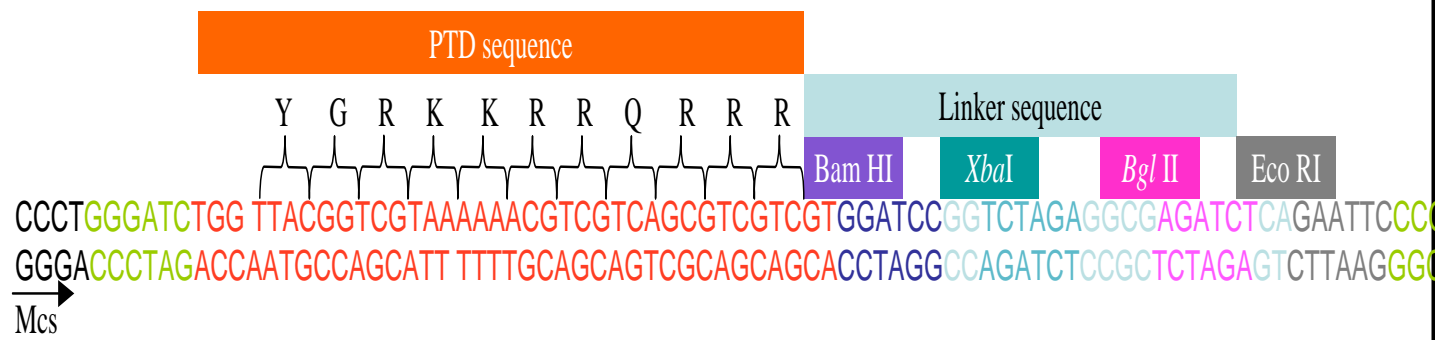
Figure 3.12: Sequence analysis verifying the presence of PTD-Linker sequences and relevant restriction sites.

The Linker sequence is shown and is flanked by *Bam HI* and *Eco RI* restriction sites.

Mcs= Multiple cloning site.
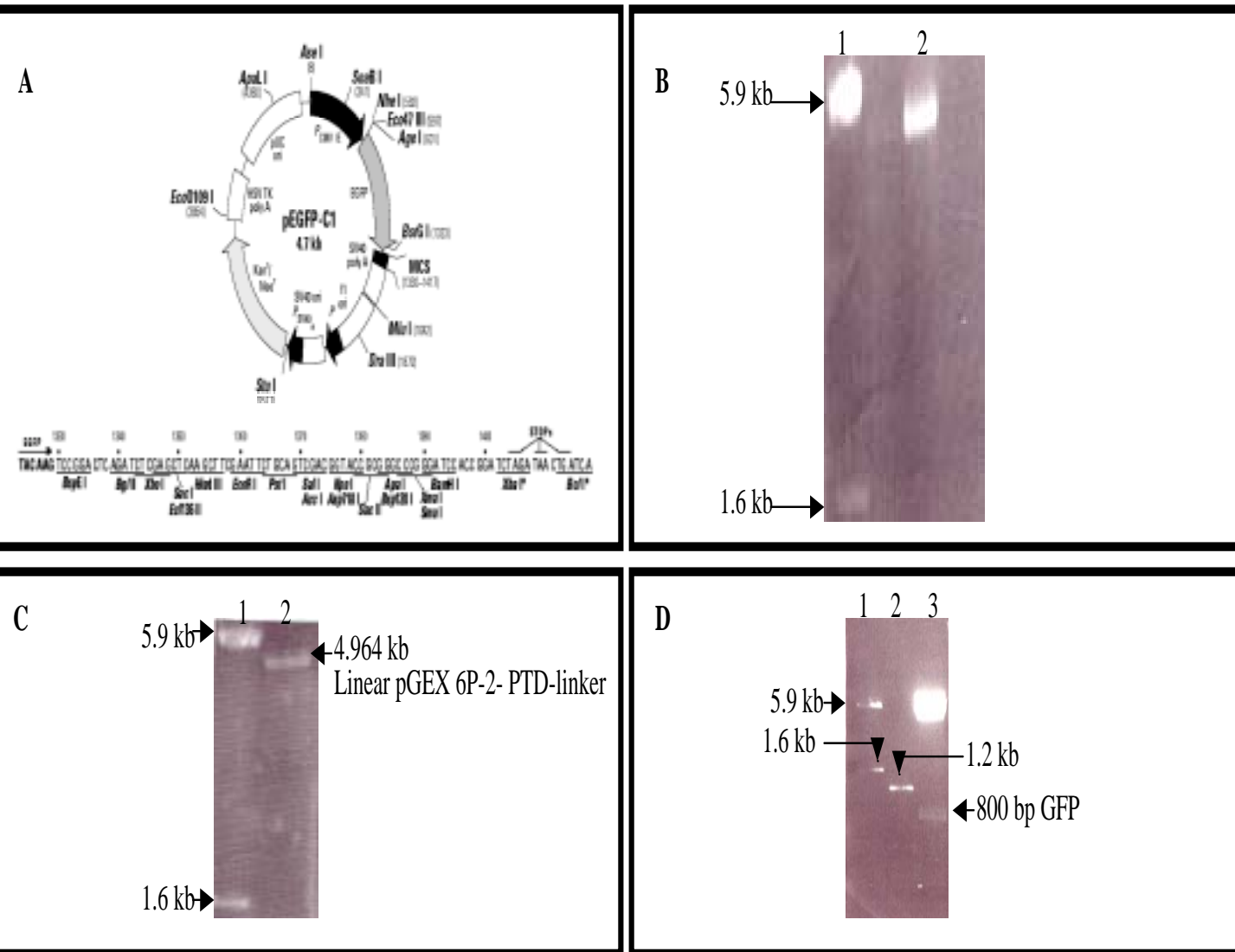
Figure 3.13: 1 %Agarose gel electrophoresis of the pGEX-6P-2-PTD-linker construct digested with *Xba*I/*Bgl*II and of pGFPC$_1$ digested with *Nhe*I/*Bam*HI.

A. Diagrammatic representation of the pGFPC$_1$ vector from which the GFP cDNA fragment was released.

B. Gel electrophoresis of the pGEX-6P-2-PTD-linker construct digested with *Xba*I (Lane 2) and Lane 1: Molecular weight marker..

C. Gel electrophoresis of the heat in-activated *Xba*I pGEX-6P-2-PTD-linker digest, digested with *Bgl*II (Lane 2) and Lane 1: Molecular weight marker.

D. Gel electrophoresis of pGFPC$_1$ digested with *Nhe*I/*Bam*HI: Lane 1: Molecular weight marker, Lane 2: Molecular weight marker, Lane 3: *Nhe*I/*Bam*HI Digest.

overhangs. pGEX-6P-2-PTD-Linker was first digested with *Xba*I, which was heat inactivated, and then with *Bgl*II. *Bgl*II was first tested for successful digestion to confirm its activity. The *Nhe*I and *Xba*I sites are compatible, i.e., one site is capable of cloning or ligating onto another, the ligation end of these sites (*Nhe*I and *Xba*I) was disrupted as is the case with *Bam*HI and *Bgl*II hence the GFP fragment was then cloned into the *Bgl*II and *Xba*I digested pGEX-6P-2-PTD-Linker. Colony PCR was used to screen for the positive clones (Fig 3.14). A small scale DNA isolation (section 2.12) was performed on the positive clones (lanes 2, 4 and 6) and further screening by restriction digestion (lanes 7 and 8) was performed (Fig 3.15). PTD remained intact, while GFP and its linker were released. Insertion was thus verified. Positive clones contained GFP fragment within the linker sequence. Fig 3.16 illustrates the pGEX-6P-2-PTD-Linker-GFP construct.

pGEX-6P-2-PTD-Linker-GFP was transformed into *E.coli* BL21 pLys S (DE3) to screen for the expression of GST-PTD-Linker-GFP (Figs 3.29 and 3.30) (section 3.9).

3.5 The cloning of DWNN$_{118}$ into pGEX-6P-2-PTD-Linker-GFP

PCR amplification of DWNN$_{118}$ generated a 363 bp fragment, which was cloned into the pGEM-T easy vector. Small-scale plasmid DNA isolation of the transformants was performed. The transformants were screened for the presence of DWNN$_{118}$ by digestion with *Bam*HI and *Xho*I (Fig 3.17 A). The pGEX-6P-2-PTD-GFP construct was digested with *Bgl*II and *Sal*I (Fig 3.17 B), after single digests to test the digestion
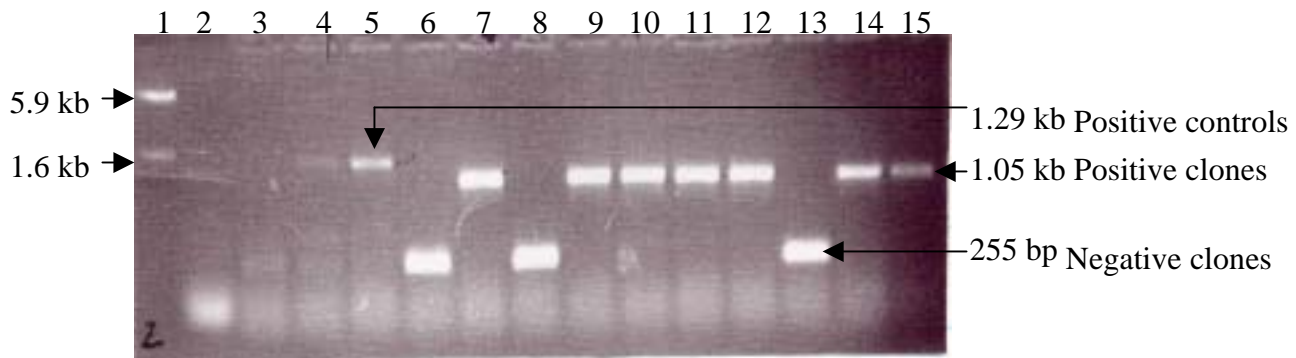
Figure 3.14: 1 %Agarose gel electrophoresis of a colony PCR screening for the presence of the GFP fragment into pGEX-6P-2-PTD-linker.

The positive controls represent GFP-DWNN$_{81}$ clones where the experiment was previously performed while the positive clones show that the GFP fragment was successfully inserted into pGEX-6P-2-PTD-linker.

Lane 1: Molecular weight marker, Lane 2: Negative control (water), Lanes 3, 6, 8 & 13: Negatives, Lanes 4 & 5: Positive controls, Lanes 7, 9, 10, 11, 12, 14 & 15: Positive clones.
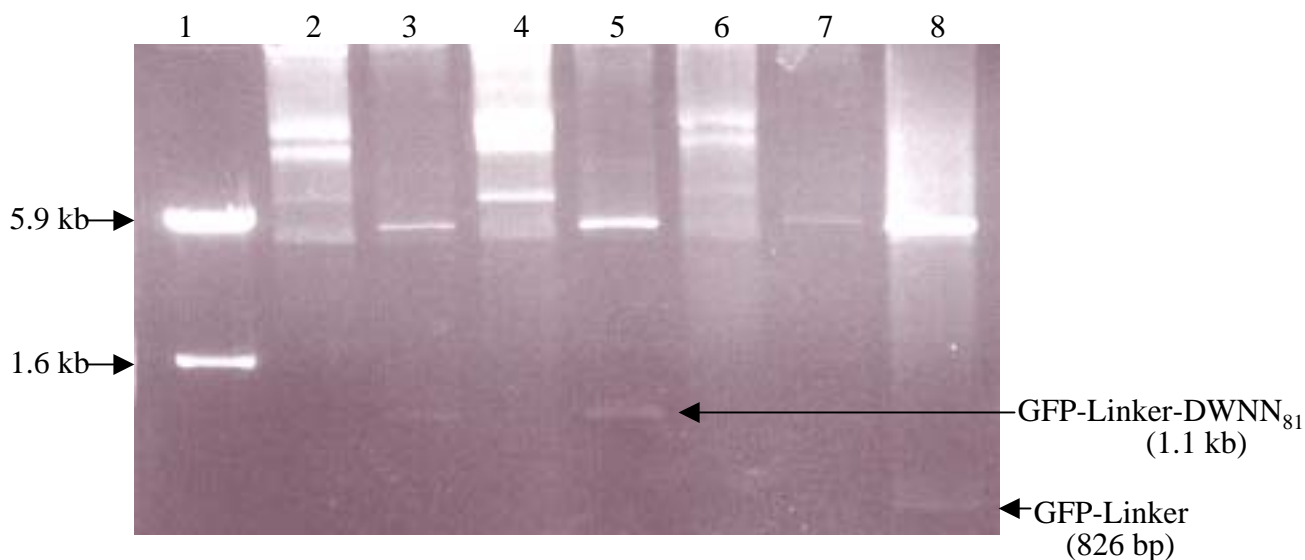
Figure 3.15: 1 %Agarose gel electrophoresis of the pGEX-6P-2-PTD-linker-GFP construct digested with *Bam*HI/*Xho*I to release GFP and its linker.

Lane 1: Molecular weight marker, Lanes 2, 4 & 6: Undigested small scale plasmid DNA isolation, Lanes 3 & 5: *Bam*HI/*Xho*I Digests of positive controls (positive control as in previous picture), Lanes 7 and 8: *Bam*HI/*Xho*I Digests of positive clones.

Figure 3.16: Diagrammatic representation of the insertion of the GFP fragment into pGEX-6P-2-PTD-Linker.

Illustrated here is how the *GFP* reporter gene fragment, obtained from the pGFPC$_1$ *Nhe*I and *Ba*mHI sites, was inserted into the pGEX-6P-2-PTD-linker *Xba*I and *Bgl*II sites within the linker sequence.
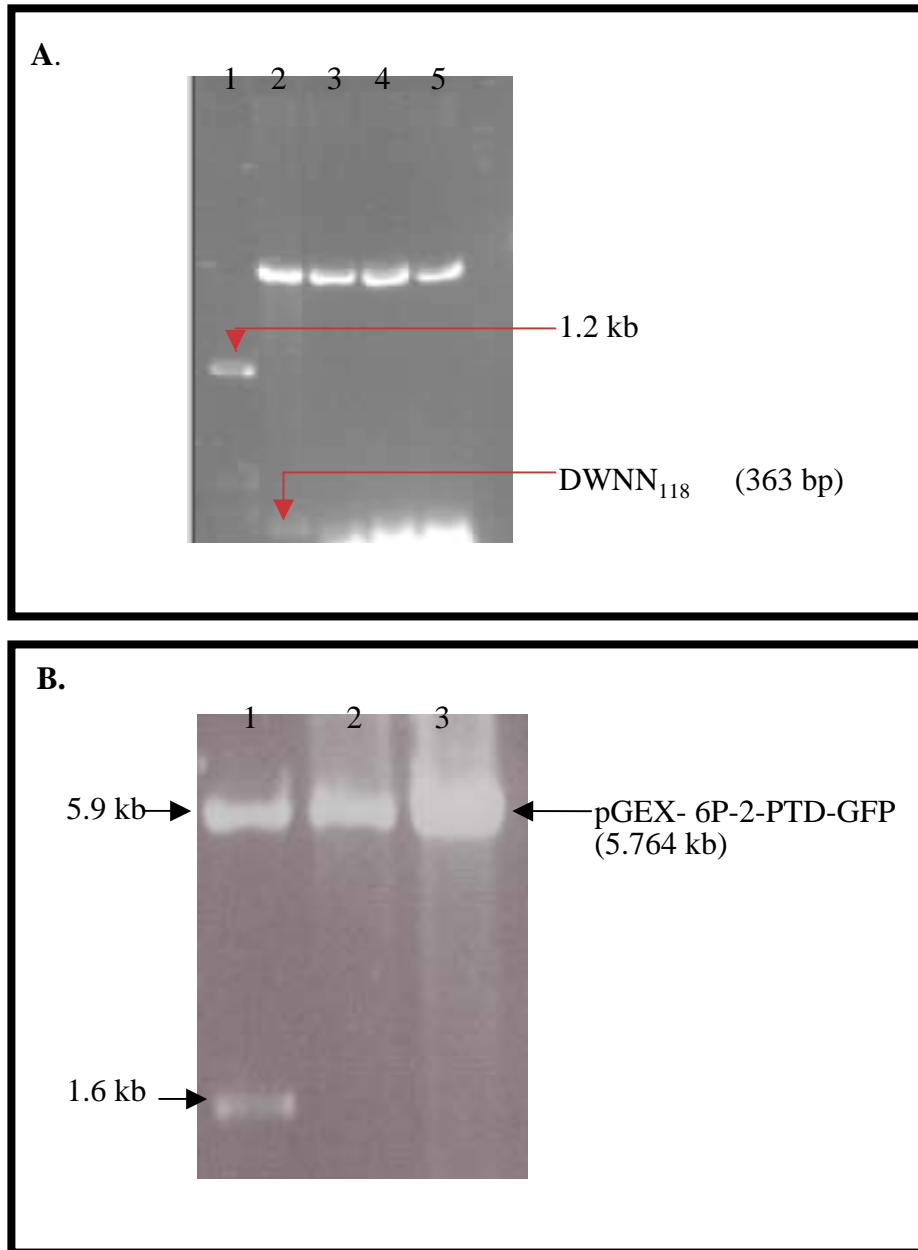
Figure 3.17: 1 % Agarose gel electrophoresis of pGEM-T easy-DWNN$_{118}$ digested with *Bam*HI/*Xho*I and of pGEX-6P-2-PTD-GFP digested with *Bgl*II/*Sal*I.

A. Gel electrophoresis of pGEM-T easy-DWNN$_{118}$ digested with *Bam*HI/*Xho*I (Lanes 2-5) and Lane 1: Molecular weight marker.

B. Gel electrophoresis of the digestion of pGEX-6P-2-PTD-GFP with *Bgl*II/*Sal*I (Lanes 2 & 3) and Lane 1: Molecular weight marker.

capability of each. These sites are respectively compatible with *Bam*HI and *Xho*I. Such sites would be disrupted after cloning though. The 363 bp long DWNN$_{118}$ PCR fragment was thus cloned into pGEX-6P-2-PTD-GFP (Fig 3.20), and colony PCR was used to screen for insertion (Fig 3.18 A and B). Small scale DNA isolation (section 2.12) was performed and a further screening by restriction digestion was performed (Fig 3.19). This analysis showed a successful insertion of DWNN$_{118}$ into pGEX-6P-2-PTD-Linker-GFP since the right sized insert was released.

pGEX-6P-2-PTD-Linker-GFP-DWNN$_{118}$ was transformed into *E.coli* BL21 pLys S (DE3) to screen for the expression of GST-PTD-Linker-GFP-DWNN$_{118}$ (Fig 3.30) (section 3.9).

3.6 The cloning of GFP into pGEX-6P-2

The GFP cDNA fragment was cut from pGEX-6P-2-PTD-GFP by digestion with *Bam*HI/*Xho*I (Fig 3.15) (section 3.4), PTD thus not included. This fragment was cloned into pGEX-6P-2, which was digested with *Bam*HI/*Xho*I. Colony PCR was performed to screen for the cloning of GFP into pGEX-6P-2 (Fig 3.21 A and B). Small-scale DNA isolations (section 2.12) were performed on the positive clones and further screening by restriction digestion with *Bam*HI/*Xho*I was used to verify the insertion of GFP (Fig 3.22). Fig 3.23 shows a diagrammatic insertion of GFP into pGEX-6P-2.
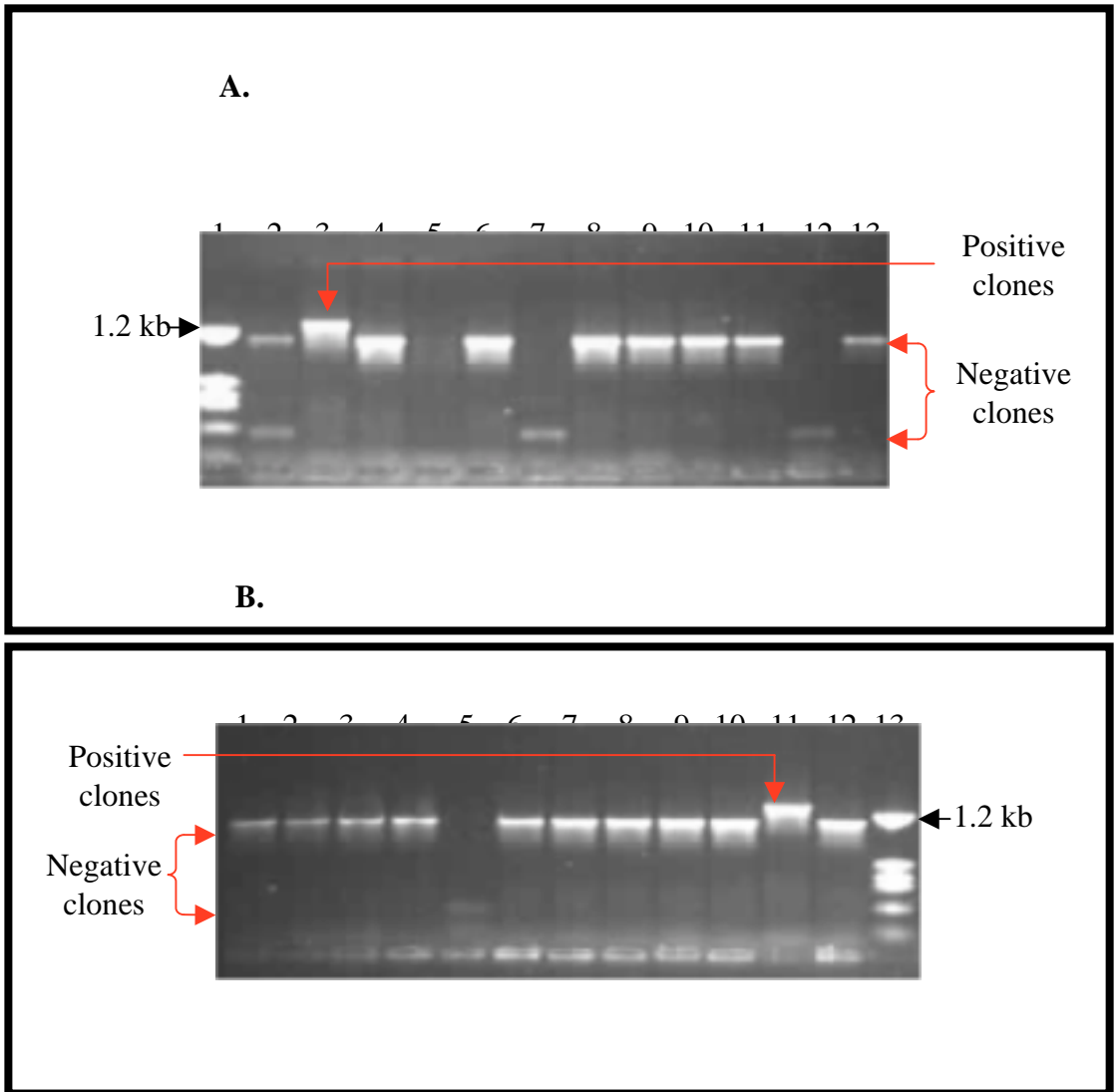
Figure 3.18: 1 % Agarose gel electrophoresis of colony PCR screening for the cloning of DWNN$_{118}$ fragment into pGEX-6P-2-PTD-GFP.

A. Lane 1: Molecular weight marker, Lanes 2, 4, 5, 6, 7, 8, 9, 10, 11, 12 & 13 : Negatives, Lane 3: Successful insertion (positive clone),

B. Lane 11: Positive clone, Remaining clones: Negatives, Lane 13: Molecular weight marker.
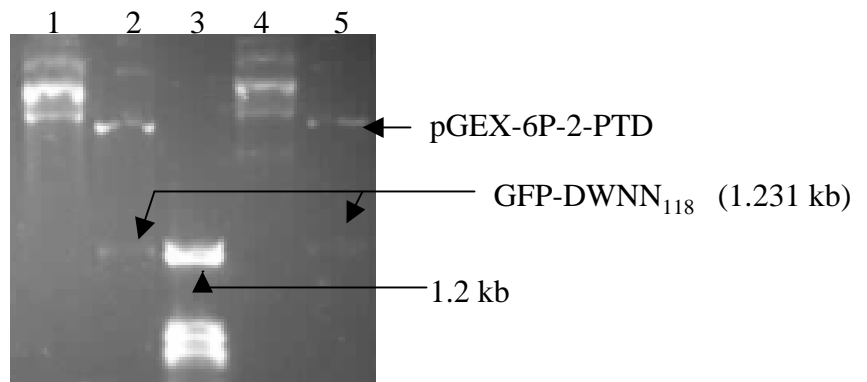
Figure 3.19: 1 % Agarose gel electrophoresis of the small scale DNA isolation of the pGEX-6P-2-PTD-GFP-DWNN$_{118}$ construct and its digestion with *Ba*mHI/*Xho*I to release GFP-DWNN$_{118}$.

Lanes 1 & 4: Undigested small scale plasmid DNA, Lane 3: Molecular weight marker, Lanes 2& 5: *Ba*mHI/*Xho*I Digests.

Figure 3.20: Diagrammatic representation of the insertion of the DWNN$_{118}$ fragment into pGEX-6P-2-PTD-GFP.

This diagram demonstrates how the DWNN$_{118}$ gene fragment, obtained from the pGEM-T easy-DWNN$_{118}$ *Ba*mHI and *Xho*I sites, was inserted into the pGEX-6P-2-PTD-linker-GFP *Bgl*II and *Sal*I sites.

Figure 3.21: 1 % Agarose gel electrophoresis of colony PCR screening for the cloning of GFP fragment into pGEX-6P-2.

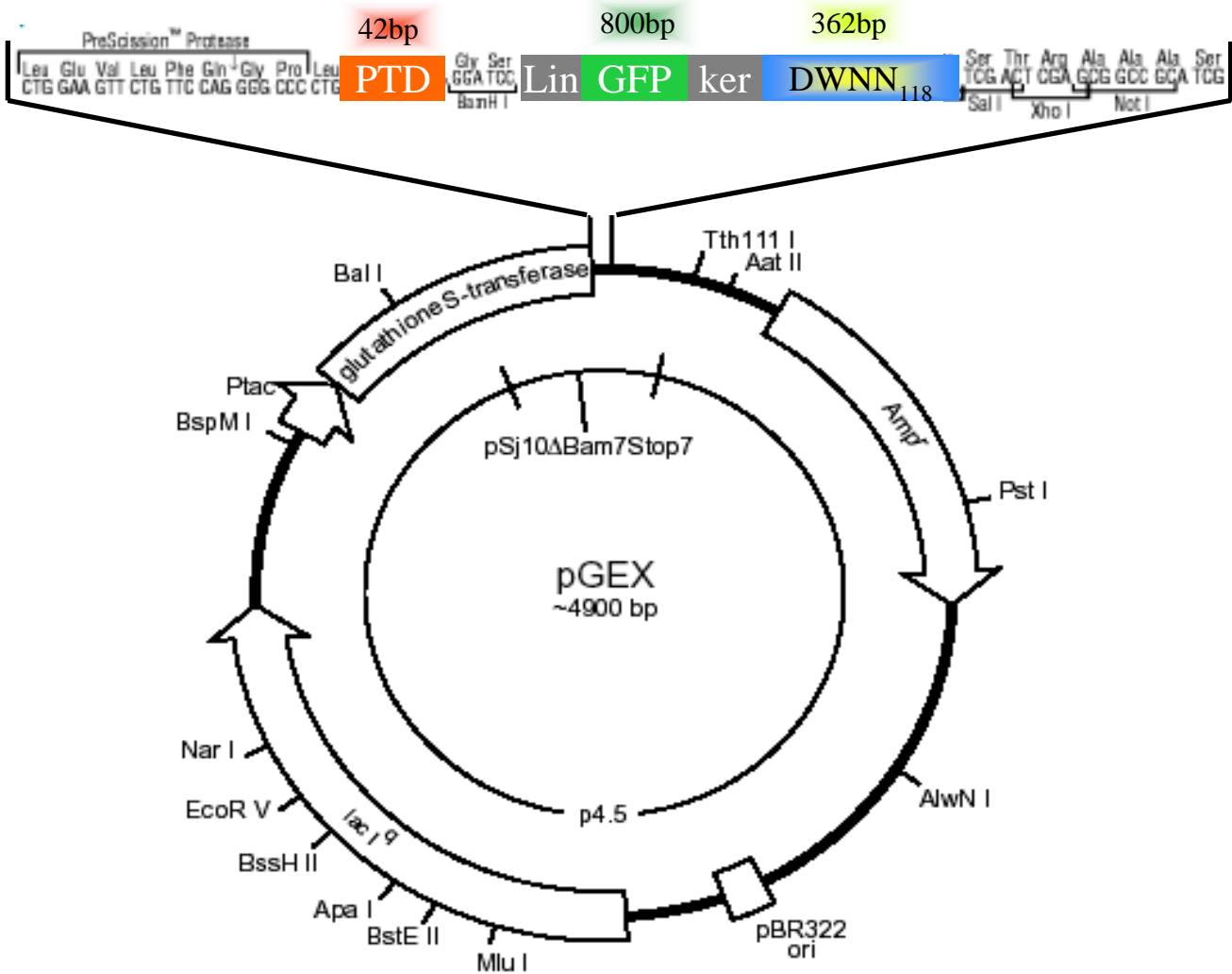**A.** Lane 1: Molecular weight marker, Lanes 2, 7 & 13: Positives, Remaining clones: negatives.

B. Lane 15: Molecular weight marker, Lanes 3, 11 , 12 & 14: Positives, Remaining clones : negatives.

Figure 3.22: 1 % Agarose gel electrophoresis of the small scale DNA isolation of the pGEX-6P-2-GFP construct and its digestion with *Bam*HI/*Xho*I to release GFP.

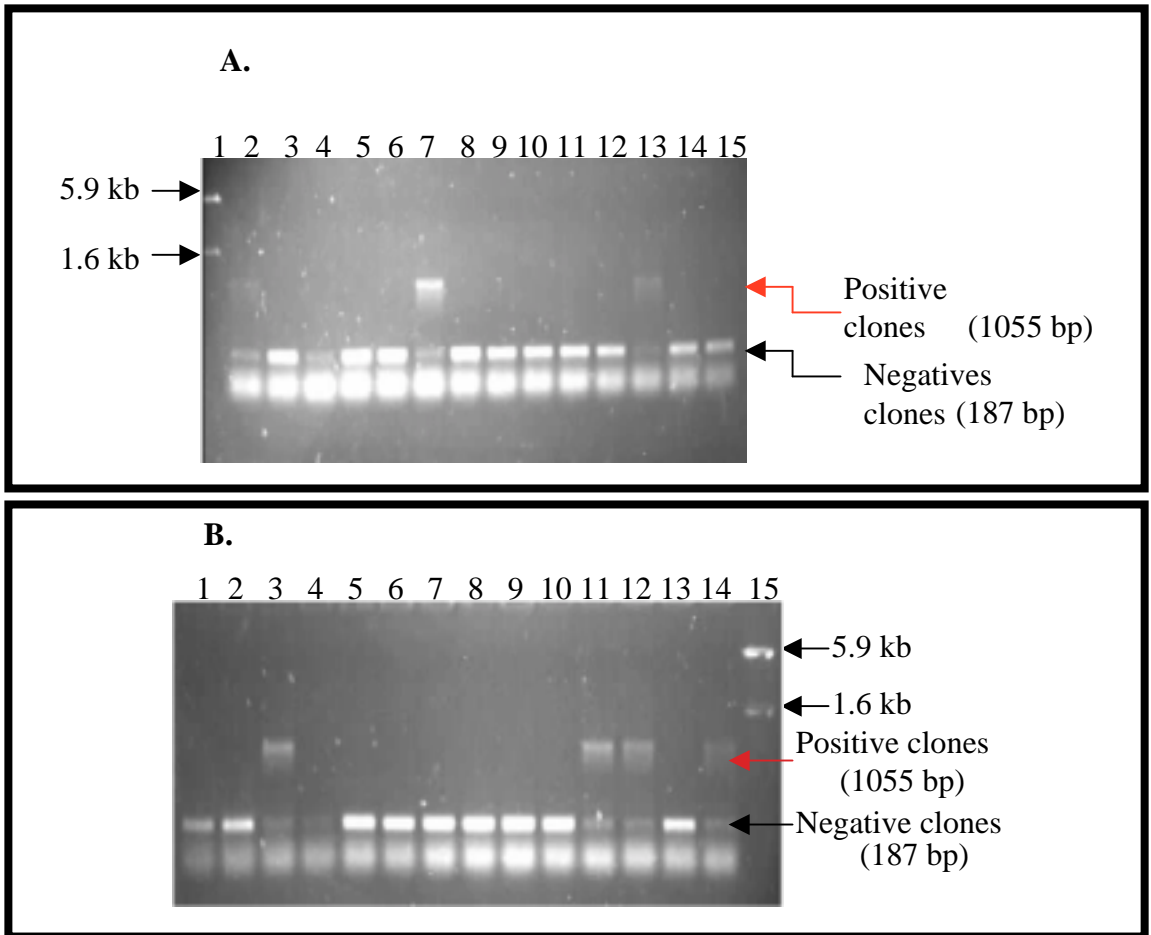Lane 1: Molecular weight marker, Lanes 2, 4, 6,8, 10, 12, and 14: Undigested small scale plasmid DNA isolation, and Lanes 3, 5, 7, 9, 11, 13 and 15: *Bam*HI/*Xho*I Digests.
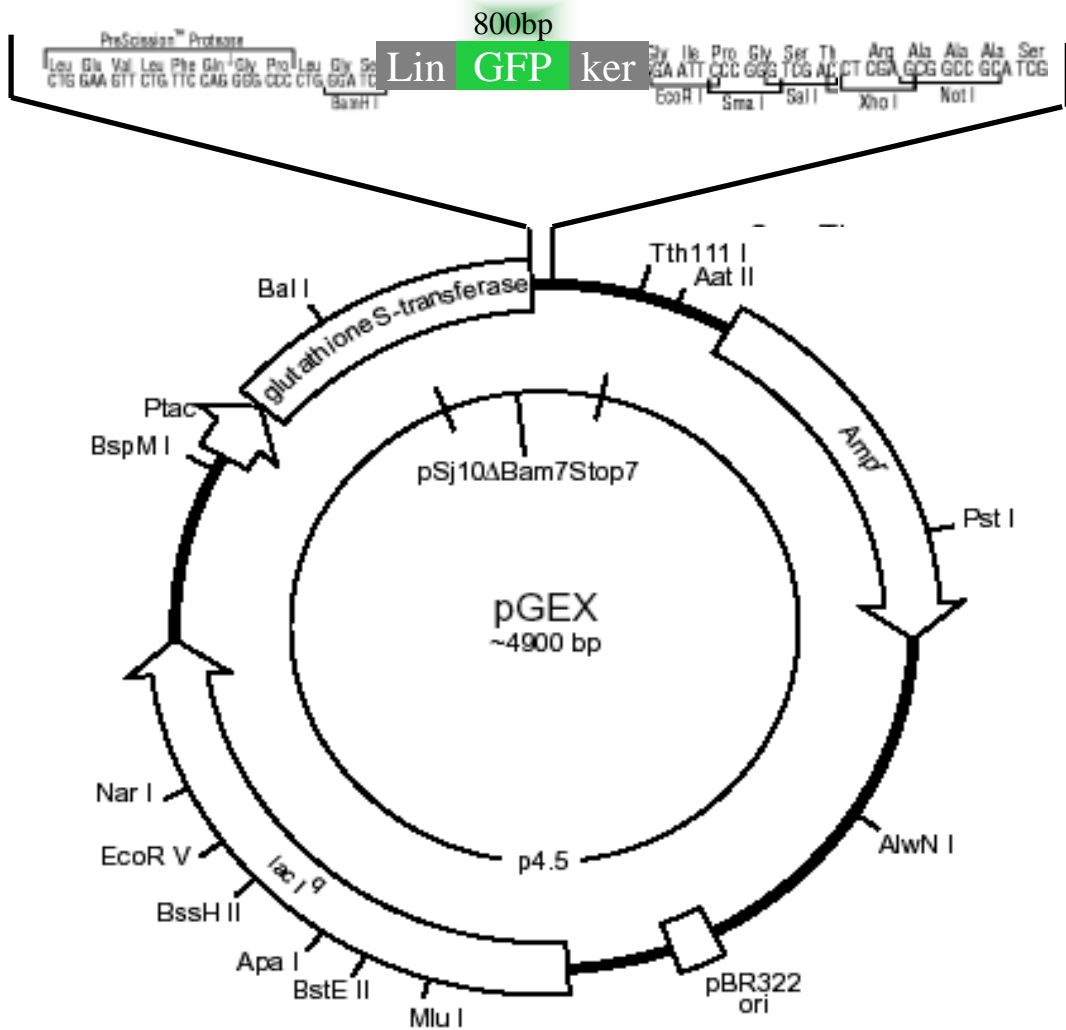
Figure 3.23: Diagrammatic representation of the insertion of the GFP fragment into pGEX-6P-2.

A demonstration on how the Linker-GFP gene fragment, digested out of the pGEX-6P-2-PTD-linker-GFP *Ba*mHI and *Xho*I sites, was inserted into the pGEX-6P-2 *Ba*mHI and *Xho*I sites.

pGEX-6P-2–GFP was transformed into *E.coli* BL21 pLys S (DE3) to screen for the expression of GST-GFP (Fig 3.30) (section 3.9).

3.7 The cloning of GFP-DWNN$_{118}$ into pGEX-6P-2

The GFP-DWNN$_{118}$ fragment released from pGEX-6P-2-PTD-GFP-DWNN$_{118}$ by digestion with *Bam*HI/*Xho*I (Fig 3.19) (section 3.5), PTD was excluded in this case too. This fragment was cloned into pGEX-6P-2 digested with *Bam*HI/*Xho*I. Colony PCR was used to screen for the GFP-DWNN$_{118}$ insertion (Fig 3.24) and a small scale DNA isolation (section 2.12) was performed on the positive colonies and restriction digestion was performed for further screening. This confirmed the construction of pGEX-6P-2-Linker-GFP-DWNN$_{118}$ (Fig 3.25).

pGEX-6P-2–Linker-GFP-DWNN$_{118}$ was transformed into *E.coli* BL21 pLys S (DE3) to screen for the expression of GST-GFP-DWNN$_{118}$ (section 3.9).

3.8 The cloning of DWNN$_{118}$ into pGEX-6P-2-PTD

The DWNN$_{118}$ PCR fragment (section 3.5) was cloned into pGEX-6P-2-PTD digested with *Bam*HI/*Xho*I. Colony PCR was performed to screen for the presence of the insert (Fig 3.26 A and B). Small scale DNA isolation (section 2.12) of the positive colonies was performed. Clones were farther screened by restriction digestion (Fig 3.27) and successful insertion was confirmed. The construct generated was pGEX-6P-2-PTD-DWNN$_{118}$ (Fig 3.28).
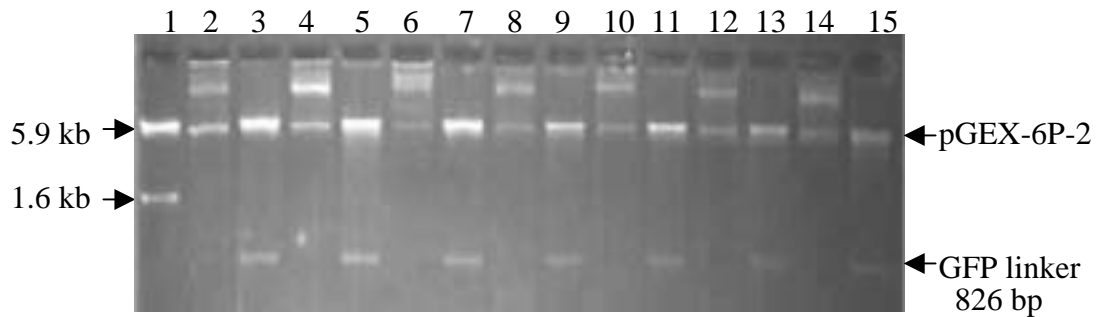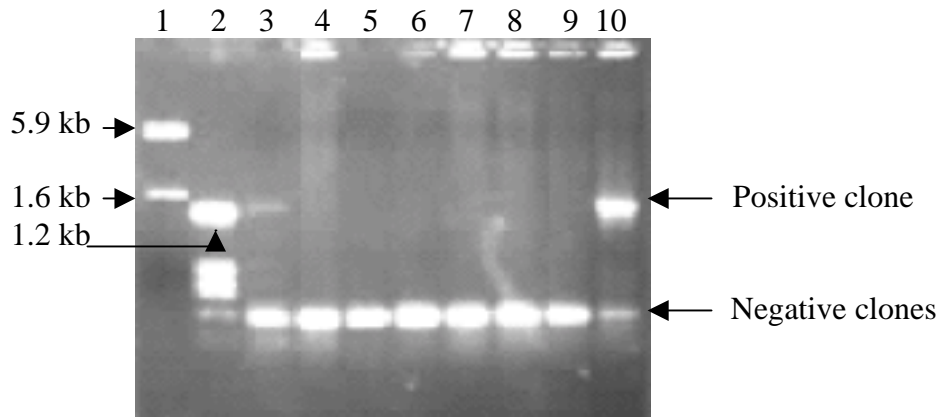
Figure 3.24: 1 % Agarose gel electrophoresis of colony PCR screening for the cloning of GFP-DWNN$_{118}$ fragment into pGEX-6P-2.

Lane 1: Molecular weight marker, Lane 2: Molecular weight marker, Lanes 3-9: Negative clones, Lane 10: Positive clone.
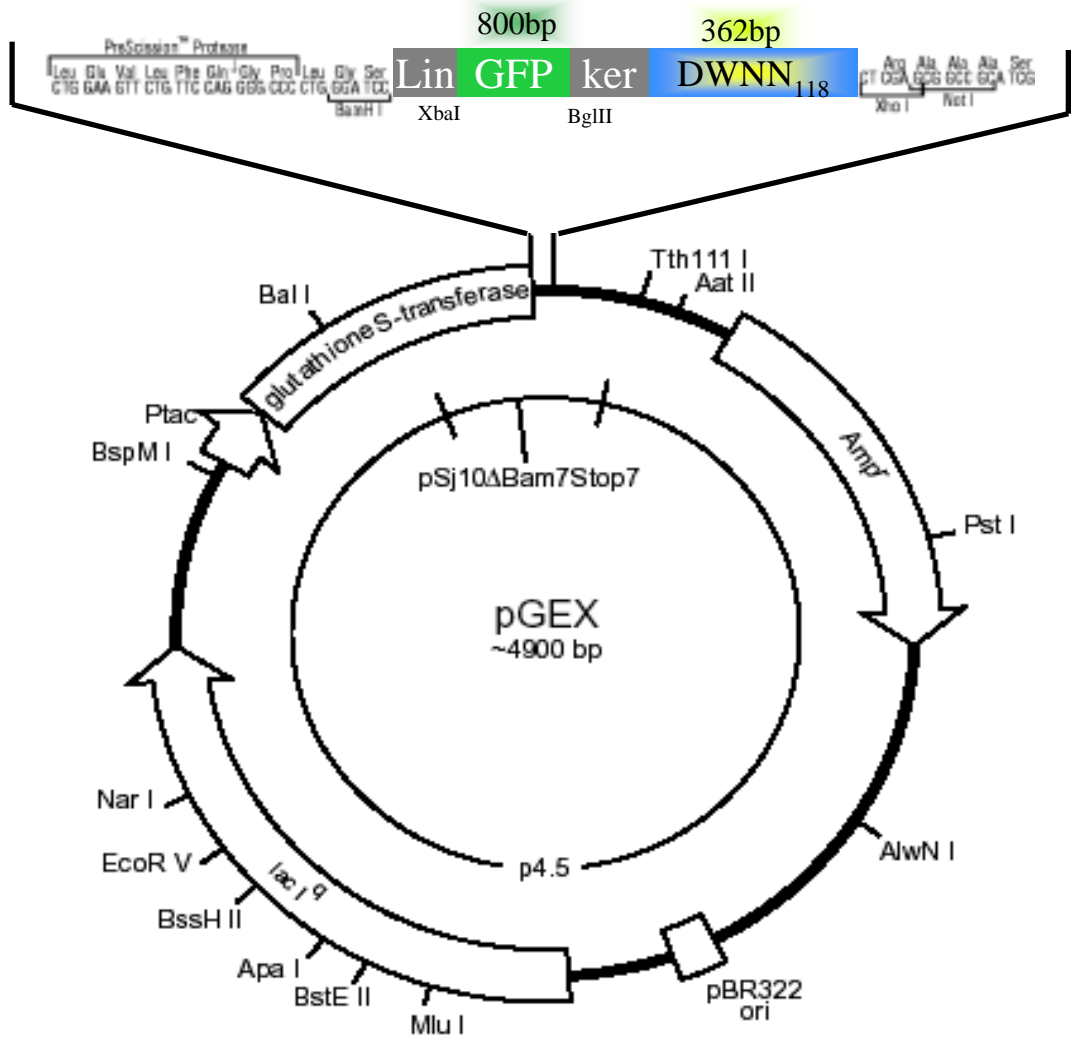
Figure 3.25: Diagrammatic representation of the insertion of the GFP-DWNN$_{118}$ fragment into pGEX-6P-2.

This serves the demonstration of how the Linker-GFP-DWNN$_{118}$ gene fragment, digested out of the pGEX-6P-2-PTD-linker-GFP *Ba*mHI and *Xho*I sites, was inserted into the pGEX-6P-2 *Ba*mHI and *Xho*I sites.
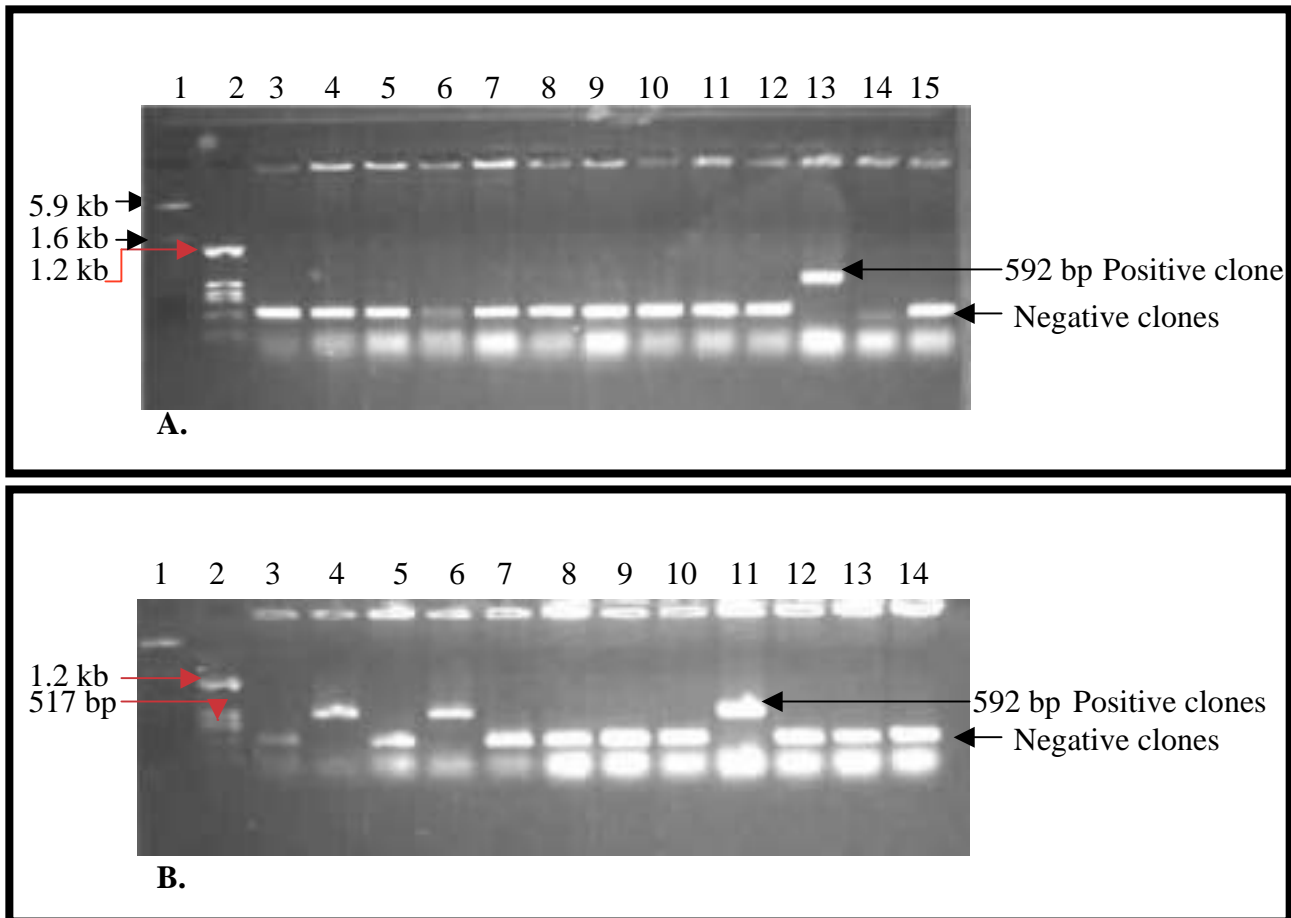
Figure 3.26: 1 % Agarose gel electrophoresis of colony PCR screening for the cloning of DWNN$_{118}$ fragment into pGEX-6P-2-PTD.

A. Lane 1: Molecular weight marker, Lane 2: Molecular weight marker, Lanes 3-12, 14 & 15: Negatives, Lane 13: Positive.

B. Lane 1: Molecular weight marker, Lane 2: Molecular weight marker, Lanes 4, 6, & 11: Positive clones, Remaining clones: Negatives.
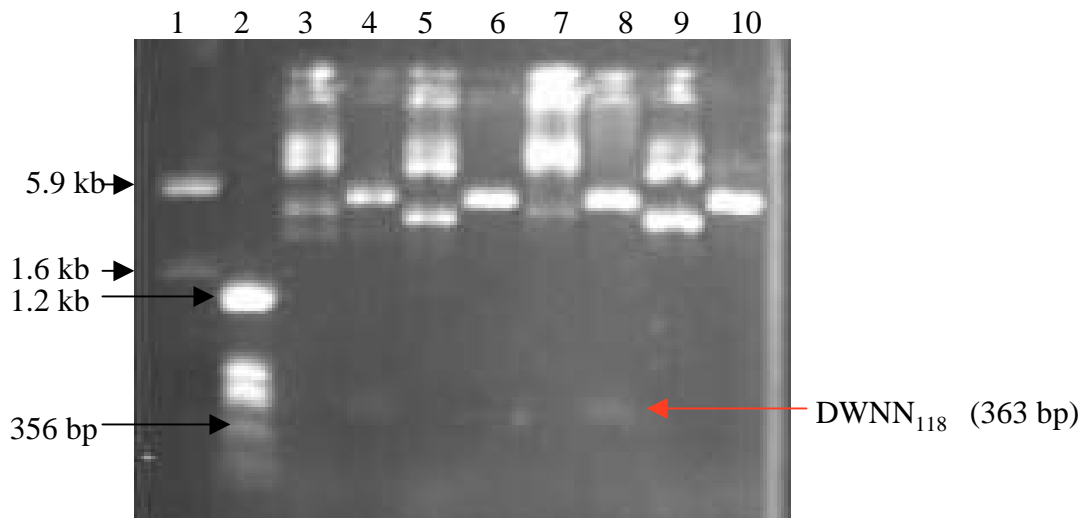
Figure 3.27 : 1 % Agarose gel electrophoresis of the small scale DNA isolation of the pGEX-6P-2-PTD-DWNN$_{118}$ construct and its digestion with *Bam*HI/*Xho*I to release DWNN$_{118}$.

Lane 1: Molecular weight marker, Lane 2: Molecular weight marker, Lanes 3, 5 ,7 and 9: Undigested small scale plasmid DNA isolation, Lanes 4, 6, 8, and 10: *Bam*HI/*Xho*I Digests.
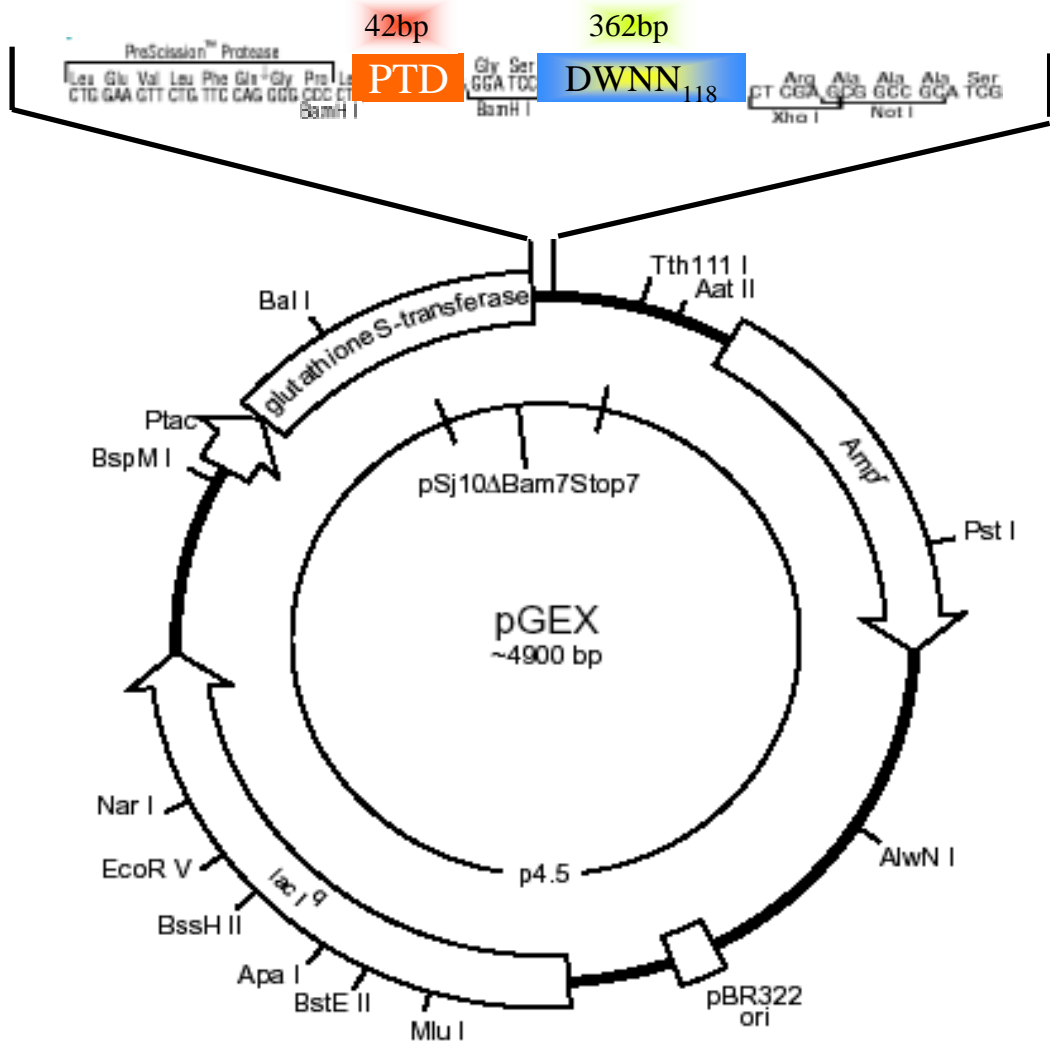
Figure 3.28: Diagrammatic representation of the insertion of the DWNN₁₁₈ fragment into pGEX-6P-2-PTD.

Demonstrated here is how the DWNN$_{118}$ gene fragment, obtained from the pGEM-T easy-DWNN$_{118}$ *Ba*mHI and *Xho*I sites, was inserted into the pGEX-6P-2-PTD *Ba*mHI and *Xho*I sites.

pGEX-6P-2–PTD-DWNN$_{118}$ was transformed into *E.coli* BL21 pLys S (DE3) to screen for the expression of GST-PTD-DWNN$_{118}$ (section 3.9).

3.9 Small Scale Expression

Expression screening of the recombinants was performed on each step of the proceedings, i.e. the expression screening from GST-TAT, GST-TAT-Linker, GST-TAT-Linker-GFP, GST-TAT-Linker-GFP-DWNN$_{118}$, GST-Linker-GFP, GST-Linker-GFP-DWNN$_{118}$ to GST-TAT-DWNN$_{118}$ (section 2.13.1). A summary experiment showing the successful expression of the constructs is depicted in figs 3.29 and 3.30, where lanes 2, 4, 6, 8, 10 represent the induced from GST through GST-TAT, GST-TAT-Linker, GST-TAT-Linker-GFP, to GST-TAT-Linker-GFP-DWNN$_{81,}$ respectively, in fig 3.29, while lanes 3, 5, 7 and 9 represent the induced GST, GST-Linker-GFP, GST-TAT-Linker-GFP, and GST-TAT-Linker-GFP-DWNN$_{118}$, in fig 3.30.

3.10 Discussion

Protein transduction involves the direct uptake of foreign proteins or peptides and protein or peptide chemical complexes by a cell. Amongst the advantages of protein transduction over other delivery methods is the ability to transfer proteins into all mammalian cells examined, while delivery by other methods into some mammalian cells have been demonstrated to be problematical. Further problems experienced with other delivery modes include the low percentage of cells targeted, over-expression
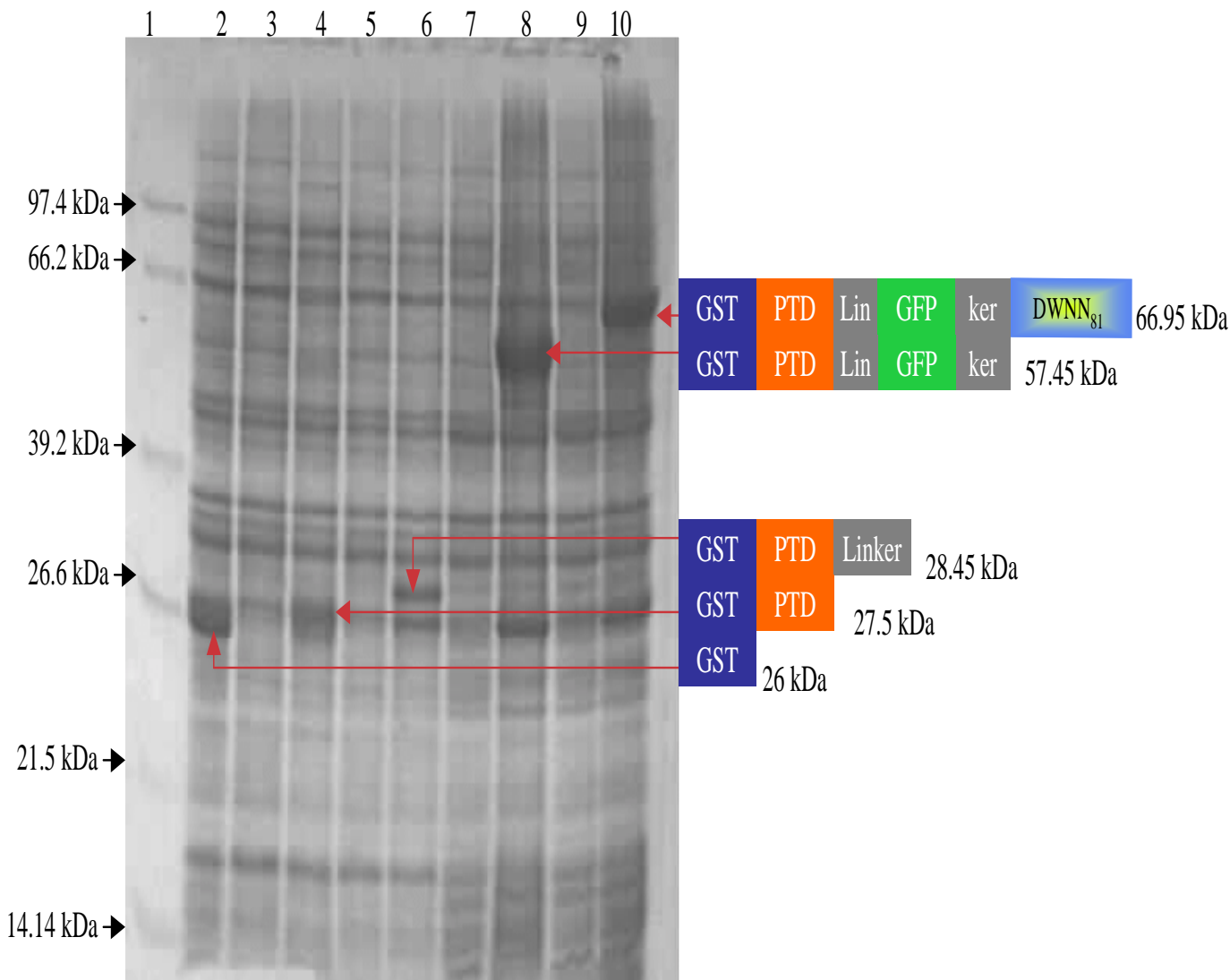
Figure 3.29: **12 % SDS PAGE gel electrophoresis of the small scale expression of soluble GST-PTD, GST-PTD-linker, GST-PTD-linker-GFP and of GST-PTD-linker-GFP-DWNN$_{81}$ at 0.3 mM IPTG and 37 ^{0}C.**

Lane 1: Protein Marker, Lanes 3, 5, 7, and 9: Un-induced, Lanes 2, 4, 6, 8, and 10: Induced. 20 µl of protein was loaded in each lane.
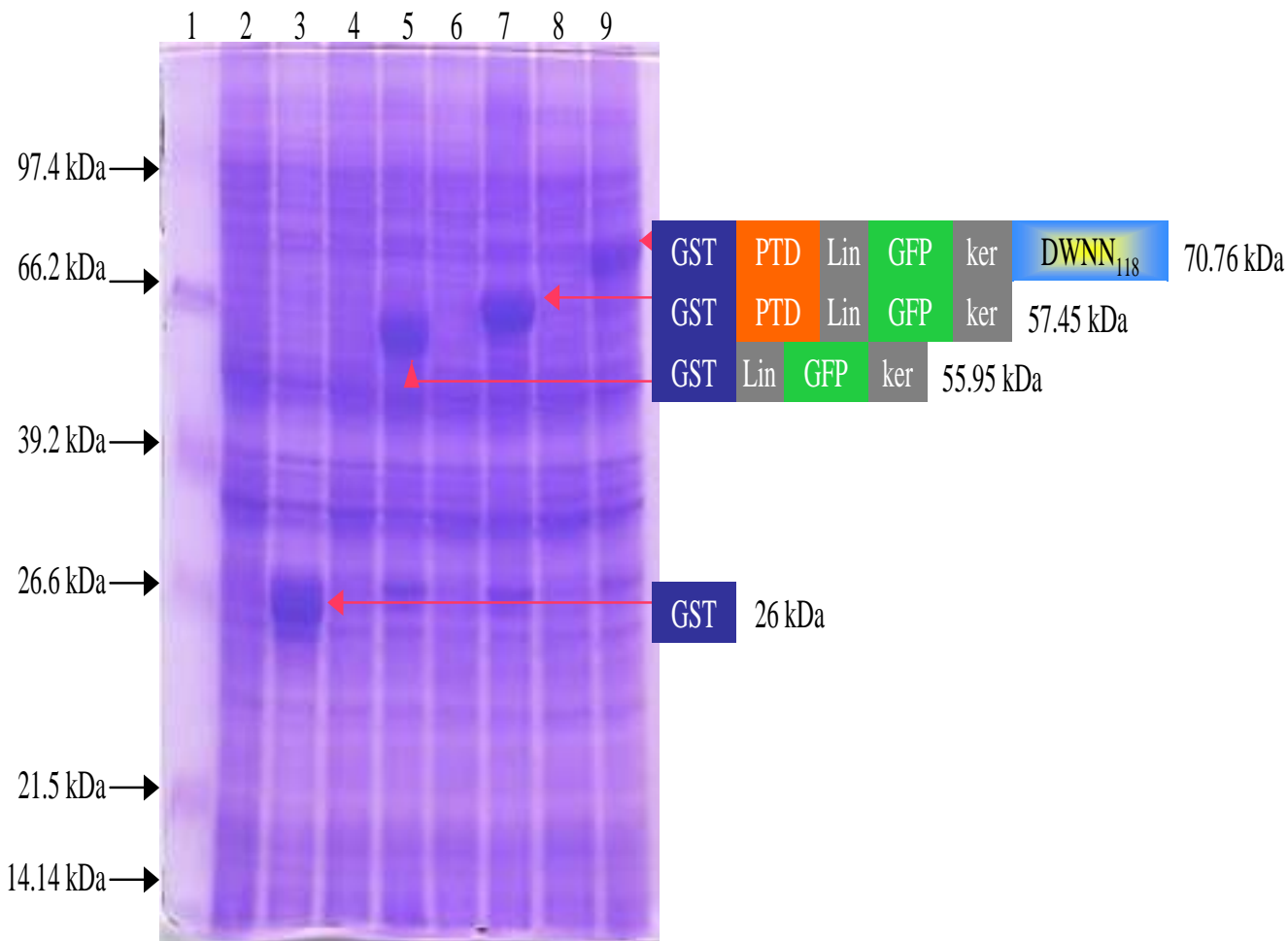
Figure 3.30: 12 % SDS PAGE gel electrophoresis of the small-scale expression of soluble GST-linker-GFP, GST-PTD-linker-GFP and that of GST-PTD-linker-GFP-DWNN$_{118}$ at 0.3 mM IPTG and 37 ^{0}C.

Lane 1: Protein Marker, Lanes 3, 5, 7 and 9: Induced, Lanes 2, 4, 6, and 8: Un-induced. 20 µl of protein was loaded in each lane.

and cell-to-cell variation in intracellular protein concentrations. Protein transduction occurs rapidly, with the protein detected inside the cell in a few minutes. Changing the amount of exogenous protein to be trafficked into cells results in the regulation of the protein concentration.

The cloning of the 11-amino acid TAT Protein Transduction Domain (PTD) into pGEX-6P-2 to be in the same reading frame of the vector was thus desired and achieved. Although the expected (theoretical) transformation efficiency was not attained, there was growth in all but one plate, with the highest concentration of the PTD, this may have been due to experimental error or the ligation may simply have not occurred due to the maximal threshold amount of insert molecules being exceeded where too high the insert concentration even hindered the vector self ligation by clogging the vector ends. The plate with no PTD (Table 3.1), where re-circularisation was expected, had more colonies than the rest. This suggests that re-circularisation is less likely in the presence of an insert.

The cloning of the linker sequence containing internal restriction sites, for the insertion of the *GFP* reporter gene was also achieved. These internal sites were tested for and shown not to be available both on the pGEX-6P-2 and pGEX-6P-2-PTD vectors by restriction digestion since a linear fragment was ideal, which would have not been possible if there was any of these sites on the vectors.

GFP was cloned into the linker sequence as a C-terminal in-frame fusion of the pGEX-6P-2-PTD vector, to act as a non-interfering marker, and no shortcomings were experienced.

$DWNN_{118}$ was cloned into the assembly and was in the right orientation and expression was optimal in M9ZB media formulation (section 2.13.2.2).

All the constructs were of their corrected sizes hence the cloning technique was appropriately conducted hence the successful insertions.

3.11 Summary

A series of TAT-PTD fusion proteins, GST-TAT-GFP, GST-TAT-GFP-$DWNN_{118}$, GST-TAT-$DWNN_{118}$ and their controls, GST-GFP and GST-GFP-$DWNN_{118}$ TAT-PTD fusion constructs attached to the N terminus of GST on the pGEX-6P-2 vector, were built (Figs 3.1 A and B). The oligonucleotides coding for the gene sequence of a **P**rotein **T**ransduction **D**omain (PTD) were synthesised, annealed and cloned into pGEX-6P-2. The presence of the PTD in the construct was confirmed by colony PCR and sequence analysis. The oligonucleotides coding for the DNA sequence of the linker, into which the GFP fragment was to be inserted, were also synthesised, annealed and cloned into pGEX-6P-2-TAT. The presence of the linker sequence was verified by colony PCR, restriction digestion and sequence analysis. The GFP fragment was released from the $pGFPC_1$ vector, cloned into the pGEX-6P-2-TAT-

Linker construct and identified by colony PCR and restriction digestion. A PCR amplification of the gene sequence of $DWNN_{118}$ generated a 363 bp fragment, which was sub-cloned into pGEM-T Easy vector. The presence of the insert was verified by colony PCR and restriction digestion. The $DWNN_{118}$ insert was released from the pGEM-T Easy vector and cloned into pGEX-6P-2-TAT-Linker-GFP and pGEX-6P-2-TAT constructs. The insertion was confirmed by colony PCR and restriction digestion. GFP and GFP-$DWNN_{118}$ were released from the pGEX-6P-2-TAT-Linker-GFP and pGEX-6P-2-TAT-Linker-GFP-$DWNN_{118}$ constructs, respectively, and cloned into pGEX-6P-2. The insertions were confirmed by colony PCR and restriction digestion. These constructs were screened for the expression of the proteins they code for and in each case the expression was satisfactory since the desired protein sizes were obtained. The constructs were to be expressed and purified, as described in the next chapter, to test the capability of TAT-PTD delivery, and to introduce TAT-PTD fusion proteins into cells.

CHAPTER 4

Expression and Purification of the Constructs

4.1 Introduction

This chapter presents the large-scale expression and purification of the fusion proteins whose design was described in the previous chapter. The power to express protein domains is a crucial means in the search of function and structure-function relationships. The GST fusion proteins are used, since they make the purification of the protein of interest possible. The cDNA of the protein of interest is cloned downstream of the gene coding for glutathione-S-transferase (GST), and introduced into bacteria. Expression in bacteria produces fusion proteins of sufficient quantities for functional and/or structural studies *in vitro*. Expression occurs through the induction of the lac promoter using IPTG. The purification, to remove the bacterial proteins, is achieved by the fusion partner, GST, which binds to the glutathione-sepharose beads. The elution of the fusion partner and anything desirable downstream of it is achieved by the addition of reduced glutathione (section 2.14.3), which displaces the GST from the glutathione column.

4.2 Purification of the constructs on GST column

The aim was to produce large amounts of PTD-GFP, PTD-GFP-DWNN$_{118}$, PTD-DWNN$_{118}$, GFP and GFP-DWNN$_{118}$ protein products with respective sizes of 31.45 kDa, 44.74 kDa, 14.79 kDa, 29.95 kDa, and 42.95 kDa, all without the 26 kDa GST.

Expression was performed (sections of 2.13.2.1 and 2.13.2.2) subsequent to which was the purification step (section 2.14.3). The fusion proteins were transformed into *E.coli* BL21 pLys S (DE3) for large-scale expression (section 2.13.2). Two media formulations (sections 2.13.2.1 and 2.13.2.2) were investigated and it was discovered that maximal expression was in M9ZB (section 2.13.2.2). Expression was carried out at 37 ^{0}C. The induction with IPTG was performed at 0.3 mM at 25 ^{0}C. Every fusion protein that contained GFP was green to the naked eye and fluoresced when illuminated with UV light (fig 4.11). Purification of the fusion proteins was carried out using GST columns on which they bound due to the GST affinity and were eluted with 15 mM glutathione, 50 mM Tris pH 8.0 (section 2.14.3). Purified GST-GFP (fig 4.1), GST-PTD-GFP (fig 4.2), GST-GFP-DWNN$_{118}$ (fig 4.3), GST-PTD-DWNN$_{118}$ (fig 4.4) and GST-PTD-GFP-DWNN$_{118}$ (fig 4.5) fusion proteins were analysed on a 12 % acrylamide denaturing gel. There was no detectable contaminating protein in each case, however some degradation products were observed despite the addition of protease inhibitors. Such proteolysis was negligible since large protein quantities were attained.

4.3 Cleavage to release GST

The purified proteins were then cleaved with a recombinant 3-C protease (figs 4.6 and 4.7) and further purification was performed to obtain protein products without GST (figs 4.8-4.10), where GST bound and remained on the column while the unbound protein product, the flow through, was the protein of interest. The cleavage
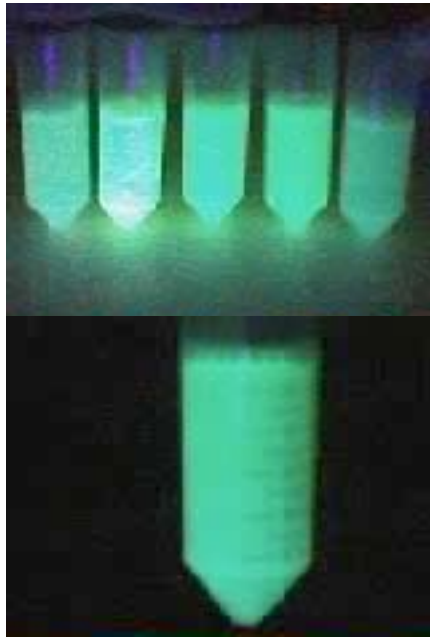
Figure 4.11: Fluorescence of GFP when illuminated by a short wavelength.

The figure shows green fluorescence achieved by an illumination using a short wavelength ultra violet.
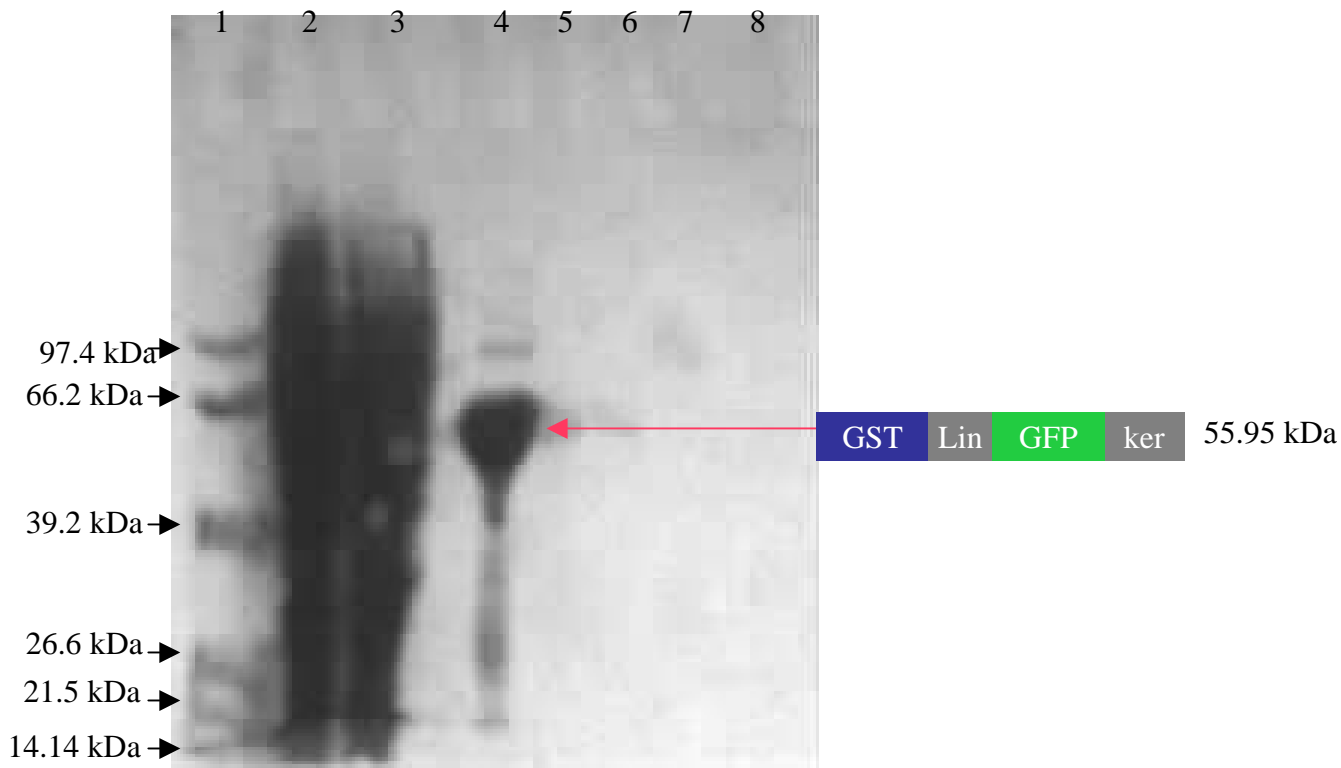
Figure 4.1: 12 % SDS PAGE gel electrophoresis of the Purification of the GST-Linker-GFP construct.

Lane 1: Protein Marker, 2: Flow through, 3: PBS Wash, 4: 1st Eluted Fraction, 5: 2nd Eluted Fraction, 6: 3rd Eluted Fraction, 7: 1st wash with 2M NaCl, 8: 2nd wash with 2M NaCl.

Illustrated here is the purification of the above expressed construct after induction by IPTG. Purification was achieved since a highly concentrated protein was eluted.
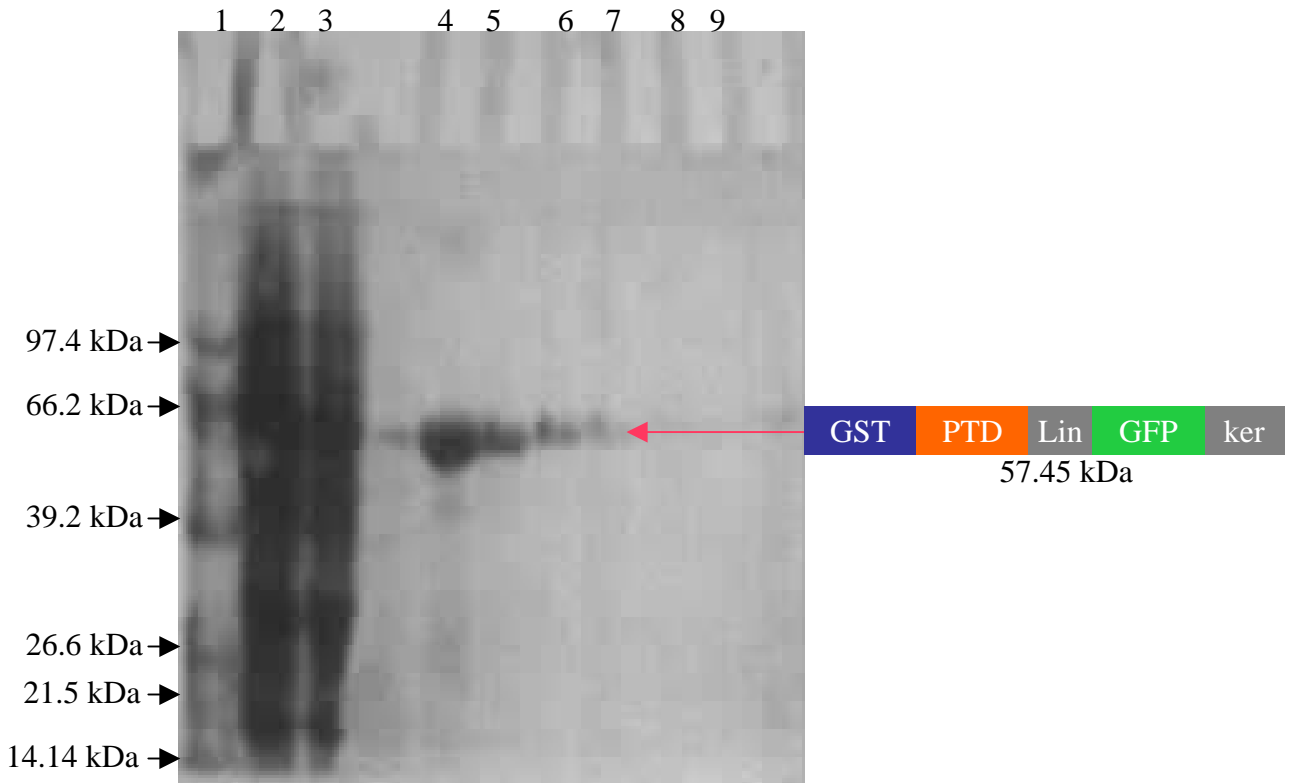
Figure 4.2: 12 % SDS PAGE gel electrophoresis of the Purification of the GST-PTD-Linker-GFP construct.

Lane 1: Protein Marker, 2: Flow through, 3: PBS Wash, 4: 1st Eluted Fraction, 5: 2nd Eluted Fraction, 6: 3rd Eluted Fraction, 7: 4th Eluted Fraction, 8: 1st wash with 2M NaCl, 9: 2nd wash with 2M NaCl.

Shown here is the purification of the above expressed construct following induction by the IPTG addition. Purification was achieved since a satisfactorily concentrated protein was eluted.

Figure 4.3: 12 % SDS PAGE gel electrophoresis of the Purification of the GST-PTD-Linker-GFP-DWNN₁₁₈ construct.

Lane 1 & 2: Pre-mixed Protein Marker, 3: Lysate protein, 4: PBS Wash, 5: Further wash, 6: 1st Eluate, 7: 2nd Eluate, 8: 3rd Eluate. 9: Salt wash.

An illustration of the purification of the above expressed construct after induction by IPTG. Purification was achieved since a highly concentrated protein was eluted.
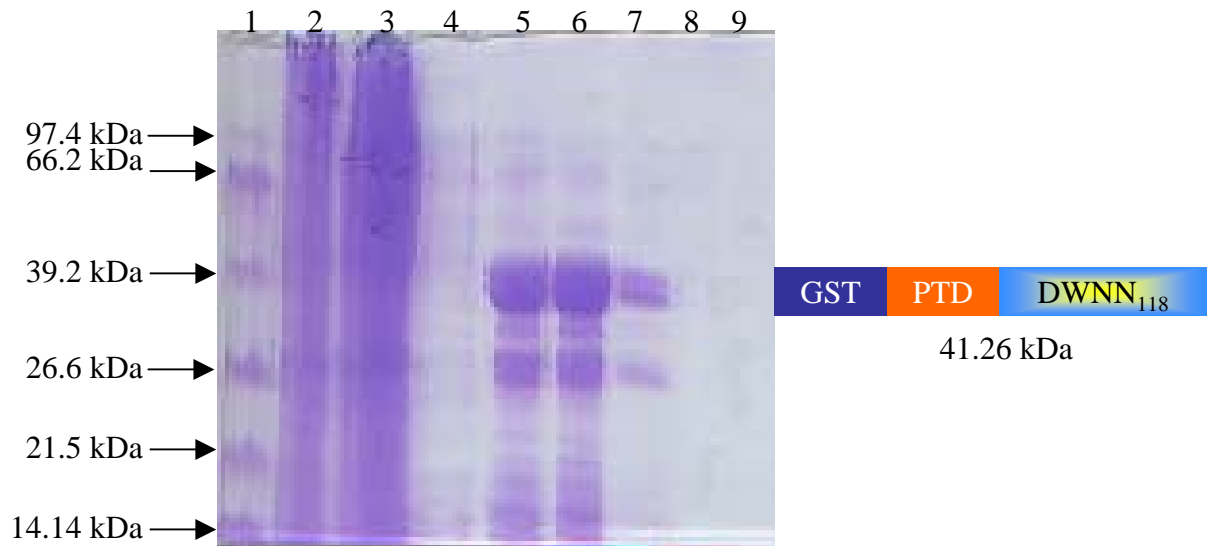
Figure 4.4: 12 % SDS PAGE gel electrophoresis of the Purification of the GST-PTD-DWNN$_{118}$ construct.

Lane 1: Pre-mixed Protein Marker, 2: Lysate protein, 3: PBS Wash, 4: Further wash, 5: 1st Eluate, 6: 2nd Eluate, 7: 3rd Eluate, 8: Salt wash.

A demonstration of the purification of the above expressed construct after induction by IPTG. Purification was achieved since a satisfactorily concentrated protein was eluted.
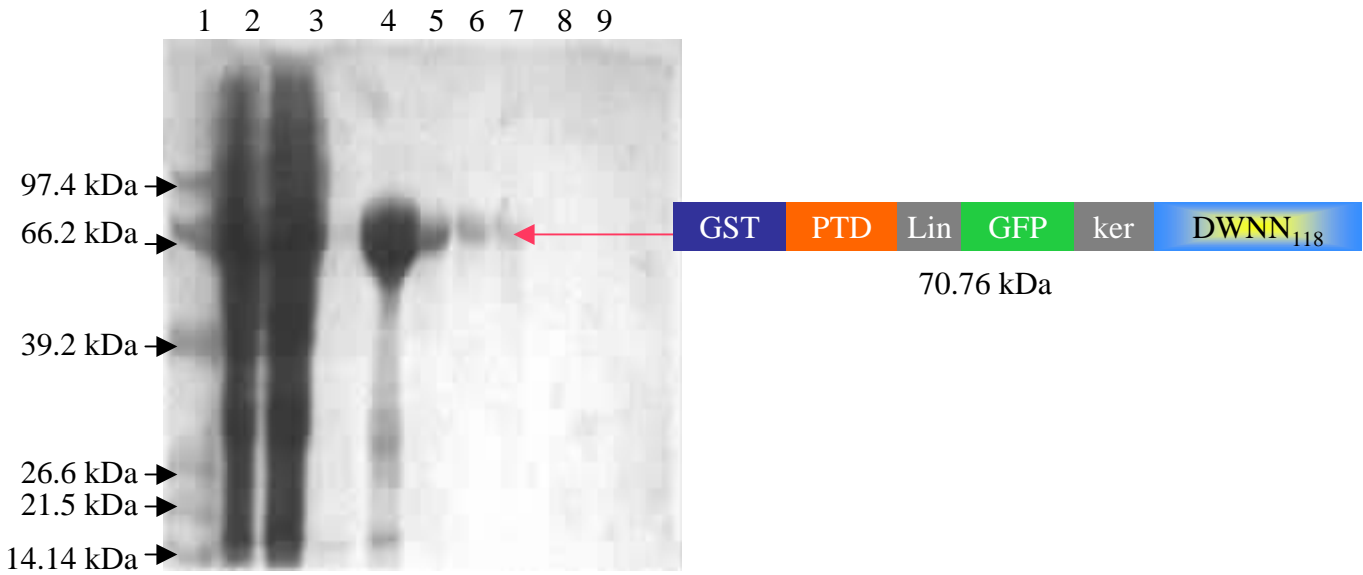
Figure 4.5: 12 % SDS PAGE gel electrophoresis of the Purification of the GST-PTD-Linker-GFP-DWNN$_{118}$ construct.

Lane 1: Protein Marker, 2: Flow through, 3: PBS Wash, 4: 1st Eluted Fraction, 5: 2nd Eluted Fraction, 6: 3rd Eluted Fraction, 7: 4th Eluted Fraction, 8: 1st wash with 2M NaCl, 9: 2nd wash with 2M NaCl.

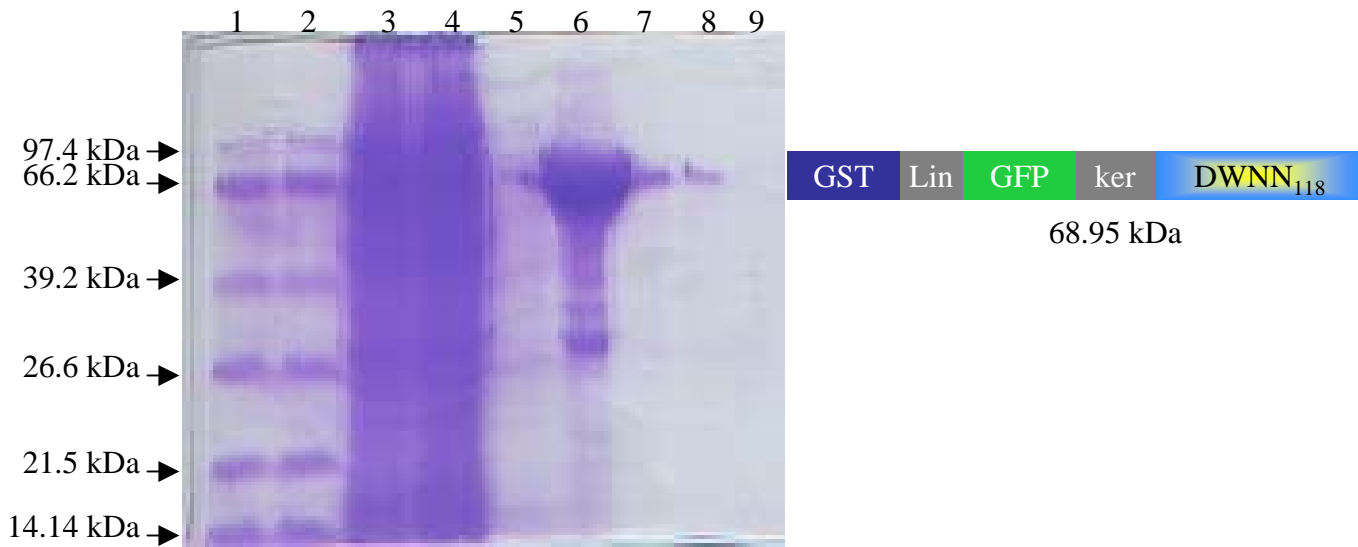Demonstrated is the purification of the above expressed construct after induction by IPTG. Purification was achieved since a highly concentrated protein was eluted.
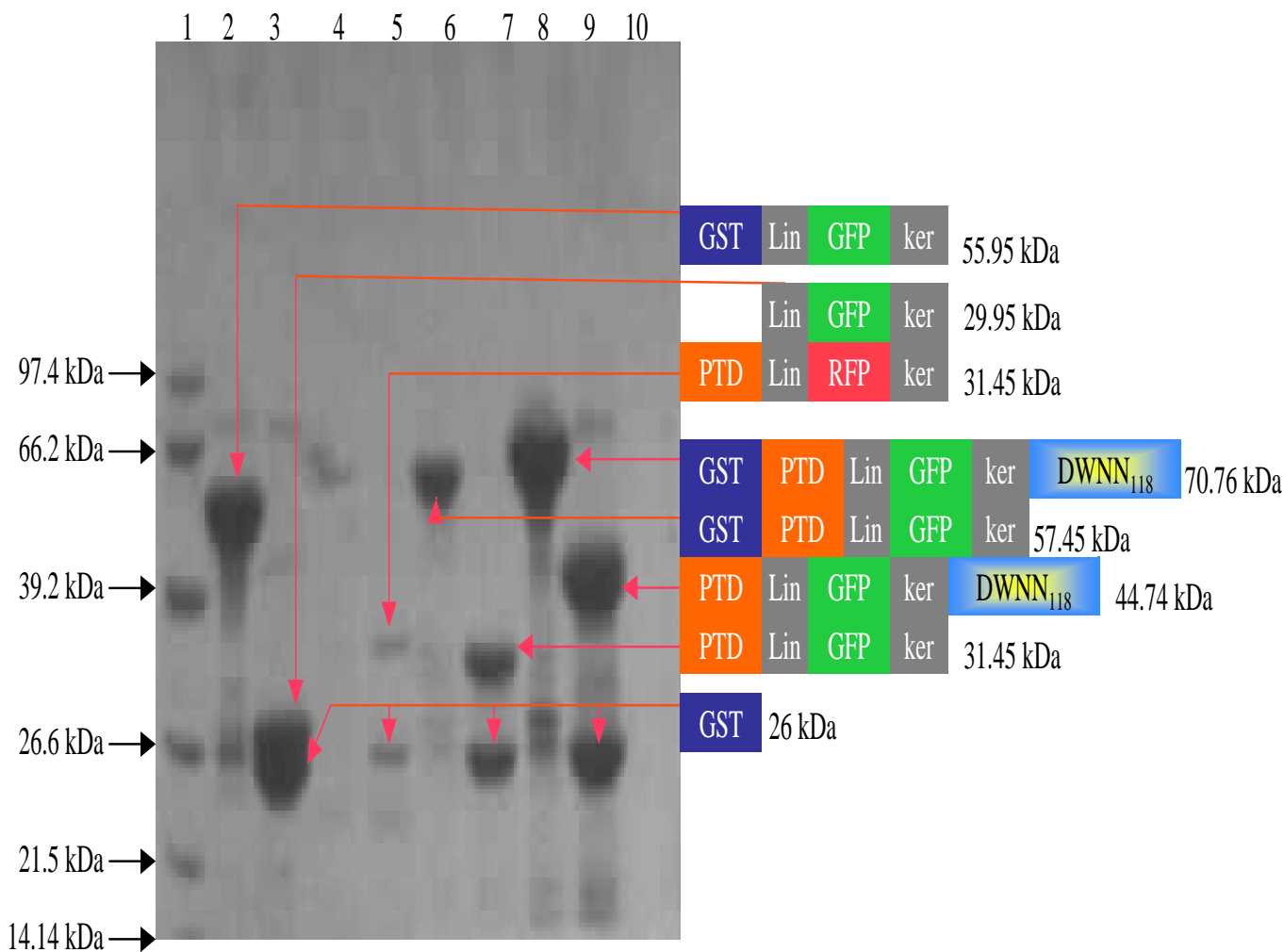
Figure 4.6: 12 % SDS PAGE gel electrophoresis of the cleavage of the constructs with 3C protease.

Lane 1: Protein Marker, Lanes 2, 4, 6 and 8:Un-cleaved constructs, Lanes 3. 5. 7 and 9, cleaved protein products.

Represented here is the cleavage of GST away from the constructs. Cleavage is shown to have been to completion.
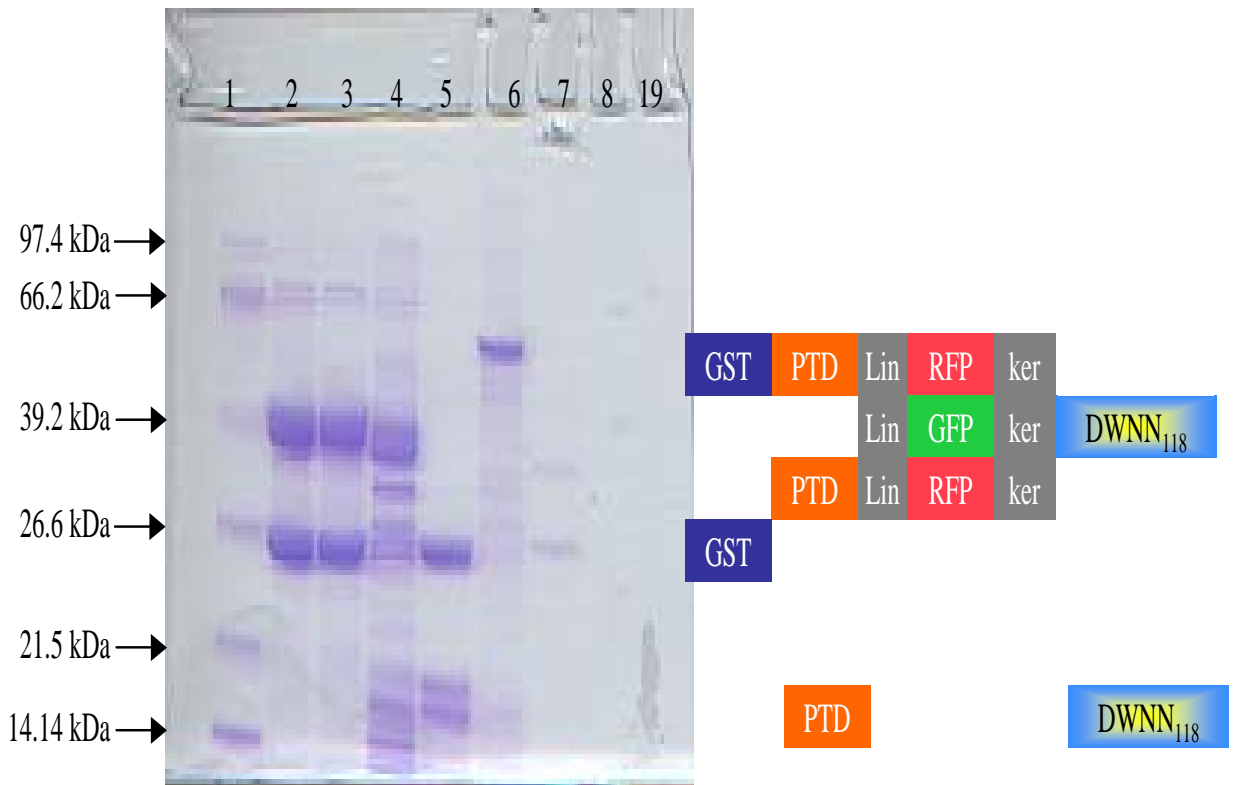
Figure 4.7: 12 % SDS PAGE gel electrophoresis of the cleavage of the constructs with 3C protease.

Lane 1: Pre-mixed Protein Marker, 2: Cleaved GST-GFP-DWNN$_{118}$, 3: Cleaved GST-GFP-DWNN$_{118}$, 4: GST-PTD-DWNN$_{118}$, 5: Cleaved GST-PTD-DWNN$_{118}$, 6: GST-PTD-RFP, 7: Cleaved GST-PTD-RFP.

Represented here is the cleavage of GST away from the constructs. Cleavage is shown to have been to completion.
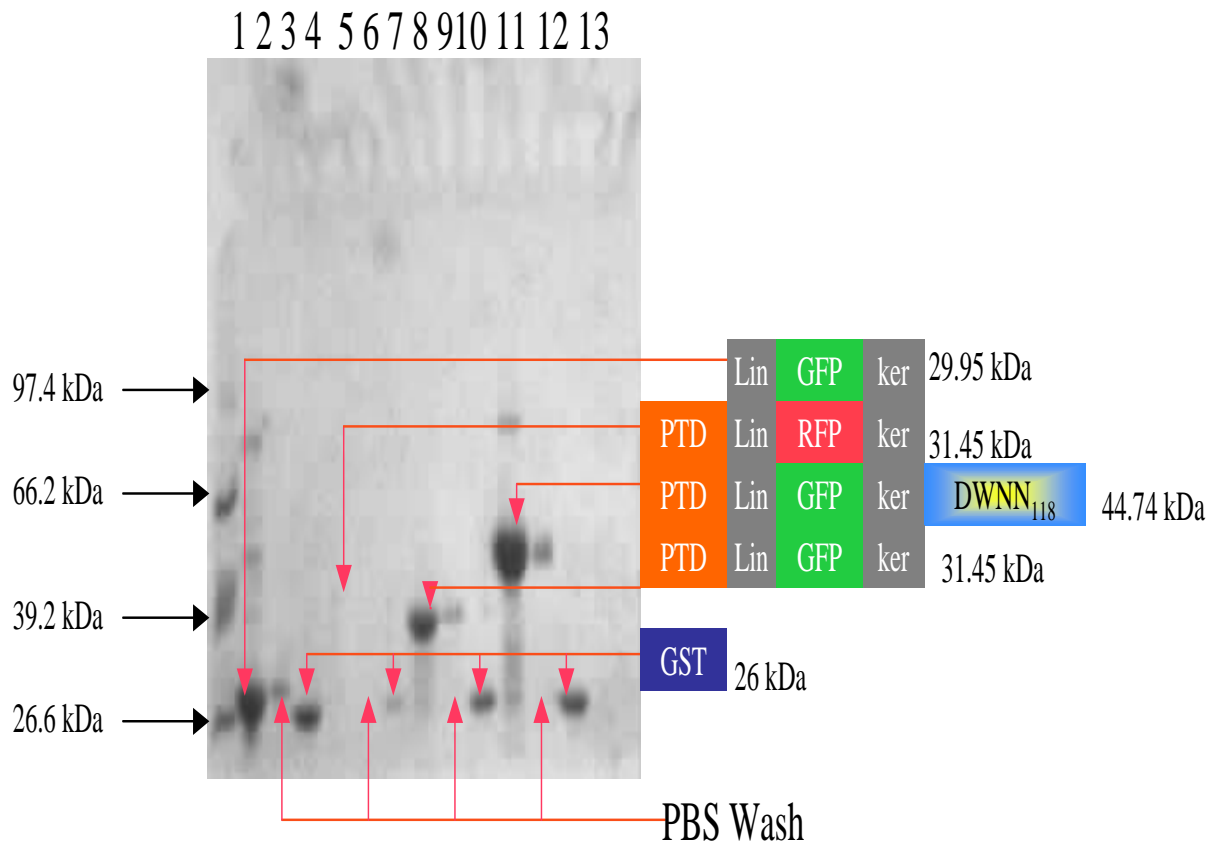
Figure 4.8: 12 % SDS PAGE gel electrophoresis of the Purification of the cleaved constructs to eliminate GST. Lane 1: Protein Marker.

A demonstration of purification of constructs away from GST. Purification was satisfactory since pure constructs were isolated and no GST was detected in each case while GST was observed after elution from the column.
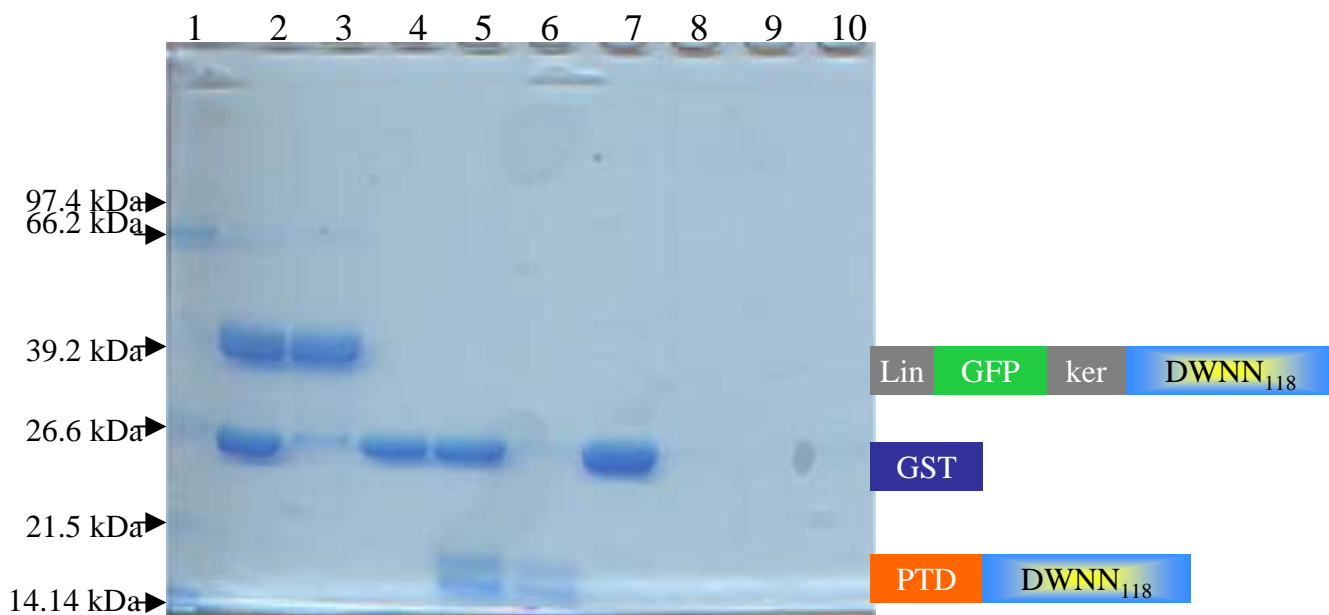
Figure 4.9: 12 % SDS PAGE gel electrophoresis of the Purification of the cleaved constructs to eliminate GST.

Lane 1: Pre-mixed Protein Marker, 2: Cleaved GST-GFP-DWNN$_{118}$, 3: GFP-DWNN$_{118}$, 4: GST sorted away from GFP-DWNN$_{118}$, 5: Cleaved GST-PTD-DWNN$_{118}$, 6: PTD-DWNN$_{118}$, 7: GST sorted away from PTD-DWNN$_{118}$, 8: Cleaved GST-PTD-RFP, 9: PTD-RFP, 10: GST sorted away from PTD-RFP.

Represented here is the purification of GST away from the constructs. Purification/isolation is unsatisfactory since GST was detected in each case while GST
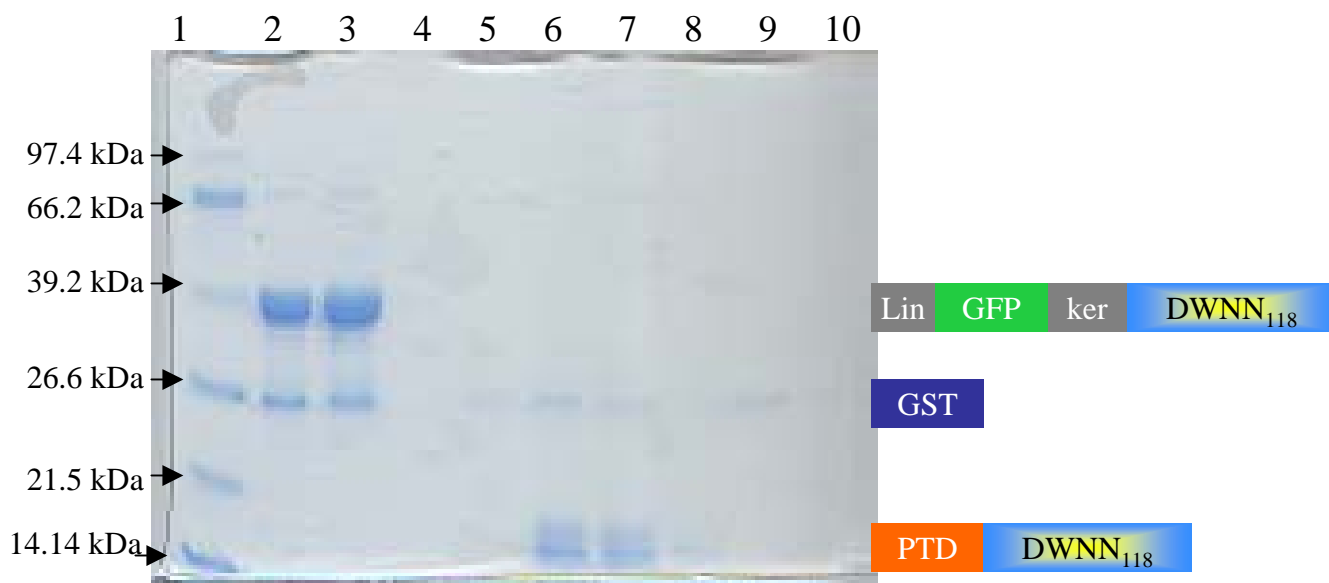
Figure 4.10: 12 % SDS PAGE gel electrophoresis of the further purification of the cleaved constructs to eliminate GST.

Lane 1: Pre-mixed Protein Marker, 2: Cleaved GST-GFP-DWNN$_{118}$, 3: GFP-DWNN$_{118}$, 4: PBS wash, 5: GST sorted away from GFP-DWNN$_{118}$, 6: Cleaved GST-PTD-DWNN$_{118}$, 7: PTD-DWNN118, 8: PBS wash, 9: GST sorted away from PTD-DWNN$_{118}$, 10: GST sorted away from PTD-RFP.

A demonstration of purification of constructs away from GST. Purification was still unsatisfactory since GST was detected in each case while GST.

products were analysed on a 12 % acrylamide gel and proteins of expected sizes were obtained. The 31.45 kDa PTD-GFP (fig 4.8, lane 8), 44.74 kDa PTD-GFP-DWNN$_{118}$ (fig 4.8, lane 11), 14.79 kDa PTD-DWNN$_{118}$ (figs 4.9 and 4.10, lanes 6 and 7 respectively), 29.95 kDa GFP (fig 4.8, lane 2) and 42.95 kDa GFP-DWNN$_{118}$ (figs 4.9 and 4.10, lanes 3 in each gel) were isolated from their cleavage products. GST was also eluted as in section 4.2 and the column regenerated.

4.4 Discussion

A single band representative of the correctly sized fusion protein was obtained in each case and no contaminating protein was detectable in every case. Complete cleavage was attained and purification satisfactory. Purification of GFP-DWNN$_{118}$ and of PTD-DWNN$_{118}$ were not as convincing as of other fusion proteins (fig 4.9) since there was detectable amount of GST. To combat this, purification was repeated (fig 4.10) and the same result was observed and no further purification was conducted since GST was not expected to interfere with the subsequent experiments. GST was eluted after the final purification step and is detectable as an isolated protein product (figs 4.8-4.10).

The desired full-length proteins were produced, even though there was some evidence of proteolysis detectable in the case of PTD-DWNN$_{118}$ fusion since two bands were observed. One of the bands represented the size of the fusion protein, while the other band was most likely the degradation product.

4.5 Summary

It is concluded that PTD-GFP, PTD-GFP-DWNN$_{118}$, PTD-DWNN$_{118}$, GFP and GFP-DWNN$_{118}$ fusion proteins associated with GST protein were produced efficiently by over-expression in bacterial cells. GST present a way for their purification. Cleavage of GST and purification resulted in homogenous domains of their respective expected sizes of 31.45 kDa, 44.74 kDa, 14.79 kDa, 29.95 kDa, and 42.95 kDa. The expressed and pure constructs were utilised in the transduction experiments in chapter 5.

CHAPTER 5

Introduction of fusion Proteins into cells by Transduction

5.1 Introduction

This chapter serves to present the transduction of the fusion proteins into cells. Urea-denatured TAT fusion proteins can transduce into cells and this is true for a broad spectrum of proteins being trafficked regardless of their size, function or structure [Vocero-Akbani *et al.*, 1999]. TAT-fusion proteins accumulate around the nucleus without any significant visible nuclear targeting after transduction. Using a Cre/Lox based functional assay, the nuclear delivery of functional TAT-Cre recombinase increased by up to 23-fold [Caron *et al.*, 2004]. The transduction of denatured TAT fusions increases the accessibility of the TAT-PTD domain by eliciting biological responses more efficiently than correctly folded soluble proteins.

CHO-Mut 8 (3 X HA8) 3.5 cell line, generated using promoter-trap mutagenesis system that identifies novel components involved in CTL-killing, CHO22, and CHO-Y10 were used for transduction in this study.

5.2 Urea Denaturation and Purification of the Constructs by G-25 Sephadex

The exact mechanism by which transduction across the bi-lipid layer of the membranes occurs is at this stage still unclear. It has been shown though that urea-denatured proteins obtain biological phenotypes more efficiently than soluble,

correctly folded protein. There is a hypothesis that due to reduced structural constraints, higher energy (Δ G), denatured proteins may transduce more efficiently into cells than lower energy, properly folded proteins [Vocero-Akbani *et al.*, 1999]. When within the cells, transduced denatured proteins would be properly refolded by chaperones such as heat shock protein 90 (HSP90) and thus re-attain their intracellular activation. In order to use TAT fusions in an aqueous milieu like tissue culture media, it is a requirement to quickly remove 8 M urea. This also accomplishes the aim of attaining high energetic (Δ G), denatured TAT fusion proteins. The TAT fusion protein in urea is applied to a G-25 Sephadex desalting column equilibrated in tissue culture media to be used for elution. Column fractions are isolated as described in section 2.16.2. The PTD-GFP, PTD-GFP-DWNN$_{118}$, PTD-DWNN$_{118}$, GFP and GFP-DWNN$_{118}$, constructs were urea denatured (section 2.16.1) and purified by buffer exchange on a G-25 Sephadex column (section 2.16.2).

5.3 *In vivo* protein transduction in tissue culture

The cells were transduced (section 2.16.3) and analysed using fluorescent microscopy (2.16.4), and FACS (section 2.16.5). Western Blot analysis was carried out (section 2.17) on the protein extracts isolated from cells cultured (section 2.15.4) with each DWNN$_{118}$ containing transduction cell products and the control GFP-DWNN$_{118}$, which contained no PTD included. Transduction responses are seen at molar concentrations of 100-200 nM (Becker-Hapak *et al.*, 2001).

5.3.1 Microscopy

The TAT-PTD containing fusion proteins and their non-TAT containing counterparts were transduced into CHO-Y10 and CHO-Mut 8 (3 X HA8) 3.5 cell lines. The cells were incubated for 72 hours to permit the GFP refolding since it was not rapid. The cells were subsequently fixed with 4 % paraformaldehyde and were stained with DAPI, which binds DNA and emits blue fluorescence. Microscopic analysis (Section 2.16.4) demonstrated that only the PTD containing constructs transduce into cells since the cells treated with non-PTD constructs, containing GFP, did not fluoresce when fluorescence microscopy was conducted. These cells showed only DAPI staining and no green fluorescence. Native PTD and GFP containing constructs targeted the cytoplasm (Figs 5.1 and 5.2) while denatured PTD and GFP containing constructs targeted both the cytoplasmic and the nuclear regions and non PTD containing constructs, though they contained GFP, could not be traced hence were not transducible, which supports the theory that transduction is PTD mediated (Figs 5.3-5.5). Cells transduced with PTD-GFP-DWNN$_{118}$ showed better nuclear uptake than their PTD-GFP transduced counterparts, which strongly supports the hypothesis that DWNN localises to the nucleus (Figs 5.4-5.5). This is backed by researchers whose TAT fusion proteins accumulated around the nucleus [Caron *et al.*, 2004].

The CHO-Mut 8 (3 X HA8) 3.5 cells transduced with PTD-DWNN$_{118}$ construct were immuno-fluorescently stained (section 2.16.4) with anti-DWNN antibody and then with a fluorescein or rhodamine labeled-anti rabbit IgG antibody (Figs 5.8-5.12).
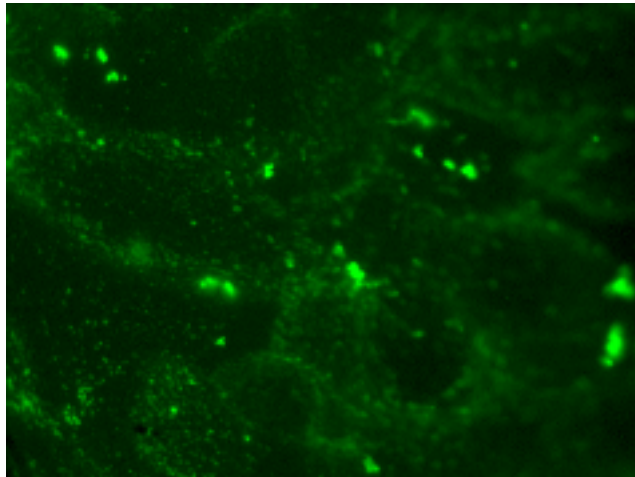
Figure 5.1: Microscopic analysis of Y10 cells transduced with native TAT PTD-GFP. This response was detected at the estimated concentration of 26 ug/µl transduced into cells. Cells were monitored by green fluorescence microscopy. Cells were viewed using a Zeiss Axioplan fluorescence microscope and imaging was by a Spot RT digital camera (Section 2.16.4).
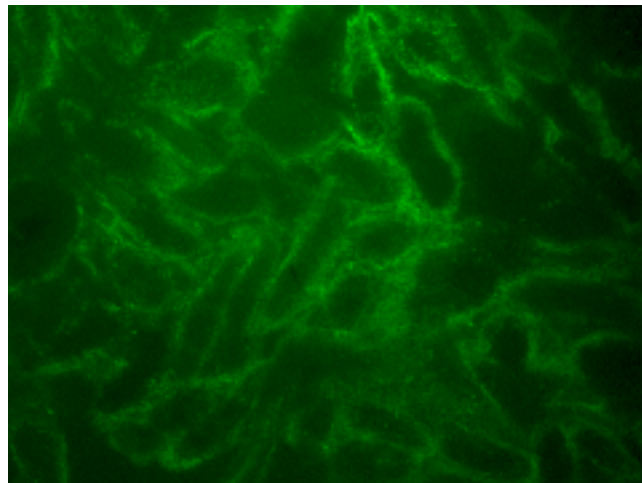
Figure 5.2: Microscopic analysis of Y10 cells transduced with native TAT PTD-GFP-DWNN$_{118}$. This response was detected at the estimated concentration of 32 ug/µl transduced into cells. Cells were monitored by green fluorescence microscopy. Cells were viewed using a Zeiss Axioplan fluorescence microscope and imaging was by a Spot RT digital camera (Section 2.16.4).
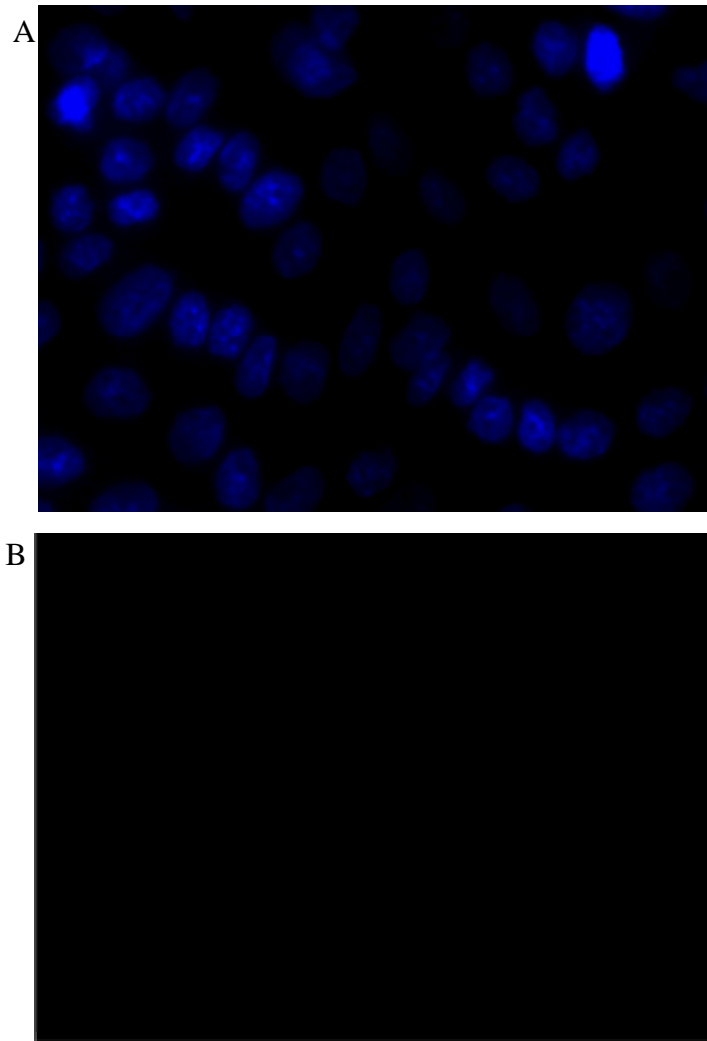
Figure 5.3: Green fluorescence microscopic analysis of untreated Y10 cells.

A: DAPI stained cells. B: Same cell population as in A showing no fluorescence. These results are the same as in the case of cells treated with GFP and GFP-DWNN$_{118}$, confirming that transduction is TAT-PTD mediated. Cells were viewed using a Zeiss Axioplan fluorescence microscope and imaging was by a Spot RT digital camera (Section 2.16.4).

Figure 5.4: Green fluorescence microscopic analysis of Y10 cells transduced with TAT-GFP. The response was detected at the estimated concentration of 26 ug/µl transduced into cells.

A: DAPI stained cells. B: Same cell population as in A showing fluorescence (Nuclear localisation observed). These results confirm that transdution is TAT-PTD mediated. Cells were viewed using a Zeiss Axioplan fluorescence microscope and imaging was by a Spot RT digital camera (Section 2.16.4).

Figure 5.5: Green fluorescence microscopic analysis of Y10 cells transduced with TAT-GFP-DWNN$_{118}$. The response was detected at the estimated concentration of 32 ug/µl transduced into cells

A: DAPI stained cells. B: Same cell population as in A showing fluorescence (Nuclear localisation observed). These results confirm that transdution is TAT-PTD mediated. Cells were viewed using a Zeiss Axioplan fluorescence microscope and imaging was by a Spot RT digital camera (Section 2.16.4).

Figure 5.6: Microscopic analysis of immuno-fluorescently labeled untreated CHO-Mut 8 (3 X HA8) 3.5 cells probed with anti-DWNN primary antibody and fluorescein. Cells were monitored by green fluorescence microscopy.

A: DAPI stained cells. B: Same cell population as in A showing successful probing (Cells showed only cytoplasmic staining). Cells were viewed using a Zeiss Axioplan fluorescence microscope and imaging was by a Spot RT digital camera (Section 2.16.4).

Courtesy of Miss Amanda Skepu, Biochemistry Research lab: UWC.
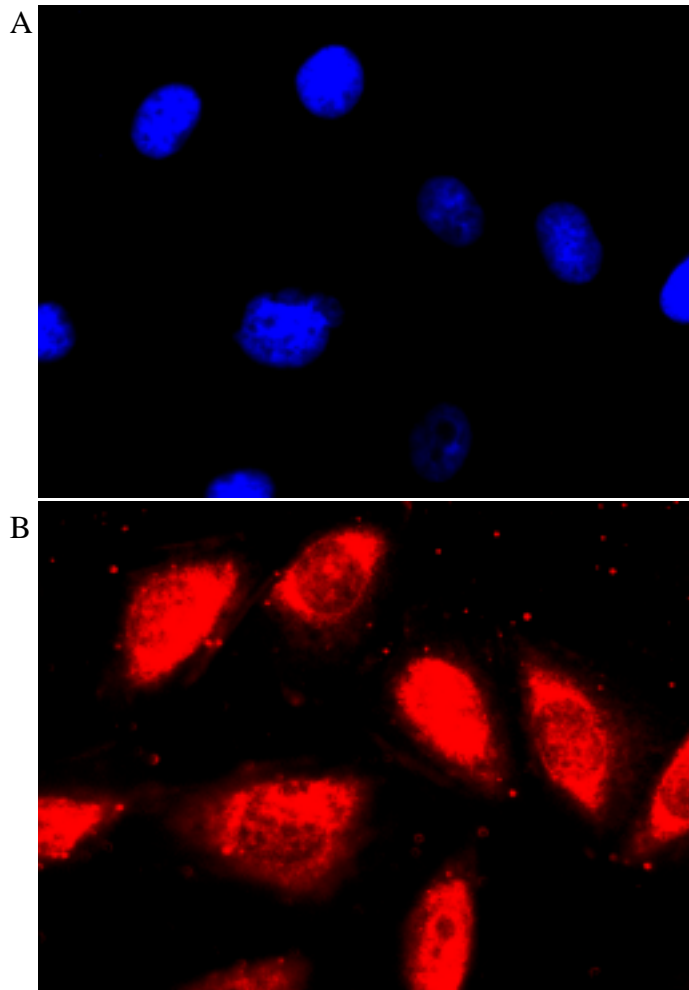
Figure 5.7: Microscopic analysis of immuno-fluorescently labeled untreated CHO-Mut 8 (3 X HA8) 3.5 cells probed with anti-DWNN primary antibody and rhodamine. Cells were monitored by red fluorescence microscopy.

A: DAPI stained cells. B: Same cell population as in A showing successful probing (Cells showed cytoplasmic staining and scanty nuclear staining). Cells were viewed using a Zeiss Axioplan fluorescence microscope and imaging was by a Spot RT digital camera (Section 2.16.4).

Courtesy of Miss Amanda Skepu, Biochemistry Research lab: UWC
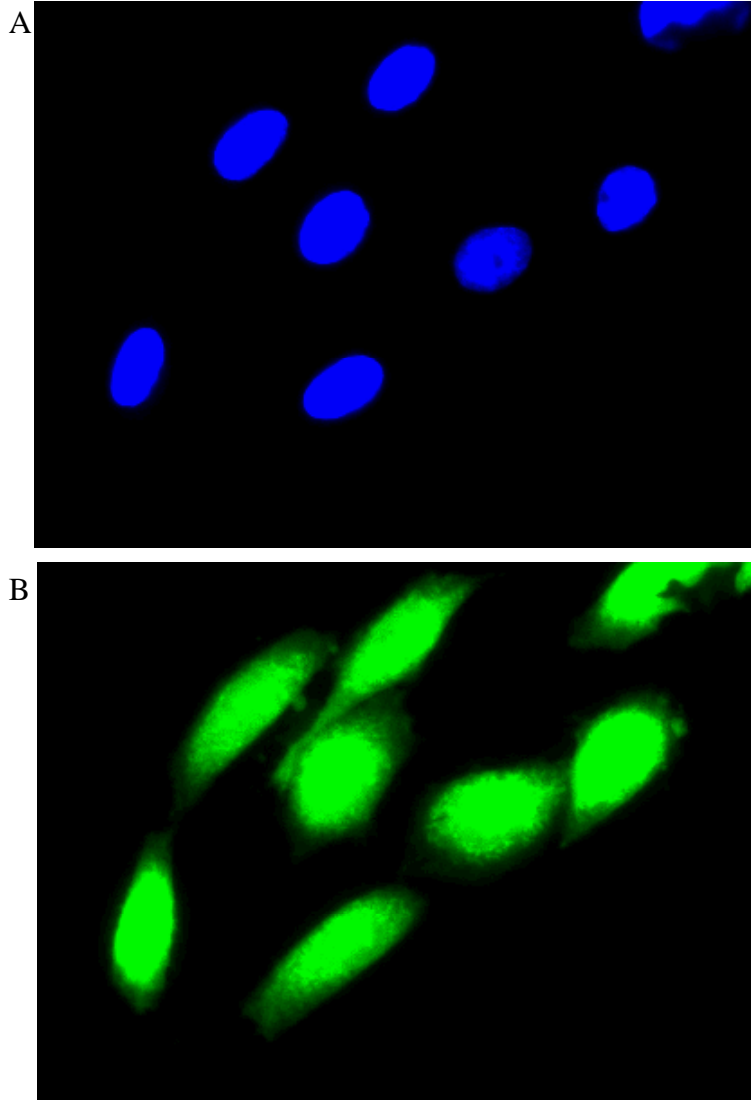
Figure 5.8: Microscopic analysis of immuno-fluorescently labeled CHO-Mut 8 (3 X HA8) 3.5 cells transduced with TAT PTD-DWNN$_{118}$ and probed with anti-DWNN primary antibody and fluorescein. The response was detected at the estimated concentration of 30 ug/µl transduced into cells. Cells were monitored by green fluorescence microscopy.

A: DAPI stained cells. B: Same cell population as in A showing successful probing (Both the cytoplasmic and nuclear regions were stained: More staining in the nuclear region). Cells were viewed using a Zeiss Axioplan fluorescence microscope and imaging was by a Spot RT digital camera (Section 2.16.4).
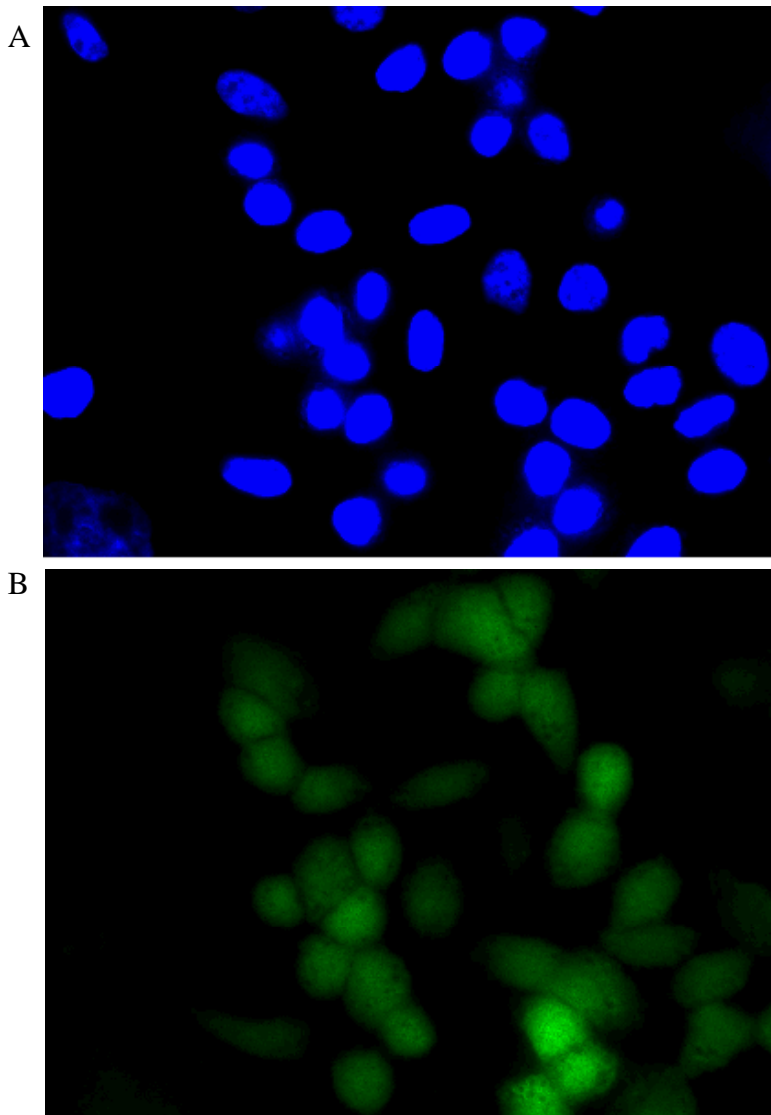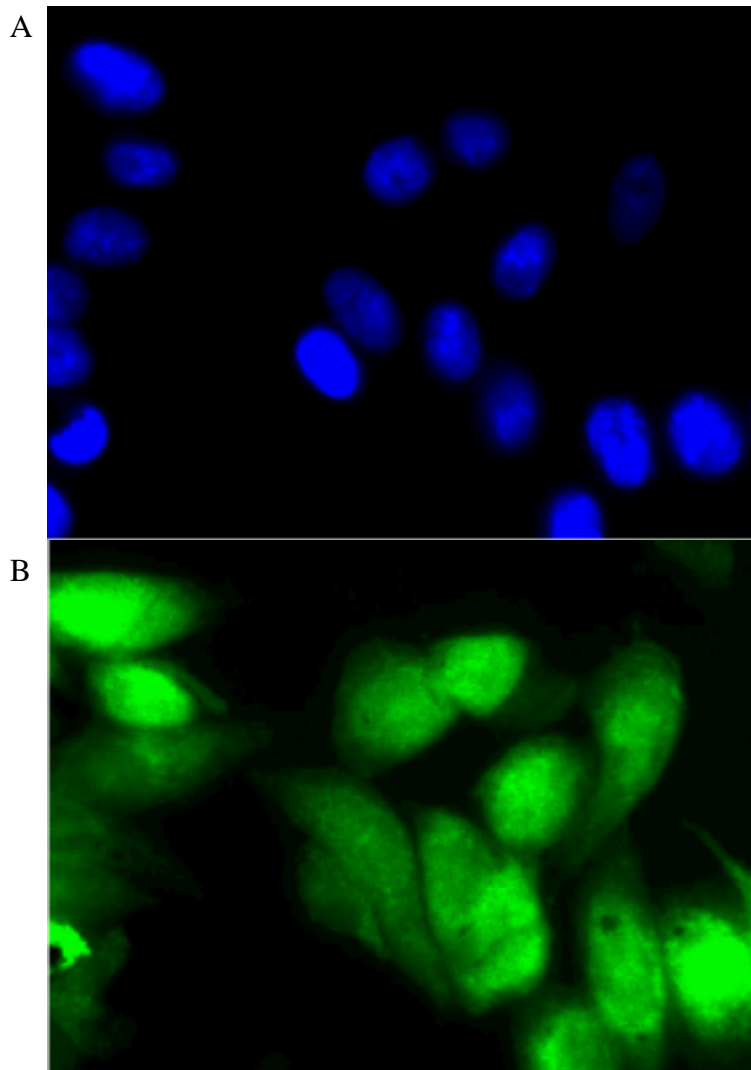
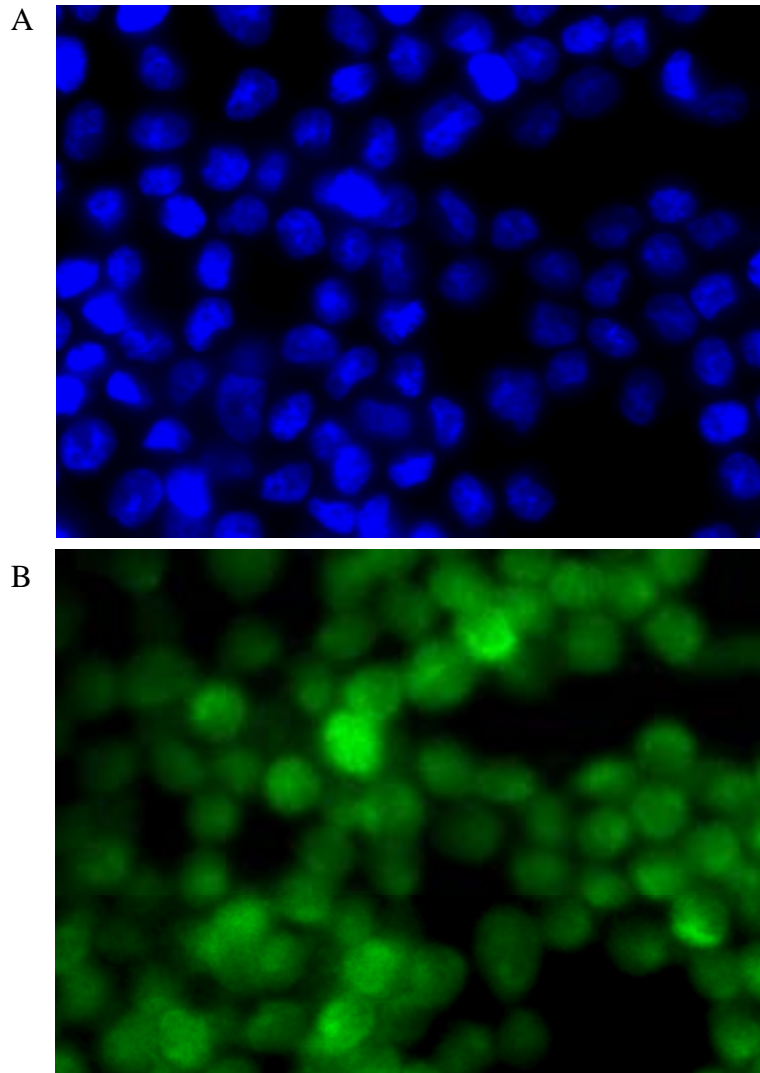**Figure 5.9: Microscopic analysis of immuno-fluorescently labeled CHO-Mut 8 (3 X HA8) 3.5 cells transduced with TAT PTD-DWNN$_{118}$ and probed with anti-DWNN primary antibody and fluorescein**. Cells were monitored by green fluorescence microscopy.

A: DAPI stained cells. B: Same cell population as in A showing successful probing (Both the cytoplasmic and nuclear regions were stained: More staining in the nuclear region). Cells were viewed using a Zeiss Axioplan fluorescence microscope and imaging was by a Spot RT digital camera (Section 2.16.4).
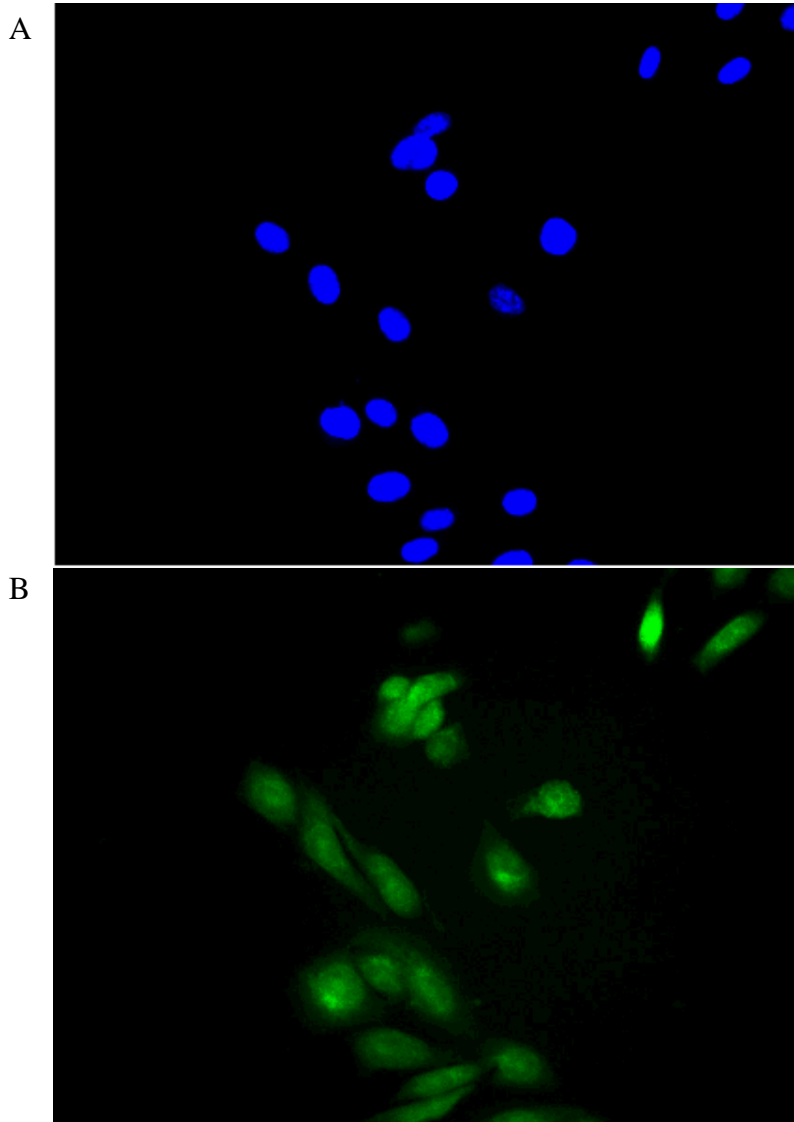
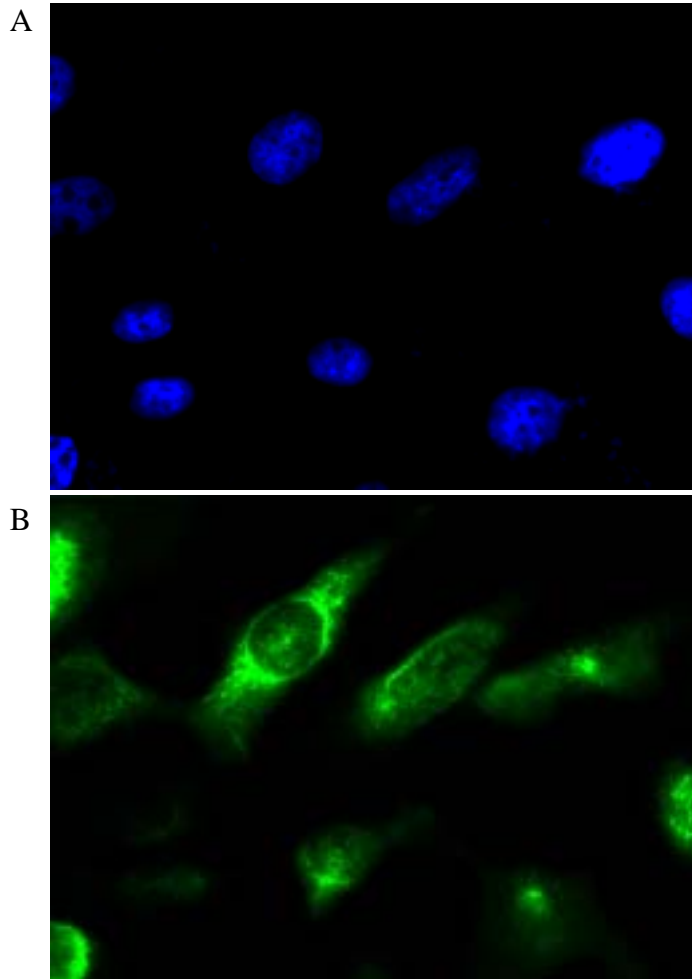**Figure 5.10: Microscopic analysis of immuno-fluorescently labeled CHO-Mut 8 (3 X HA8) 3.5 cells transduced with TAT PTD-DWNN$_{118}$ and probed with anti-DWNN primary antibody and fluorescein.** Cells were monitored by green fluorescence microscopy.

A: DAPI stained cells. B: Same cell population as in A showing successful probing (Both the cytoplasmic and nuclear regions were stained: More staining in the nuclear region). Cells were viewed using a Zeiss Axioplan fluorescence microscope and imaging was by a Spot RT digital camera (Section 2.16.4).
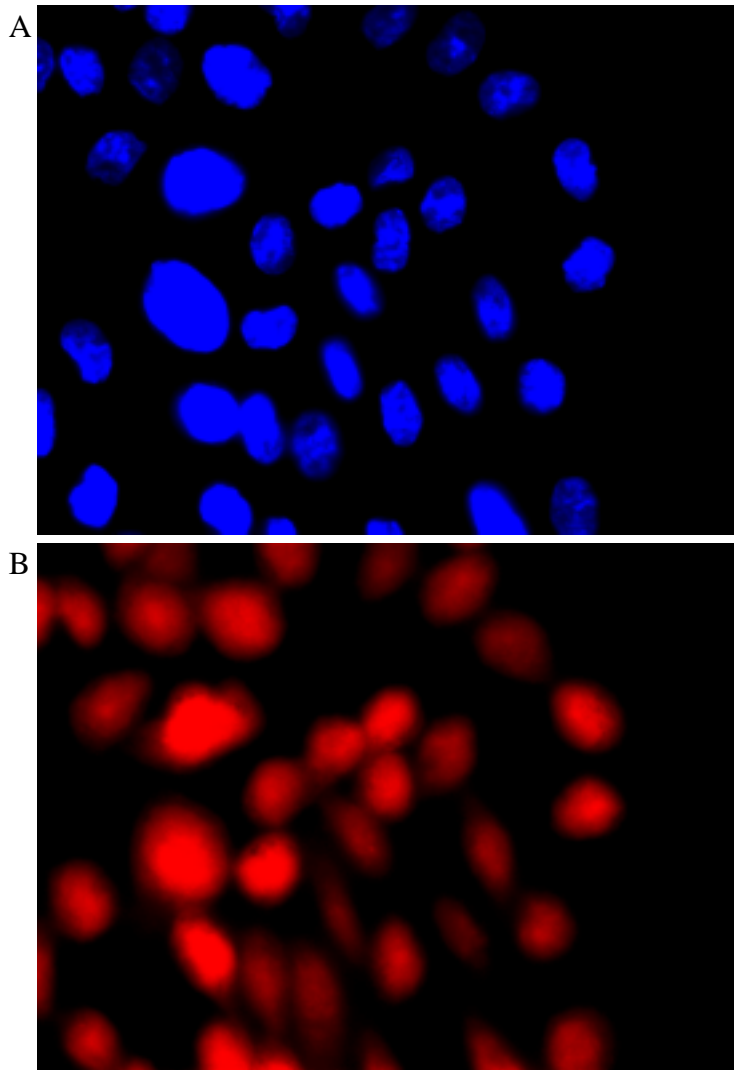
Figure 5.11: Microscopic analysis of immuno-fluorescently labeled CHO-Mut 8 (3 X HA8) 3.5 cells transduced with TAT PTD-DWNN$_{118}$ and probed with anti-DWNN primary antibody and rhodamine. Cells were monitored by red fluorescence microscopy.

A: DAPI stained cells. B: Same cell population as in A showing successful probing (Both the cytoplasmic and nuclear regions were stained: More staining in the nuclear region). Cells were viewed using a Zeiss Axioplan fluorescence microscope and imaging was by a Spot RT digital camera (Section 2.16.4).
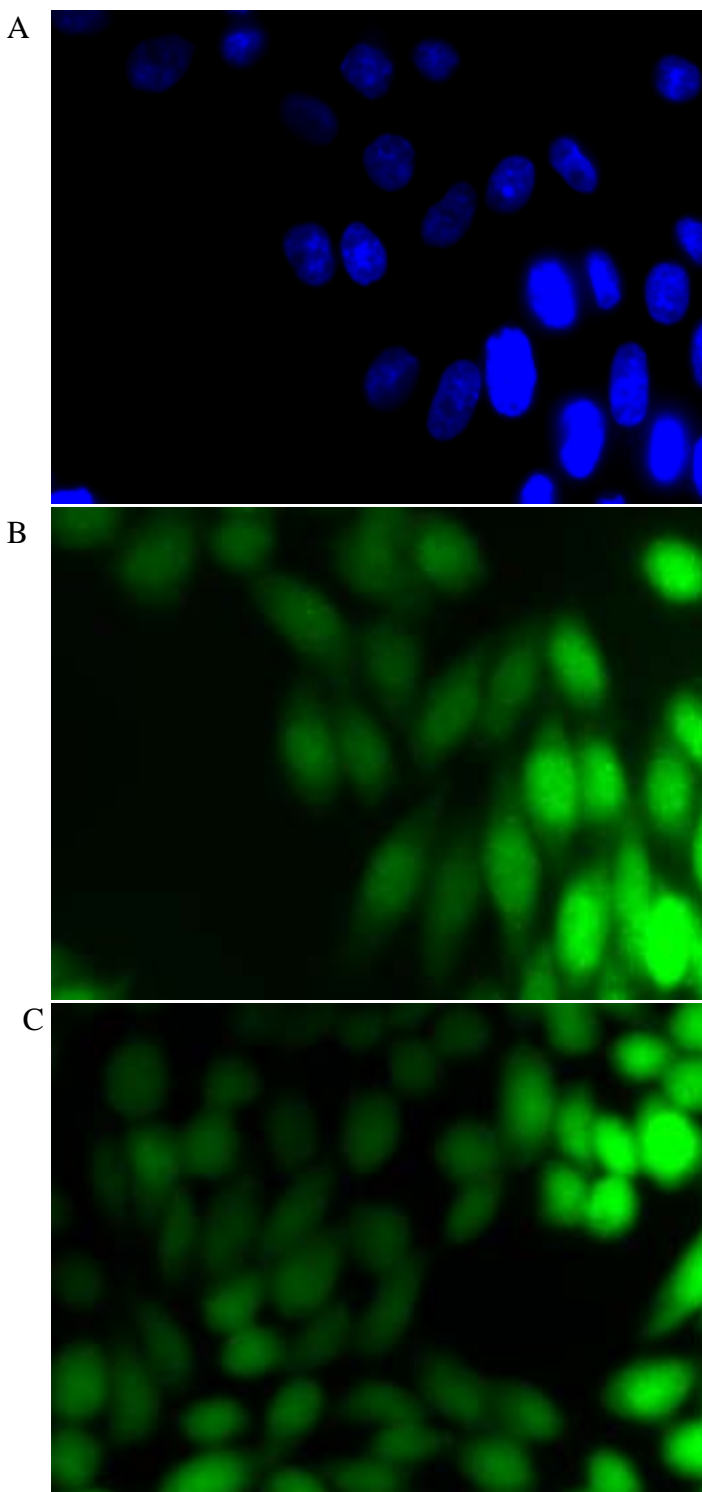
Figure 5.12: Microscopic analysis of immuno-fluorescently labeled CHO-Mut 8 (3 X HA8) 3.5 cells transduced with TAT PTD-DWNN$_{118}$ and probed with anti-DWNN primary antibody and fluorescein. Cells were monitored by green fluorescence microscopy.

A: DAPI stained cells. B: Same cell population as in A showing successful probing (Both the cytoplasmic and nuclear regions were stained: More staining in the nuclear region). C: Population of cells without DAPI staining, also showing successful probing. Cells were viewed using a Zeiss Axioplan fluorescence microscope and imaging was by a Spot RT digital camera (Section 2.16.4).

Untreated cells showed localisation of DWNN to the cytoplasm since staining was observed in the cytoplasmic region (Figs 5.6-5.7). The CHO-Mut 8 (3 X HA8) 3.5 cells are cells from which DWNN had been knocked out and it is clear that there is no nuclear staining in figs 5.6 and 5.7 while when DWNN was reintroduced into cells it localised to both the cytoplamic and the nuclear regions (Figs 5.8-5.12).

5.3.2 Flow Cytometry (FACScan)

The TAT-PTD containing fusion proteins and their non-TAT containing counterparts were transduced into CHO22 cell lines. The cells were incubated for 72 hours to permit the GFP expression. The cells were washed and briefly trypsinised, transferred to FACS test tubes. Flow cytometric analysis (section 2.16.5) verified the results obtained in microscopic analysis (fig 5.13), that transduction by TAT result into GFP fusion proteins uptake since the untreated cells were at the 10^1 region of the gating, M1, demonstrating little to no fluorescence as expected, while cells transduced with TAT-GFP-DWNN$_{118}$ and TAT-GFP showed a shift into the 10^2 region of the gating, M2, thus signifying protein uptake by cells.

5.3.3 Western Blot

The TAT-PTD containing fusion proteins and their non-TAT containing counterparts were transduced into CHO-Y10 and CHO-Mut 8 (3 X HA8) 3.5 cell lines grown in 75 cm^2 flasks. The cells were incubated for 72 hours to permit the GFP refolding. The cells were trypsinised, thoroughly washed and Western Blot analysis (Section 2.17)
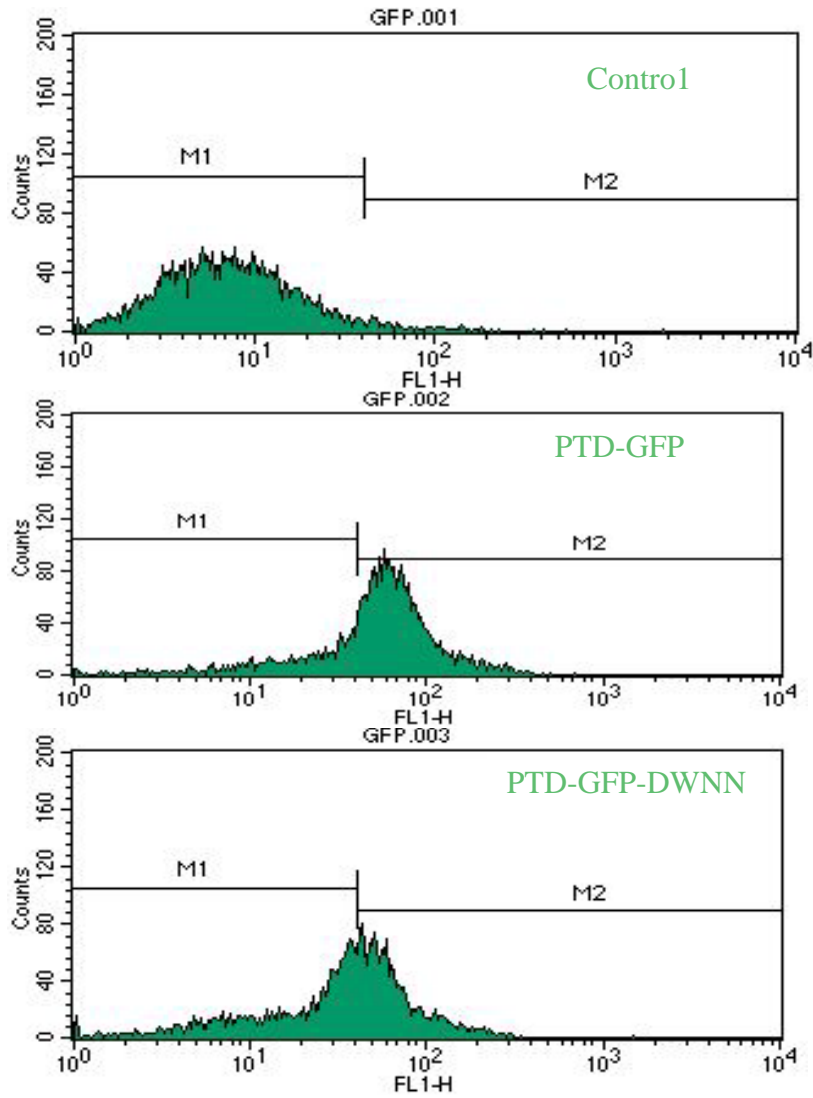
Figure 5.13: Flow cytometric analysis of shifts in green fluorescence.

The figure compares the shifts in green fluorescence in CHO22 cells that were monitored after 72 hours of treatment. Indicated are the untreated cells=Control and the transduced cells. M1 = non fluorescent cells and M2 = fluorescent cells. The cells were analysed for fluorescence by FACS.

was conducted. The analysis demonstrated that DWNN associates with some other higher molecular weight protein product after entering the cell (Figs 5.14 and 5.15). Fig 5.15 shows the association product in lanes 2, 3, and 5, wherein more concentrated TAT-GFP-DWNN$_{118}$ (extracted from transduced CHO-Y10 cells), TAT-GFP-DWNN$_{118}$ (extracted from transduced CHO-Y10 cells), and TAT-DWNN$_{118}$ [extracted from transduced CHO-Mut 8 (3 X HA8) 3.5 cells], respectively, were loaded. Lane 6 contained protein extract from untreated cells. Both the untreated cell lines show the same result of no signal after the analysis has been conducted. Transduction is TAT mediated since the control GFP-DWNN$_{118}$ with no TAT (lane 4) did not yield any association to a higher molecular weight protein just as was the case in untreated cells. The blot of the TAT-GFP-DWNN$_{118}$, GFP-DWNN$_{118}$, and TAT-DWNN$_{118}$, recombinant proteins are shown to be of their right sizes in lanes 7, 8, and 9 respectively and show a strong signal due to their high concentration as recombinants.

5.4 Discussion

Microscopic, flow cytometric and Western Blot analyses verified the mode of delivery was TAT mediated since PTD containing fusion proteins were successfully transduced, while their counterparts without PTD were not detected, as expected, in cells. Western Blot analysis further demonstrated that DWNN, once in cells, links to a higher molecular weight protein product. This supports the hypothesis that DWNN
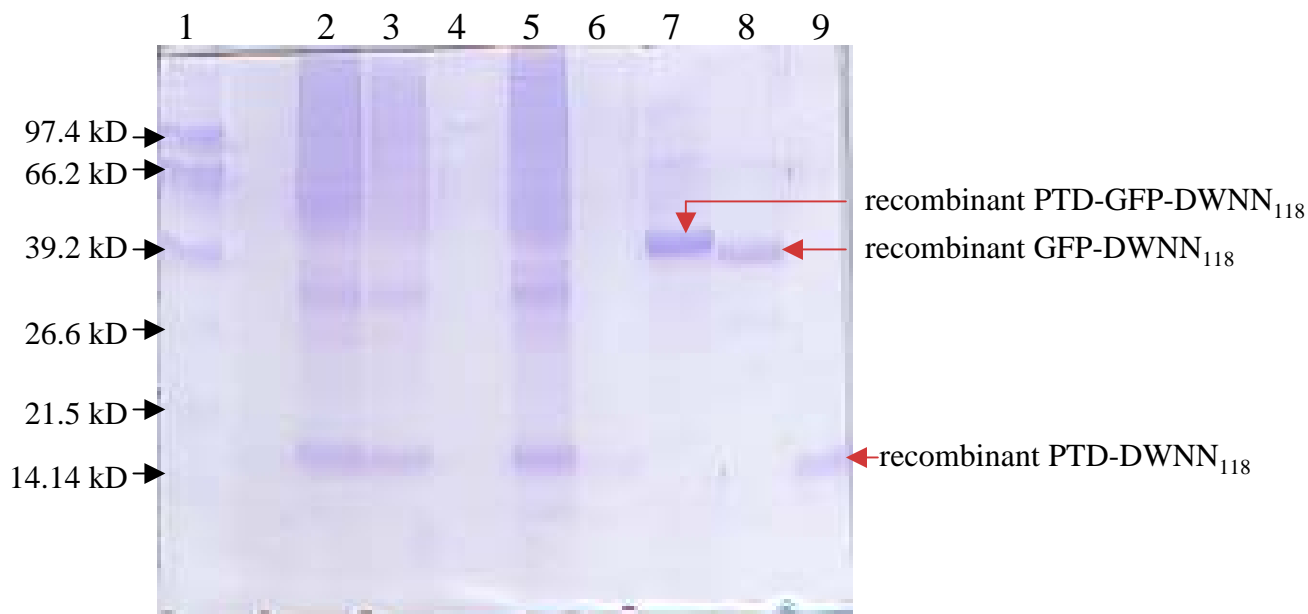
Figure 5.14: 16 % SDS-PAGE gel analysis from which the blot in Fig 5.15 was transferred.

Lane 1: Pre-mixed Protein Marker, CHO/DWNN-ve (Y10) cells transduced with: 2: TAT-GFP-DWNN$_{118}$, 3: TAT-GFP-DWNN$_{118}$, 4: GFP-DWNN$_{118}$, Mut 8 (3 X HA8) 3.5 cells transduced with 5: TAT-DWNN$_{118}$, 6: Untreated cells, and recombinant 7: Purified TAT-GFP-DWNN$_{118}$, 8: Purified GFP-DWNN$_{118}$ 9: Purified TAT-DWNN$_{118}$.
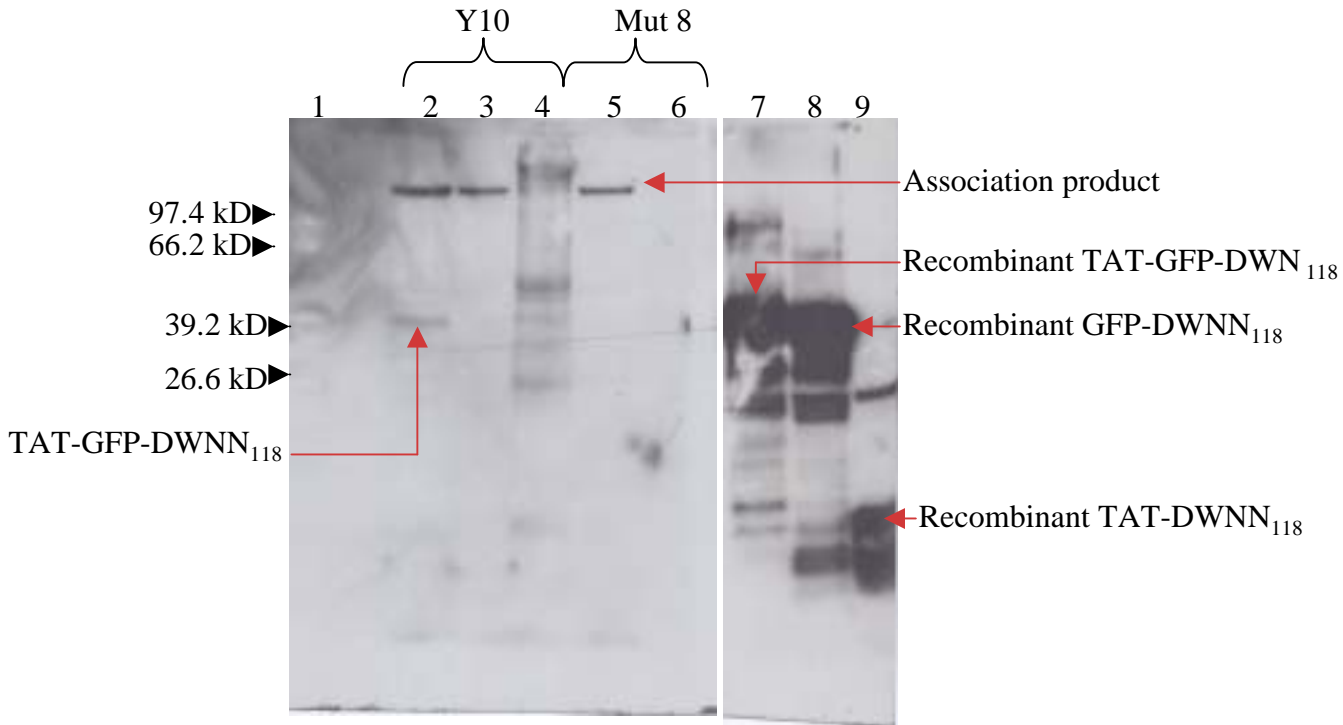
Figure 5.15: Western Blot analysis of transduction protein extracts and the controls, blotted from protein gel in Fig 5.14. Blot probed with anti-DWNN primary antibody.

This response was detected at the estimated concentration of 64 ug/µl transduced into cells in lane 2, 32 ug/µl in lane 3 and 30 ug/µl in lane 5.

Lane 1: Pre-mixed Protein Marker, CHO/DWNN-ve (Y10) cells transduced with: 2: TAT-GFP-DWNN$_{118}$, 3: TAT-GFP-DWNN$_{118}$, 4: GFP-DWNN$_{118}$, Mut 8 (3 X HA8) 3.5 cells transduced with 5: TAT-DWNN$_{118}$, 6: Untreated cells, and recombinant 7: Purified TAT-GFP-DWNN$_{118}$, 8: Purified GFP-DWNN$_{118}$ 9: Purified TAT-DWNN$_{118}$.

associates covalently with other proteins. It is probable that the association is covalent since it is stable in the reducing and denaturing condition of SDS-PAGE gel.

The blot in figure 5.15 was blotted from the protein gel in figure 5.14, where lane 2 represents protein extract of transduction with more concentrated TAT-GFP-DWNN$_{118}$ hence both the association product and the transduced TAT-GFP-DWNN$_{118}$ are clearly detected, while lane 3 represents protein extract of transduction with less concentrated TAT-GFP-DWNN$_{118}$, which thus explains why TAT-GFP-DWNN$_{118}$ does not show. This may well be attributed to association having reached saturation where the remaining protein would be free in the cell if the sites for ligation to the higher molecular weight protein product were saturated (fig 5.16: lane 2). The result thus supports the hypothesis that DWNN domain is attached to other proteins since it attaches to a larger protein once introduced into cells. The control GFP-DWNN$_{118}$ represented in lane 4 did not show the same pattern as the experimental TAT-GFP-DWNN$_{118}$ and TAT-DWNN$_{118}$, thus showing that the transduction was TAT mediated. TAT-DWNN$_{118}$ demonstrated to form the same association pattern as TAT-GFP-DWNN$_{118}$, which suggests that, once in cells, DWNN was localised without being hindered by GFP.

No size difference was observable, suggesting that the association product was of a very high molecular weight, and beyond the effective size resolution of the 16 % gel used. This same pattern was obtained in both the CHO-Y10 and the CHO-Mut 8 cell

112

lines since one line was treated with TAT-GFP-DWNN$_{118}$ while the other was treated with TAT-DWNN$_{118}$ respectively.

5.5 Summary

"*In vivo* protein transduction" is PTD mediated since the constructs without the PTD showed no cellular uptake while their PTD containing counterparts did. This was shown by all the analyses performed in this study.

GFP fluoresces when excited by the filter representing the right wavelength for its fluorescence and thus was used to report the presence of the desired protein by microscopy and flow cytometry. The TAT-GFP-DWNN$_{118}$ fusion protein is localised to the nucleus of the transduced cells.

DWNN was successfully trafficked into cells and was demonstrated to associate with some other protein product once in cells by Western Blot analysis, which verifies the fact that it may be linked to domains that play a role in apoptosis.

CHAPTER 6

General Discussion

6.1 Introduction

The aim of this study was to undertake localisation studies and functional analysis of a novel protein, DWNN, in order to characterise its involvement in apoptosis. The approach used the cloning of an HIV derived TAT protein transduction domain that traverses the plasma membrane along with proteins it is covalently linked to, which in this case were the green fluorescent protein (GFP) and $DWNN_{118}$. The constructs were generated in pGEX-6P-2 containing GST for both the experiment and controls, where the latter consisted of the constructs without the transduction domain and without GFP (Section 3.11). Fusion proteins were expressed in large amounts in bacterial cells, purified, GST cleaved and a final purification step conducted to eliminate GST (section 4.3). Homogeneous fusion proteins were urea denatured, desalted by buffer exchange and introduced into mammalian cells. The TAT mediated mode of delivery was then detected by fluorescence microscopy, immuno-fluorescent labelling for non-GFP containing $DWNN_{118}$ construct, flow cytometric and Western blot analyses.

6.2 DWNN

Amongst the evidence that DWNN plays a role in the apoptotic pathway and CTL-killing is that DWNN knock-out confers resistance to cytotoxic T-cell (CTL). The 1.1 kb DWNN full-length cDNA encodes a 118 residues protein ($DWNN_{118}$)

consisting of a highly conserved globular domain and a hydrophobic C terminal tail. Although DWNN has not yet been fully characterised functionally, its high level of sequence conservation across species (Section 1.5) suggests that it survived being eliminated during evolution due to its function in these organisms.

6.3 Green Fluorescent Protein

The vast flexibility of GFP as a non-interfering marker in living cells allows for various applications such as a cell lineage tracer, reporter of gene expression and to measure of protein-protein interactions [Chalfie, 1995; Chalfie, 1994; Cubitt et al, 1995; Hawley et al, 2004; Heim et al, 1995; Mitra et al, 1996]. It was exploited as a reporter tag in this study, where it was used to trace the cellular localisation of the fusion proteins (Section 1.6).

6.4 Construction, Expression and Transduction

The constructs consisting of the TAT protein transduction domain, for their delivery into the cellular environment, were successfully generated (Section 3.11), expressed, shown to be of their expected sizes (Section 4.5), and transduced into cells (Section 5.5). Denaturation facilitates transduction, thus the fusion proteins were urea denatured. However, urea kills cells, hence a desalting process had to be conducted. The desalting was achieved by buffer exchange through a G-25 Sephadex column (Section 2.16.2).

6.5 Fluorescence microscopy, Flow cytometric and Western blot analyses

Fluorescence microscopy, Flow cytometric and Western blot analyses were used to confirm that proteins were successfully trafficked into cells.

6.5.1 Fluorescence microscopy

Fluorescence microscopy demonstrated that TAT mediated transduction of native DWNN fusion proteins resulted in localisation into the cytoplasm while their denatured counterparts also reach the nuclear region (Section 5.3.1). This confirms that the transduction means used in this study results in protein delivery to both the cytoplasm and the nucleus, not merely attachment to the cell membrane, and that DWNN localises to the nuclear compartment.

6.5.2 Flow cytometry

Flow cytometry also verified the TAT mediated transduction by showing the fluorescence shifts compared to the untransduced counterparts (Section 5.3.2). The analysis might have been limited since the proportion of transduced cells would not be shown the same as that demonstrated by fluorescence microscopy. Microscopy showed 100 % of cells to be transduced as reported in literature (Section 5.2.1). The limitation in flow cytometry is that the gating in fig 5.13 only serves to demonstrate fluorescence shift, i.e., that there is a difference in fluorescence in the transduced cell population compared to the untransduced where little to no fluorescence is observed nor expected. Despite this limitation, this analysis served the purpose it is meant to,

116

namely, that a quantitative shift in the fluorescence of the cells, resulting from GFP transduction, could be shown. In both of the analyses, fluorescence microscopy and flow cytometry, TAT transduction technology was shown to be a useful tool for cell biological and biochemical analysis.

6.5.3 Western blot analysis

Western blot analysis confirmed the hypothesis that DWNN associates with other proteins in the cell (Sections 1.5 and 5.3.3) since when the protein extract of transduced cells was probed, using anti-DWNN antibody in a Western blot, both the recombinant protein and a probable association product, which was significantly larger than 100 kD were detected. The protein extracts were examined on a comparatively small high percentage gel, thus the exact sizes could not be easily determined. An increase in gel size would increase the resolution and show a difference in size, of the PTD-DWNN$_{118}$ and PTD-GFP-DWNN$_{118}$ association products. Two-dimensional SDS PAGE gels from which the proteins were to be transferred for Western blot analysis would also aid in the characterisation of the nature of the association product. Western blot analysis with antibodies against proteins thought to be linked to DWNN, i.e., Rb, p53 and etc., would also help in this regard.

Nuclear localisation verified by fluorescence microscopy (sections 5.3.1 and 6.5.1) also makes it evident that the probable association product demonstrated by Western

blot analysis could be with the proteins it is thought to associate with since they, p53 and Rb, are localised to the nucleus. This research did not investigate the character of the association product, thus the exact proteins DWNN associates with is ongoing research.

The results obtained by Western blotting supports DWNN being implicated in apoptosis and CTL killing, with the already demonstrated data that P2P-R, PACT and its homologue RbBP6, all partial cDNA's of DWNN-200, all shown to bind both p53 and Rb proteins that are implicated in tumor suppression, thus are implicated in programmed cell death, and all localising to the nucleus (section 1.5). The whole network, viz., nuclear localisation, conjugation to a higher molecular weight protein product, the already known data that DWNN is linked to proteins that play prominent roles in apoptosis, supports the hypothesis that DWNN is a pro-apoptotic protein hence also is required in CTL killing.

DWNN protein possibly functions as a p53 ubiquitin-like ligases. They may be part of a novel E3 ubiquitin ligase and play a role in regulating levels of p53 or Rb due to the presence of the RING finger domain, found in a number of E3 ubiquitin ligases where they target protein for degradation by catalysis of the addition of ubiquitin-like proteins. This imply that the protein may comprise a novel E3 ubiquitin ligase and play a role in regulating p53 or Rb levels.

6.6 Summary

The plasma membrane limits the passage of proteins and peptides, which may be pharmacologically important. There are currently a number of alternative means to overcome this difficulty. Amongst these strategies are transfection technologies, which exhibit a number of shortcomings, some of which include toxicity, undesirable dosage and permanent genetic modifications. To mitigate some of these impediments, protein transduction technology has been developed, where proteins are fused to an 11 residue transduction tag from HIV-TAT domain to produce a plasma membrane permeable fusion that is capable of traversing the lipid bi-layer [Nagahara et al, 1998; Schwarze et al, 1999; Wadia and Dowdy, 2002, Wadia and Dowdy, 2003]. This technology has advantages over other means of protein delivery (Section 1.9) with the high proportion of cells targeted being the most significant.

This study illustrated the use of TAT protein transduction technology to introduce proteins through the selectively permeable cell membrane to facilitate the analysis of their localisation and function.

The study verified nuclear localisation of $DWNN_{118}$, and provided evidence to support the hypothesis that there is an association of DWNN with a higher molecular weight protein product, which suggest that DWNN conjugates to some other proteins. Further studies are underway to explore a link between DWNN and cell death. Such studies include further characterisation of the domain by Western blot analysis to

determine the character of the association protein product, where the antibodies used would be specific for the proteins DWNN is thought to be associated with, i.e., p53, zinc knuckle, ring finger, SR and Rb.

There is also a study to determine the region of DWNN required for its localisation and its association to higher molecular weight product. This will be achieved by truncation of the wild type DWNN.

It is thus shown that the use of protein transduction technology allows the detection of roles for proteins, using rapid introduction of proteins into cells, which then allows the biochemical analysis of their function.

REFERENCES

Abraham MC, Shaham S. Death without caspases, caspases without death. *Trends Cell Biol*. 2004 Apr; 14 (4): 184-93.

Abrams JM. An emerging blueprint for apoptosis in Drosophila. *Trends Cell Biol*. 1999 Nov; 9 (11): 435-40.

Adams JM, Cory S. Apoptosomes: engines for caspase activation. *Curr Opin Cell Biol*. 2002 Dec; 14 (6): 715-20.

Ahmad A, Khan M, Raykundalia C, Catty D. Study of the mechanisms of killing of Mycobacterium bovis BCG by apoptosis in J774 murine macrophages. *J Pak Med Assoc*. 1999 Nov; 49 (11): 273-8.

Akagi K, Sandig V, Vooijs M, Van der Valk M, Giovannini M, Strauss M, Berns A. Cre-mediated somatic site-specific recombination in mice. *Nucleic Acids Res*. 1997 May 1; 25 (9): 1766-73.

Alexeyev MF, Pastukh VV, Shokolenko IN, Wilson GL. alpha-Complementation-Enabled T7 Expression Vectors and Their Use for the Expression of Recombinant Polypeptides for Protein Transduction Experiments. *Methods Mol Biol*. 2004; 267: 91-100.

Ameisen JC. On the origin, evolution, and nature of programmed cell death: a timeline of four billion years. *Cell Death Differ*. 2002 Apr; 9 (4): 367-93.

Aravind L, Koonin EV. The U box is a modified RING finger - a common domain in ubiquitination. *Curr Biol*. 2000 Feb 24;10 (4):R132-4.

Ashkenazi A. Targeting death and decoy receptors of the tumor-necrosis factor superfamily. *Nat Rev Cancer*. 2002 Jun; 2 (6): 420-30.

Ashwell JD, Berger NA, Cidlowski JA, Lane DP, Korsmeyer SJ. Coming to terms with death: apoptosis in cancer and immune development. *Immunology Today*. 1994 Apr; 15 (4): 147-51.

Aung S, Graham BS. IL-4 diminishes perforin-mediated and increases Fas ligand-mediated cytotoxicity *In vivo*. *J Immunol*. 2000 Apr 1; 164 (7): 3487-93.

Barisic K, Petrik J, Rumora L. Biochemistry of apoptotic cell death. *Acta Pharm*. 2003 Sep; 53 (3): 151-64.

Bayley H. Protein therapy-delivery guaranteed. *Nat Biotechnol*. 1999 Nov; 17 (11): 1066-7.

Becker-Hapak M, McAllister SS, Dowdy SF. TAT-mediated protein transduction into mammalian cells. Methods. 2001 Jul; 24 (3): 247-56. Review.

Behrens CK, Igney FH, Arnold B, Moller P, Krammer PH. CD95 ligand-expressing tumors are rejected in anti-tumor TCR transgenic perforin knockout mice. *J Immunol*. 2001 Mar 1; 166 (5): 3240-7

Bennett RP, Dalby B, Guy PM. Protein delivery using VP22. *Nat Biotechnol*. 2002 Jan; 20 (1): 20.

Bokman SH, Ward WW. Renaturation of Aequorea gree-fluorescent protein. *Biochem Biophys Res Commun*. 1981 Aug 31; 101 (4): 1372-80.

Bouillet P, Cory S, Zhang LC, Strasser A, Adams JM. Degenerative disorders caused by Bcl-2 deficiency prevented by loss of its BH3-only antagonist Bim. *Dev Cell*. 2001 Nov; 1 (5): 645-53.

Brossart P, Bevan MJ. Selective activation of Fas/Fas ligand-mediated cytotoxicity by a self peptide. *Journal of Experimental Medicine*. 1996 Jun 1; 183 (6): 2449-58.

Bruckheimer EM, Spurgers K, Weigel NL, Logothetis C, McDonnell TJ. Regulation of Bcl-2 expression by dihydrotestosterone in hormone sensitive LNCaP-FGC prostate cancer cells. *J Urol.* 2003 Apr; 169 (4): 1553-7.

Budihardjo I, Oliver H, Lutter M, Luo X, Wang X. Biochemical pathways of caspase activation during apoptosis. *Annu Rev Cell Dev Biol.* 1999; 15:269-90.

Cain K. Chemical-induced apoptosis: formation of the Apaf-1 apoptosome. *Drug Metab Rev.* 2003 Nov; 35 (4): 337-63.

Caron NJ, Quenneville SP, Tremblay JP. Endosome disruption enhances the functional nuclear delivery of Tat-fusion proteins. *Biochem Biophys Res Commun.* 2004 Jun 18; 319 (1): 12-20.

Casadaban MJ, Cohen SN. Analysis of gene control signals by DNA fusion and cloning in Escherichia coli. *J Mol Biol.* 1980 Apr; 138 (2): 179-207.

Catz SD, Johnson JL. BCL-2 in prostate cancer: a minireview. *Apoptosis.* 2003 Jan; 8 (1): 29-37.

Cecconi F. Apaf1 and the apoptotic machinery. *Cell Death Differ.* 1999 Nov; 6 (11): 1087-98.

Chalfie M. Green fluorescent protein. *Photochem Photobiol*. 1995 Oct; 62 (4): 651-6.

Chalfie M, Tu Y, Euskirchen G, Ward WW, Prasher DC. Green fluorescent protein as a marker for gene expression. *Science*. 1994 Feb 11; 263 (5148): 802-5.

Chambers CA, Allison JP. Costimulatory regulation of T cell function. *Current Opinion in Cell Biology*. 1999 Apr; 11 (2): 203-10.

Changsen C, Franzblau SG, Palittapongarnpim P. Improved green fluorescent protein reporter gene-based microplate screening for antituberculosis compounds by utilizing an acetamidase promoter. *Antimicrob Agents Chemother*. 2003 Dec; 47 (12): 3682-7.

Chen P, Ho SI, Shi Z, Abrams JM. Bifunctional killing activity encoded by conserved reaper proteins. *Cell Death Differ*. 2004 Feb 27 [Epub ahead of print].

Chen P, Rodriguez A, Erskine R, Thach T, Abrams JM. Dredd, a novel effector of the apoptosis activators reaper, grim, and hid in Drosophila. *Dev Biol*. 1998 Sep 15; 201 (2): 202-16.

Chen P, Abrams JM. Drosophila apoptosis and Bcl-2 genes: outliers fly in. *J Cell Biol*. 2000 Feb 21; 148 (4): 625-7.

Chen P, Nordstrom W, Gish B, Abrams JM. grim, a novel cell death gene in Drosophila. *Genes Dev*. 1996 Jul 15; 10 (14): 1773-82.

Chinnaiyan AM, Hanna WL, Orth K, Duan H, Poirier GG, Froelich CJ, Dixit VM. Cytotoxic T-cell-derived granzyme B activates the apoptotic protease ICE-LAP3. *Current Biology*. 1996 Jul 1; 6 (7): 897-9.

Cikala M, Wilm B, Hobmayer E, Bottger A, David CN. Identification of caspases and apoptosis in the simple metazoan Hydra. *Curr Biol*. 1999 Sep 9; 9 (17): 959-62.

Clark JM. Novel non-templated nucleotide addition reactions catalyzed by prokaryotic and eukaryotic DNA polymerases. *Nucleic Acids Res*. 1988 Oct 25; 16 (20): 9677-86.

Cohen JJ. Apoptosis: the physiologic pathway of cell death. *Hosp Pract (Off Ed)*. 1993 Dec 15; 28 (12): 35-43.

Cohen JJ. Programmed cell death and apoptosis in lymphocyte development and function. *Chest*. 1993 Feb; 103 (2 Suppl): 99S-101S.

Cohen JJ. Apoptosis. *Immunology Today*. 1993 Mar; 14 (3): 126-30.

Conus S, Rosse T, Borner C. Failure of Bcl-2 family members to interact with Apaf-1 in normal and apoptotic cells. *Cell Death Differ*. 2000 Oct; 7 (10): 947-54.

Cordingley MG, Callahan PL, Sardana VV, Garsky VM, Colonno RJ Substrate requirements of human rhinovirus 3C protease for peptide cleavage in vitro. *J Biol Chem*. 1990 Jun 5; 265 (16): 9062-5.

Cormack BP, Valdivia RH, Falkow S. FACS-optimized mutants of the green fluorescent protein (GFP). *Gene*. 1996; 173 (1 Spec No): 33-8.

Cory S, Adams JM. The Bcl2 family: regulators of the cellular life-or-death switch. *Nat Rev Cancer*. 2002 Sep; 2 (9): 647-56.

Cubitt AB, Heim R, Adams SR, Boyd AE, Gross LA, Tsien RY. Understanding, improving and using green fluorescent proteins. *Trends Biochem Sci*. 1995 Nov; 20 (11): 448-55.

Cuende E, Ales-Martinez JE, Ding L, Gonzalez-Garcia M, Martinez C, Nunez G. Programmed cell death by bcl-2-dependent and independent mechanisms in B lymphoma cells. *EMBO J*. 1993 Apr; 12 (4): 1555-60.

Darmon AJ, Nicholson DW, Bleackley RC. Activation of the apoptotic protease CPP32 by cytotoxic T-cell-derived granzyme B. *Nature*. 1995 Oct 5; 377 (6548): 446-8.

Davis JE, Smyth MJ, Trapani JA. Granzyme A and B-deficient killer lymphocytes are defective in eliciting DNA fragmentation but retain potent *in vivo* anti-tumor capacity. *Eur J Immunol.* 2001 Jan; 31 (1): 39-47.

De Felici M, Pesce M. Growth factors in mouse primordial germ cell migration and proliferation. *Prog Growth Factor Res*. 1994; 5 (2): 135-43.

Deigner HP, Haberkorn U, Kinscherf R. Apoptosis modulators in the therapy of neurodegenerative diseases*. Expert Opin Investig* Drugs. 2000 Apr; 9 (4): 747-64.

Delagrave S, Hawtin RE, Silva CM, Yang MM, Youvan DC. Red-shifted excitation mutants of the green fluorescent protein. *Biotechnology* (N Y). 1995 Feb; 13 (2): 151-4.

Denecker G, Vercammen D, Declercq W, Vandenabeele P. Apoptotic and necrotic cell death induced by death domain receptors. *Cell Mol Life Sci*. 2001 Mar; 58 (3): 356-70.

Doherty PC, Topham DJ, Tripp RA, Cardin RD, Brooks JW, Stevenson PG. Effector CD4+ and CD8+ T-cell mechanisms in the control of respiratory virus infections. *Immunol Rev*. 1997 Oct; 159: 105-17.

Durfee T, Mancini MA, Jones D, Elledge SJ, Lee WH. The amino-terminal region of the retinoblastoma gene product binds a novel nuclear matrix protein that co-localizes to centers for RNA processing. *J Cell Biol*. 1994 Nov; 127 (3): 609-22.

Earnshaw WC, Martins LM, Kaufmann SH. Mammalian caspases: structure, activation, substrates, and functions during apoptosis. *Annu Rev Biochem*. 1999; 68: 383-424.

Elliott G, O'Hare P. Intercellular trafficking and protein delivery by a herpesvirus structural protein. Cell. 1997 Jan 24; 88 (2): 223-33.

Esser MT, Krishnamurthy B, Braciale VL. Distinct T cell receptor signalling requirements for perforin- or FasL-mediated cytotoxicity. *Journal of Experimental Medicine*. 1996 Apr 1; 183 (4): 1697-706.

Evan G, Littlewood T. A matter of life and cell death. *Science.* 1998 Aug 28; 281(5381): 1317-22.

Fadeel B, Orrenius S, Zhivotovsky B. Apoptosis in human disease: a new skin for the old ceremony? *Biochem Biophys Res Commun*. 1999 Dec 29; 266 (3): 699-717.

Fanidi A, Evan G. Applications of apoptosis: making death pay. *Trends in Biotechnology*. 1994 Jun; 12 (6): 219-21.

Fawell S, Seery J, Daikh Y, Moore C, Chen LL, Pepinsky B, Barsoum J. Tat-mediated delivery of heterologous proteins into cells. *Proc Natl Acad Sci* U S A. 1994 Jan 18; 91 (2): 664-8.

Figueroa B Jr, Sauerwald TM, Mastrangelo AJ, Hardwick JM, Betenbaugh MJ. Comparison of Bcl-2 to a Bcl-2 deletion mutant for mammalian cells exposed to culture insults. *Biotechnol Bioeng*. 2001 May 5; 73 (3): 211-22.

Fortinea N, Trieu-Cuot P, Gaillot O, Pellegrini E, Berche P, Gaillard JL. Optimization of green fluorescent protein expression vectors for in vitro and *in vivo* detection of Listeria monocytogenes. *Res Microbiol*. 2000 Jun; 151 (5): 353-60.

Frankel AD, Pabo CO. Cellular uptake of the tat protein from human immunodeficiency virus. *Cell*. 1988 Dec 23; 55 (6): 1189-93.

Frohlich KU, Madeo F. Apoptosis in yeast--a monocellular organism exhibits altruistic behaviour. *FEBS Lett*. 2000 May 4; 473 (1): 6-9.

Futaki S, Suzuki T, Ohashi W, Yagami T, Tanaka S, Ueda K, Sugiura Y. Arginine-rich peptides. An abundant source of membrane-permeable peptides having potential as carriers for intracellular protein delivery. *J Biol Chem*. 2001 Feb 23; 276 (8): 5836-40. Epub 2000 Nov 17.

Gao S, Witte MM, Scott RE. P2P-R protein localizes to the nucleolus of interphase cells and the periphery of chromosomes in mitotic cells which show maximum P2P-R immunoreactivity. *J Cell Physiol*. 2002 May;191 (2): 145-54. *Erratum in: J Cell Physiol* 2002 Sep;192 (3): 359-60.

Gao S, Scott RE. P2P-R protein overexpression restricts mitotic progression at prometaphase and promotes mitotic apoptosis. *J Cell Physiol*. 2002 Nov; 193 (2): 199-207.

Gao S, Scott RE. Stable overexpression of specific segments of the P2P-R protein in human MCF-7 cells promotes camptothecin-induced apoptosis. *J Cell Physiol*. 2003 Dec; 197 (3): 445-52.

Gaumer S, Guenal I, Brun S, Theodore L, Mignotte B. Bcl-2 and Bax mammalian regulators of apoptosis are functional in Drosophila. *Cell Death Differ*. 2000 Sep; 7 (9): 804-14.

German-Retana S, Redondo E, Tavert-Roudet G, Le Gall O, Candresse T. Introduction of a NIa proteinase cleavage site between the reporter gene and HC-Pro only partially restores the biological properties of GUS- or GFP-tagged LMV. *Virus Res*. 2003 Dec; 98 (2): 151-62.

Gerschenson LE, Rotello RJ. Apoptosis: a different type of cell death. *FASEB journal*. 1992 Apr; 6 (7): 2450-5.

Gilman CP, Chan SL, Guo Z, Zhu X, Greig N, Mattson MP. p53 is present in synapses where it mediates mitochondrial dysfunction and synaptic degeneration in response to DNA damage, and oxidative and excitotoxic insults. *Neuromolecular Med*. 2003; 3 (3): 159-72.

Gius DR, Ezhevsky SA, Becker-Hapak M, Nagahara H, Wei MC, Dowdy SF. Transduced p16INK4a peptides inhibit hypophosphorylation of the retinoblastoma protein and cell cycle progression prior to activation of Cdk2 complexes in late G1. *Cancer Res*. 1999 Jun 1; 59 (11): 2577-80.

Green M, Loewenstein PM. Autonomous functional domains of chemically synthesized human immunodeficiency virus tat trans-activator protein. *Cell*. 1988 Dec 23; 55 (6): 1179-88.

Grunenfelder J, Miniati DN, Murata S, Falk V, Hoyt EG, Kown M, Koransky ML, Robbins RC. Upregulation of Bcl-2 through caspase-3 inhibition ameliorates ischemia/reperfusion injury in rat cardiac allografts. *Circulation*. 2001 Sep 18; 104 (12 Suppl 1): I202-6.

Guzman-Rojas L, Sims-Mourtada JC, Rangel R, Martinez-Valdez H. Life and death within germinal centres: a double-edged sword. *Immunology*. 2002 Oct; 107 (2): 167-75.

Hahn K, DeBiasio R, Tishon A, Lewicki H, Gairin JE, LaRocca G, Taylor DL, Oldstone M. Antigen presentation and cytotoxic T lymphocyte killing studied in individual, living cells. *Virology*. 1994 Jun; 201 (2): 330-40.

Hawiger J. Noninvasive intracellular delivery of functional peptides and proteins. *Curr Opin Chem Biol*. 1999 Feb; 3 (1): 89-94.

Haslett C. Granulocyte apoptosis and its role in the resolution and control of lung inflammation. *Am J Respir Crit Care Med.* 1999 Nov; 160 (5 Pt 2): S5-11.

Hawley TS, Herbert DJ, Eaker SS, Hawley RG. Multiparameter flow cytometry of fluorescent protein reporters. *Methods Mol Biol*. 2004; 263: 219-38.

Heim R, Cubitt AB, Tsien RY. Improved green fluorescence. *Nature*. 1995 Feb 23; 373 (6516): 663-4.

Hengartner MO. Programmed cell death in invertebrates. *Curr Opin Genet Dev*. 1996 Feb; 6 (1): 34-8.

Hengartner MO, Horvitz HR. Programmed cell death in *Caenorhabditis elegans*. *Curr Opin Genet Dev*. 1994 Aug; 4 (4): 581-6.

Hengartner MO, Horvitz HR. The ins and outs of programmed cell death during *C. elegans* development. *Philos Trans R Soc Lond B Biol Sci*. 1994 Aug 30; 345 (1313): 243-6.

Hengartner MO, Horvitz HR. Activation of *C. elegans* cell death protein CED-9 by an amino-acid substitution in a domain conserved in Bcl-2. *Nature*. 1994 May 26; 369 (6478): 318-20.

Hengartner MO, Horvitz HR. C. elegans cell survival gene ced-9 encodes a functional homolog of the mammalian proto-oncogene bcl-2. *Cell*. 1994 Feb 25; 7 6 (4): 665-76.

Hengartner MO, Ellis RE, Horvitz HR. *Caenorhabditis elegans* gene ced-9 protects cells from programmed cell death. *Nature*. 1992 Apr 9; 56(6369): 494-9.

Henkart PA. Apoptosis: O death, where is thy sting? *J Immunol*. 1995 May 15; 154 (10): 4905-8.

Ho A, Schwarze SR, Mermelstein SJ, Waksman G, Dowdy SF. Synthetic protein transduction domains: enhanced transduction potential in vitro and *in vivo*. *Cancer Res*. 2001 Jan 15; 61 (2): 474-7.

Ho E, Courtemanche C, Ames BN. Zinc deficiency induces oxidative DNA damage and increases p53 expression in human lung fibroblasts. *J Nutr*. 2003 Aug; 133 (8): 2543-8.

Hockenbery DM, Oltvai ZN, Yin XM, Milliman CL, Korsmeyer SJ. Bcl-2 functions in an antioxidant pathway to prevent apoptosis. *Cell*. 1993 Oct 22; 75 (2): 241-51.

Holtz J, Heinrich H. [Apoptosis--what is it? Significance in coronary heart disease and myocardial infarct] *Herz*. 1999 May; 24 (3): 196-210.

Horvitz HR, Shaham S, Hengartner MO. The genetics of programmed cell death in the nematode *Caenorhabditis elegans*. *Cold Spring Harb Symp Quant Biol*. 1994; 59:377-85.

Hoyes KP, Cai WB, Potten CS, Hendry JH. Effect of bcl-2 deficiency on the radiation response of clonogenic cells in small and large intestine, bone marrow and testis. *Int J Radiat Biol*. 2000 Nov; 76 (11): 1435-42.

Huppertz B, Frank HG, Kaufmann P. The apoptosis cascade--morphological and immunohistochemical methods for its visualization. *Anat Embryol (Berl).* 1999 Jul; 200 (1): 1-18.

Hutchins JB, Barger SW. Why neurons die: cell death in the nervous system. *Anat Rec*. 1998 Jun; 253 (3): 79-90.

Igaki T, Miura M. Role of Bcl-2 family members in invertebrates. *Biochim Biophys Acta*. 2004 Mar 1; 1644 (2-3): 73-81.

Inouye S, Tsuji FI. Aequorea green fluorescent protein. Expression of the gene and fluorescence characteristics of the recombinant protein. *FEBS Lett*. 1994 Mar 21; 341 (2-3): m277-80.

Inouye S, Tsuji FI. Evidence for redox forms of the Aequorea green fluorescent protein. *FEBS Lett*. 1994 Sep 5; 351 (2) :211-4.

Isaaz S, Baetz K, Olsen K, Podack E, Griffiths GM. Serial killing by cytotoxic T lymphocytes: T cell receptor triggers degranulation, re-filling of the lytic granules and secretion of lytic proteins via a non-granule pathway. *European Journal of Immunology*. 1995 Apr; 25 (4): 1071-9.

Jacobson MD, Weil M, Raff MC. Programmed cell death in animal development. *Cell*. 1997 Feb 7; 88 (3): 347-54.

Jo D, Nashabi A, Doxsee C, Lin Q, Unutmaz D, Chen J, Ruley HE. Epigenetic regulation of gene structure and function with a cell-permeable Cre recombinase. *Nature Biotechnology*. 2001 Oct;19 (10): 929-33.

Johnson S, Young-Chan CS, Laping NJ, Finch CE. Perforant path transection induces complement C9 deposition in hippocampus. *Exp Neurol*. 1996 Apr; 138 (2): 198-205.

Ju ST, Panka DJ, Cui H, Ettinger R, el-Khatib M, Sherr DH, Stanger BZ, Marshak-Rothstein A. Fas (CD95)/FasL interactions required for programmed cell death after T-cell activation. *Natur*e. 1995 Feb 2; 373 (6513): 444-8.

Karray S, Kress C, Cuvellier S, Hue-Beauvais C, Damotte D, Babinet C, Levi-Strauss M. Complete loss of Fas ligand gene causes massive lymphoproliferation and early death, indicating a residual activity of gld allele. J Immunol. 2004 Feb 15; 172 (4): 2118-25.

Kerr JF, Wyllie AH, Currie AR. Apoptosis: a basic biological phenomenon with wide-ranging implications in tissue kinetics. *Br J Cancer*. 1972 Aug; 26 (4): 239-57.

Kirsch DG, Doseff A, Chau BN, Lim DS, de Souza-Pinto NC, Hansford R, Kastan MB, Lazebnik YA, Hardwick JM. Caspase-3-dependent cleavage of Bcl-2 promotes release of cytochrome c. *J Biol Chem*. 1999 Jul 23; 274 (30): 21155-61.

Lang F, Uhlemann AC, Lepple-Wienhues A, Szabo I, Siemen D, Nilius B, Gulbins E. Cell volume regulatory mechanisms in apoptotic cell death. Herz. 1999 May; 24 (3): 232-5.

Lee SH, Bar-Haim E, Goldberger O, Reich-Zeliger S, Vadai E, Tzehoval E, Eisenbach L. Expression of FasL by tumor cells does not abrogate anti-tumor CTL function. *Immunol Lett*. 2004 Feb 15; 91 (2-3): 119-26.

Liang CY, Wang HZ, Li TX, Hu ZH, Chen XW. High efficiency gene transfer into mammalian kidney cells using baculovirus vectors. *Arch Virol*. 2004 Jan; 149 (1):51-60. Epub 2003 Sep 22.

Lin YZ, Yao SY, Veach RA, Torgerson TR, Hawiger J. Inhibition of nuclear translocation of transcription factor NF-kappa B by a synthetic peptide containing a cell membrane-permeable motif and nuclear localization sequence. *J Biol Chem*. 1995 Jun 16; 270 (24): 14255-8.

Liu QA, Hengartner MO. The molecular mechanism of programmed cell death in C. elegans. *Ann N Y Acad Sci*. 1999; 887:92-104.

Lundberg M, Johansson M. Is VP22 nuclear homing an artifact? *Nat Biotechnol*. 2001 Aug; 19 (8): 713-4.

Mai JC, Shen H, Watkins SC, Cheng T, Robbins PD. Efficiency of protein transduction is cell type-dependent and is enhanced by dextran sulfate. *J Biol Chem*. 2002 Aug 16; 277 (33): 30208-18. Epub 2002 May 28.

McGuire MJ, Lipsky PE, Thiele DL. Generation of active myeloid and lymphoid granule serine proteases requires processing by the granule thiol protease dipeptidyl peptidase I. *J Biol Chem*. 1993 Feb 5; 268 (4): 2458-67.

Medema JP, Scaffidi C, Kischkel FC, Shevchenko A, Mann M, Krammer PH, Peter ME. FLICE is activated by association with the CD95 death-inducing signaling complex (DISC). *EMBO J*. 1997 May 15; 16 (10): 2794-804.

Meier P, Finch A, Evan G. Apoptosis in development. *Nature*. 2000 Oct 12; 407 (6805): 796-801.

Metzstein MM, Stanfield GM, Horvitz HR. Genetics of programmed cell death in C. elegans: past, present and future. *Trends Genet*. 1998 Oct; 14 (10): 410-6.

Mitra RD, Silva CM, Youvan DC. Fluorescence resonance energy transfer between blue-emitting and red-shifted excitation derivatives of the green fluorescent protein. *Gene*. 1996; 173 (1 Spec No): 13-7.

Miyawaki A. Green fluorescent protein-like proteins in reef Anthozoa animals. *Cell Struct Funct*. 2002 Oct; 27 (5): 343-7.

Morris MC, Depollier J, Mery J, Heitz F, Divita G. A peptide carrier for the delivery of biologically active proteins into mammalian cells. *Nat Biotechnol*. 2001 Dec; 19 (12): 1173-6.

Morris MC, Chaloin L, Heitz F, Divita G. Translocating peptides and proteins and their use for gene delivery. *Curr Opin Biotechnol*. 2000 Oct; 11 (5): 461-6.

Morris MC, Vidal P, Chaloin L, Heitz F, Divita G. A new peptide vector for efficient delivery of oligonucleotides into mammalian cells. *Nucleic Acids Res.* 1997 Jul 15; 25 (14): 2730-6.

Morris MC, Chaloin L, Mery J, Heitz F, Divita G. A novel potent strategy for gene delivery using a single peptide vector as a carrier. *Nucleic Acids Res*. 1999 Sep 1; 27 (17): 3510-7.

Mullauer L, Gruber P, Sebinger D, Buch J, Wohlfart S, Chott A. Mutations in apoptosis genes: a pathogenetic factor for human disease. *Mutat Res*. 2001 Jul; 488 (3): 211-31.

Nagahara H, Vocero-Akbani AM, Snyder EL, Ho A, Latham DG, Lissy NA, Becker-Hapak M, Ezhevsky SA, Dowdy SF. Transduction of full-length TAT fusion proteins into mammalian cells: TAT-p27Kip1 induces cell migration. *Nat Med*. 1998 Dec; 4 (12): 1449-52.

Nagata S, Golstein P. The Fas death factor. *Science*. 1995 Mar 10; 267 (5203): 1449-56.

Nicholson DW. Caspase structure, proteolytic substrates, and function during apoptotic cell death. *Cell Death Differ*. 1999 Nov; 6 (11): 1028-42.

Nomura Y Neuronal apoptosis and protection:effects of nitric oxide and endoplasmic reticulum-related proteins. *Biol Pharm Bull*. 2004 Jul; 27 (7): 961-3.

Ohman L, Franzen L, Rudolph U, Birnbaumer L, Hornquist EH. Regression of Peyer's patches in G alpha i2 deficient mice prior to colitis is associated with reduced expression of Bcl-2 and increased apoptosis. Gut. 2002 Sep; 51 (3): 392-7.

Ohta S, Ishibashi Y. [Molecular mechanism of apoptosis] *No To Hattatsu*. 1999 Mar; 31 (2): 122-8.

Palumbo A, Yeh J. Apoptosis as a basic mechanism in the ovarian cycle: follicular atresia and luteal regression. *J Soc Gynecol Investig*. 1995 May-Jun; 2 (3): 565-73.

Pan H, Feng L, Lu H, Xu C, Zhang P, Zhang Z. Aging of human mature erythrocytes is like a process of apoptosis in enucleated cell. *Chin Med Sci J*. 1998 Mar; 13 (1): 20-3.

Papaconstantinou HT, Xie C, Zhang W, Ansari NH, Hellmich MR, Townsend CM Jr, Ko TC. The role of caspases in methotrexate-induced gastrointestinal toxicity. *Surgery*. 2001 Nov; 130 (5): 859-65.

Parrish J, Li L, Klotz K, Ledwich D, Wang X, Xue D. Mitochondrial endonuclease G is important for apoptosis in C. elegans. *Nature*. 2001 Jul 5; 412 (6842): 90-4.

Peter ME, Heufelder AE, Hengartner MO. Advances in apoptosis research. *Proc Natl Acad Sci* U S A. 1997 Nov 25; 94 (24): 12736-7.

Peter ME, Krammer PH. Mechanisms of CD95 (APO-1/Fas)-mediated apoptosis. *Curr Opin Immunol*. 1998 Oct; 10 (5): 545-51.

Pham CT, Thomas DA, Mercer JD, Ley TJ. Production of fully active recombinant murine granzyme B in yeast. *J Biol Chem*. 1998 Jan 16; 273 (3): 1629-33.

Phelan A, Elliott G, O'Hare P. Intercellular delivery of functional p53 by the herpesvirus protein VP22. *Nat Biotechnol*. 1998 May; 16 (5): 440-3.

Pinkoski MJ, Hobman M, Heibein JA, Tomaselli K, Li F, Seth P, Froelich CJ, Bleackley RC. Entry and trafficking of granzyme B in target cells during granzyme B-perforin-mediated apoptosis. *Blood*. 1998 Aug 1; 92 (3): 1044-54.

Pinkoski MJ, Waterhouse NJ, Heibein JA, Wolf BB, Kuwana T, Goldstein JC, Newmeyer DD, Bleackley RC, Green DR. Granzyme B-mediated apoptosis proceeds predominantly through a Bcl-2-inhibitable mitochondrial pathway. *J Biol Chem*. 2001 Apr 13; 276 (15): 12060-7. *Epub* 2001 Jan 12.

Prochiantz A. [Messenger proteins] *J Soc Biol*. 2000; 194 (3-4): 119-23.

Prochiantz A. Messenger proteins: homeoproteins, TAT and others. *Curr Opin Cell Biol*. 2000 Aug; 12 (4): 400-6.

Proskuryakov SY, Konoplyannikov AG, Gabai VL. Necrosis: a specific form of programmed cell death? Exp Cell Res. 2003 Feb 1; 283 (1): 1-16.

Putcha GV, Johnson EM Jr. Men are but worms: neuronal cell death in C elegans and vertebrates. *Cell Death Differ*. 2004 Jan;11(1):38-48.

Raff MC. Social controls on cell survival and cell death. *Nature*. 1992 Apr 2; 356 (6368): 397-400.

Reed JC. Bcl-2 and the regulation of programmed cell death. *J Cell Biol*. 1994 Jan; 124 (1-2): 1-6.

Rich T, Allen RL, Wyllie AH. Defying death after DNA damage. *Nature*. 2000 Oct 12; 407 (6805): 777-83.

Richardson H, Kumar S. Death to flies: Drosophila as a model system to study programmed cell death. *J Immunol Methods*. 2002 Jul 1; 265 (1-2): 21-38.

Rodriguez A, Chen P, Abrams JM. Molecular prophets of death in the fly. *Am J Hum Genet*. 1998 Mar; 62 (3): 514-9.

Rosochacki SJ, Kozikova LV, Korwin-Kossakowski M, Matejczyk M, Poloszynowicz J, Duszewska AM. Noninvasive fluorescent screening of microinjected bovine embryos to predict transgene integration. *Folia Biol* (Krakow). 2003; 51 (1-2): 97-104.

Ryu J, Han K, Park J, Choi SY. Enhanced uptake of a heterologous protein with an HIV-1 Tat protein transduction domains (PTD) at both termini. *Mol Cells*. 2003 Dec 31; 16 (3): 385-91.

Sakai Y, Saijo M, Coelho K, Kishino T, Niikawa N, Taya Y. cDNA sequence and chromosomal localization of a novel human protein, RBQ-1 (RBBP6), that binds to the retinoblastoma gene product. *Genomics*. 1995 Nov 1; 30 (1): 98-101.

Saraste A, Pulkki K. Morphologic and biochemical hallmarks of apoptosis. *Cardiovasc Res*. 2000 Feb; 45 (3): 528-37.

Saunders JW Jr. Death in embryonic systems. *Science*. 1966 Nov 4; 154 (749): 604-12.

Sayers TJ, Brooks AD, Ward JM, Hoshino T, Bere WE, Wiegand GW, Kelly JM, Smyth MJ, Kelley JM. The restricted expression of granzyme M in human lymphocytes. *J Immunol*. 2001 Jan 15; 166(2): 765-71. Erratum in: *J Immunol* 2001 Mar 1; 166 (5): 3622.
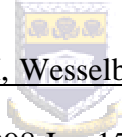
Schulze-Osthoff K, Ferrari D, Los M, Wesselborg S, Peter ME. Apoptosis signaling by death receptors. *Eur J Biochem*. 1998 Jun 15; 254 (3): 439-59.

Schwartz LM, Smith SW, Jones ME, Osborne BA. Do all programmed cell deaths occur via apoptosis? *Proc Natl Acad Sc* U S A. 1993 Feb 1; 90 (3): 980-4.

Schwartz LM, Osborne BA. Programmed cell death, apoptosis and killer genes. *Immunology Today*. 1993 Dec; 14 (12): 582-90.

Schwarze SR, Ho A, Vocero-Akbani A, Dowdy SF. *In vivo* protein transduction: delivery of a biologically active protein into the mouse. *Science*. 1999 Sep 3; 285 (5433): 1569-72.

Schwarze SR, Hruska KA, Dowdy SF. Protein transduction: unrestricted delivery into all cells? *Trends Cell Biol*. 2000 Jul; 10 (7): 290-5.

Schwarze SR, Dowdy SF. *In vivo* protein transduction: intracellular delivery of biologically active proteins, compounds and DNA. *Trends Pharmacol Sci*. 2000 Feb; 21(2): 45-8.

Scott RE, Giannakouros T, Gao S, Peidis P. Functional potential of P2P-R: a role in the cell cycle and cell differentiation related to its interactions with proteins that bind to matrix associated regions of DNA? *J Cell Biochem*. 2003 Sep 1; 90 (1): 6-12.

Scott RE, Gao S. P2P-R deficiency modifies nocodazole-induced mitotic arrest and UV-induced apoptosis. Anticancer Res. 2002 Nov-Dec; 22 (6C): 3837-42.

Simon MM, Hausmann M, Tran T, Ebnet K, Tschopp J, ThaHla R, Mullbacher A. In vitro- and ex vivo-derived cytolytic leukocytes from granzyme A x B double knockout mice are defective in granule-mediated apoptosis but not lysis of target cells. *J Exp Med*. 1997 Nov 17; 186 (10): 1781-6.

Simons A, Melamed-Bessudo C, Wolkowicz R, Sperling J, Sperling R, Eisenbach L, Rotter V. PACT: cloning and characterization of a cellular p53 binding protein that interacts with Rb. *Oncogene*. 1997 Jan 16; 14 (2): 145-55.

Skulachev VP. Programmed death in yeast as adaptation? *FEBS Lett*. 2002 Sep 25; 528 (1-3): 23-6.

Smith DB, Johnson KS. Single-step purification of polypeptides expressed in Escherichia coli as fusions with glutathione S-transferase. *Gene.* 1988 Jul 15; 67 (1): 31-40.

Smyth MJ, O'Connor MD, Trapani JA. Granzymes: a variety of serine protease specificities encoded by genetically distinct subfamilies. *J Leukoc Biol*. 1996 Nov; 60 (5): 555-62.

Smyth MJ, Street SE, Trapani JA. Cutting edge: granzymes A and B are not essential for perforin-mediated tumor rejection. *J Immunol*. 2003 Jul 15; 171 (2): 515-8.

Snyder EL, Dowdy SF. Cell penetrating peptides in drug delivery. *Pharm Res*. 2004 Mar; 21 (3): 389-93.

Solomon M, Belenghi B, Delledonne M, Menachem E, Levine A. The involvement of cysteine proteases and protease inhibitor genes in the regulation of programmed cell death in plants. *Plant Cell*. 1999 Mar; 11 (3): 431-44.

Soria Gonzalez JE, Orea Solano M. [Apoptosis] *Rev Alerg Mex*. 2002 Jul-Aug; 49 (4): 121-8.

Soriano P. Generalized lacZ expression with the ROSA26 Cre reporter strain. *Nat Genet*. 1999 Jan; 21 (1): 70-1

Stein CA. Mechanisms of action of taxanes in prostate cancer. *Semin Oncol*. 1999 Oct; 26 (5 Suppl 17): 3-7.

Takahashi T, Tanaka M, Inazawa J, Abe T, Suda T, Nagata S. Human Fas ligand: gene structure, chromosomal location and species specificity. *Int Immunol*. 1994 Oct; 6 (10): 1567-74.

Takahashi T, Tanaka M, Brannan CI, Jenkins NA, Copeland NG, Suda T, Nagata S. Generalized lymphoproliferative disease in mice, caused by a point mutation in the Fas ligand. *Cell*. 1994 Mar 25; 76 (6): 969-76.

Taylor JE, Fernandez-Patron C. Delivery of bioactive, gel-isolated proteins into live cells. Electrophoresis. 2003 May; 24 (9): 1331-7.

Thompson CB. Apoptosis in the pathogenesis and treatment of disease. *Science*. 1995 Mar 10; 267 (5203): 1456-62.

Tittel JN, Steller H. A comparison of programmed cell death between species. Genome Biol. 2000; 1 (3):REVIEWS0003. *Epub* 2000 Sep 13.

Tooze SA, Flatmark T, Tooze J, Huttner WB. Characterization of the immature secretory granule, an intermediate in granule biogenesis. *J Cell Biol*. 1991 Dec; 115 (6): 1491-503.

Trapani JA. Granzymes: a family of lymphocyte granule serine proteases. *Genome Biol*. 2001; 2 (12): REVIEWS3014. Epub 2001 Nov 23.

Van Cruchten S, Van Den Broeck W. Morphological and biochemical aspects of apoptosis, oncosis and necrosis. *Anat Histol Embryol*. 2002 Aug; 31 (4): 214-23.

Varfolomeev EE, Schuchmann M, Luria V, Chiannilkulchai N, Beckmann JS, Mett IL, Rebrikov D, Brodianski VM, Kemper OC, Kollet O, Lapidot T, Soffer D, Sobe T, Avraham KB, Goncharov T, Holtmann H, Lonai P, Wallach D. Targeted disruption of the mouse Caspase 8 gene ablates cell death induction by the TNF receptors, Fas/Apo1, and DR3 and is lethal pre-natally. *Immunity*. 1998 Aug; 9 (2): 267-76.

Vaux DL, Cory S, Adams JM. Bcl-2 gene promotes haemopoietic cell survival and cooperates with c-myc to immortalize pre-B cells. *Nature*. 1988 Sep 29; 335 (6189): 440-2.

Vaux DL, Korsmeyer SJ. Cell death in development. *Cell*. 1999 Jan 22; 96 (2): 245-54.

Vaux DL, Wilhelm S, Hacker G. Requirements for proteolysis during apoptosis. *Mol Cell Biol*. 1997 Nov; 17 (11): 6502-7.

Vives E, Brodin P, Lebleu B. A truncated HIV-1 Tat protein basic domain rapidly translocates through the plasma membrane and accumulates in the cell nucleus. *J Biol Chem*. 1997 Jun 20; 272 (25): 16010-7.

Vo LT, Minet M, Schmitter JM, Lacroute F, Wyers F. Mpe1, a zinc knuckle protein, is an essential component of yeast cleavage and polyadenylation factor required for the cleavage and polyadenylation of mRNA. *Mol Cell Biol*. 2001 Dec; 21 (24): 8346-56.

Vocero-Akbani AM, Heyden NV, Lissy NA, Ratner L, Dowdy SF. Killing HIV-infected cells by transduction with an HIV protease-activated caspase-3 protein. *Nat Med*. 1999 Jan; 5 (1): 29-33.

Wadia JS, Dowdy SF. Modulation of cellular function by TAT mediated transduction of full-length proteins. *Curr Protein Pept Sci.* 2003 Apr; 4 (2): 97-104.

Wadia JS, Dowdy SF. Protein transduction technology. *Curr Opin Biotechnol*. 2002 Feb; 13 (1): 52-6.

Wadia JS, Stan RV, Dowdy SF. Transducible TAT-HA fusogenic peptide enhances escape of TAT-fusion proteins after lipid raft macropinocytosis. *Nat Med*. 2004 Mar;10 (3): 310-5. Epub 2004 Feb 08.

Ward WW, Bokman SH. Reversible denaturation of Aequorea green-fluorescent protein: physical separation and characterization of the renatured protein. *Biochemistry*. 1982 Sep 14; 21 (19): 4535-40.

Waterhouse NJ, Trapani JA. CTL: Caspases Terminate Life, but that's not the whole story. *Tissue Antigens*. 2002 Mar; 59 (3): 175-83.

Weil M, Jacobson MD, Raff MC. Is programmed cell death required for neural tube closure? *Current Biology*. 1997 Apr 1; 7 (4): 281-4.

White K, Grether ME, Abrams JM, Young L, Farrell K, Steller H. Genetic control of programmed cell death in *Drosophila*. *Science*. 1994 Apr 29; 264 (5159): 677-83.

Will E, Klump H, Heffner N, Schwieger M, Schiedlmeier B, Ostertag W, Baum C, Stocking C. Unmodified Cre recombinase crosses the membrane. *Nucleic Acids Res*. 2002 Jun 15; 30 (12): e59.

Witte MM, Scott RE. The proliferation potential protein-related (P2P-R) gene with domains encoding heterogeneous nuclear ribonucleoprotein association and Rb1 binding shows repressed expression during terminal differentiation. *Proc Natl Acad Sci* U S A. 1997 Feb 18; 94 (4): 1212-7.

Yeh ET. Life and death of the cell. *Hosp Pract* (Off Ed). 1998 Aug 15; 33 (8): 85-7, 91-2.

Zador Z, Lacza Z, Benyo Z, Harkany T, Hortobagyi T. Apoptosis in focal brain ischemia. *Ideggyogy Sz*. 2003 Jul 20; 56 (7-8): 216-28.

Zajac AJ, Dye JM, Quinn DG. Control of lymphocytic choriomeningitis virus infection in granzyme B deficient mice. *Virology*. 2003 Jan 5; 305 (1): 1-9.

Ziegler U, Groscurth P. Morphological features of cell death. News *Physiol Sci*. 2004 Jun; 19: 124-8.

Zhang D, Beresford PJ, Greenberg AH, Lieberman J. Granzymes A and B directly cleave lamins and disrupt the nuclear lamina during granule-mediated cytolysis. *Proc Natl Acad Sci* U S A. 2001 May 8; 98 (10): 5746-51. Epub 2001 May 01.

Zhang QH, Sheng HP, Loh TT. bcl-2 protects HL-60 cells from apoptosis by stabilizing their intracellular calcium pools. *Life Sci*. 2001 May 11; 68 (25): 2873-83.

APPENDIX

Amino Acids

Here is a list of the standard one-letter amino acid codes and their three-letter equivalents. The synonymous codons are shown. The amino acid codes included in this appendix are meant to cover the PTD sequence.

Symbol	3-letter	Meaning	Codons
G	Gly	Glycine	GGT, GGC, GGA, GGG
K	Lys	Lysine	AAA, AAG
Q	Gln	Glutamine	CAA, CAG
R	Arg	Arginine	CGT, CGC, CGA, CGG, AGA, AGG
Y	Tyr	Tyrosine	TAT, TAC
Q		Glutamine	GAA, GAG, CAA, CAG
*	End	Terminator	TAA, TAG, TGA